ATRX: A New Player in DNA Damage Repair.

Sam Shepherd

M.Res Oncology

St. Cross College

ABSTRACT

A key requisite for indefinite growth of cancer cells is the ability to continuously elongate telomeres to circumvent the onset of senescence or apoptosis, this is known as a telomere maintenance mechanism. Most cancers use an enzyme called telomerase, however, in approximately 10 – 15% of cancers this is achieved through the Alternative Lengthening of Telomeres (ALT) mechanism, a Break Induced Replication (BIR) mediated mechanism of telomere copying. ATRX has emerged as the key tumour suppressor in ALT cancers but its loss is insufficient to drive induction of the pathway. Here, we report that depletion of ATRX and/or DAXX in the presence of various genotoxic agents is sufficient to induce ALT. We have additionally showed that these effects occur most strongly when telomere clustering is both exaggerated and prevalent. Moreover, co-deletion of ATRX and SETD2, commonly mutated in high grade gliomas (HGGs), elicits induction of ALT. Mechanistically, SETD2 restricts the accumulation of telomeric R-loops, which, in the absence of ATRX, leads to fork collapse and the loss of telomere sister chromatid cohesion. Cumulatively this provides a substrate for out of register BIR and telomere lengthening.

CHAPTER 1.0: INTRODUCTION

Due to the inherent inability of DNA polymerases to fully replicate the distal ends of linear chromosomes, chromosomal DNA is progressively shortened with each round of cell division. To circumvent potentially detrimental effects to genome stability and loss of genetic information, humans, like many other species, have developed specialised nucleoprotein structures, called telomeres, shown in figure 1. Telomeres are comprised of many kilobases (kb) of a tandem repeat sequence, TTAGGG, culminating in a 3' protrusion of single stranded G-rich DNA of 50 – 400 nucleotides. Telomeric sequence is bound by a specialised protein complex, denoted Shelterin, which comprises the proteins TRF1, TRF2, POT1, TIN1, TPP1 and RAP1 (de Lange, 2018). Telomeres range from 3 to 12 kb in humans and progressively shorten by about 200 base pairs per cell division due to the end-replication problem, this is due to the lack of replication occurring at the 5' end primer. Once telomeres reach a critical length, termed the 'Hayflick limit', they elicit DNA damage checkpoint activation, leading to cellular senescence or telomere-induced apoptosis.

A key hallmark of cancer cells is their ability to circumvent telomere shortening via a telomere length maintenance mechanism (TMM). In the majority of cancers, this is achieved through the upregulation of telomerase, a specialised ribonucleoprotein that acts to progressively add telomeric repeats to the end of chromosomes. More recently it has emerged that approximately 15% of cancers maintain telomere length through a telomerase independent TMM, known as the Alternative Lengthening of Telomeres (ALT) pathway. No in depth studies have been done to determine the prevalence of both telomerase activity and ALT in the same tumour. The ALT pathway is particularly

prevalent in cancers of mesenchymal origin, including several cancers of the central nervous system (CNS), with rates as high as 63% (Heaphy et al., 2011). ALT in human cancer cells is generally considered to be a form of aberrant telomere recombination and conservative DNA synthesis known as Break Induced Replication (BIR), occurring during both the G2 and Mitosis phases of the cell cycle. A three-protein axis has been implicated in facilitating ALT-mediated telomere synthesis; POLD3, PCNA and RAD52 (Dilley et al., 2016; Min et al., 2017; Roumelioti et al., 2016). A second Rad52 independent pathway has also recently been reported, suggesting that ALT is in fact a bifurcated pathway, with similarities to telomerase independent telomere maintenance pathways originally described in budding yeast (Cho et al., 2014; Zhang et al., 2019a).

Further work in human cells has suggested that replication stress arising at telomeres can potentiate the ALT pathway (Min et al., 2017). Indeed, owing to their repetitive nature, telomeres are thought to be inherently difficult sequences to replicate and telomeres have been shown to phenotypically resemble common fragile sites due to the overt fragility they exhibit under conditions of replication stress (Sfeir et al., 2009). This is likely in large part due to the propensity of the G-rich repetitive telomeric sequence to adopt non-canonical DNA secondary structures, including the G-quadruplex (G4) conformation and R-loops; three-stranded nucleic acid structures consisting of an RNA:DNA hybrid and a displaced piece of single stranded DNA (Aguilera and García-Muse, 2012). In line with this notion, abrogation of FANCM activity, which has known roles in R-loop resolution and fork stabilisation (Lu et al., 2019a; Pan et al., 2019; Silva et al., 2019), or depletion of RNase H, which can degrade DNA:RNA hybrids, have both recently been shown to potentiate markers of

the ALT pathway (Arora et al., 2014; Lu et al., 2019b; Pan et al., 2017a, 2017b; Silva et al., 2019).

A near unifying feature of ALT positive cancer cells is loss of the alpha thalassemia/mental retardation syndrome X-linked chromatin remodeller (ATRX) and/or its interaction partner DAXX (death domain-associated protein) (Heaphy et al., 2011; Lovejoy et al., 2012; Schwartzentruber et al., 2012a). Indeed, previous work by the lab and others has demonstrated that ectopic expression of ATRX leads to a DAXX-dependent suppression of the ALT pathway (Clynes et al., 2015a; Napier et al., 2015). Of note, depletion or knockout (KO) of ATRX in telomerase positive or primary cell lines is generally insufficient to induce markers of the ALT pathway (Clynes et al., 2014; Eid et al., 2015; Lovejoy et al., 2012; Napier et al., 2015), with the notable exception of a minority of glioma cell lines (Brosnan-Cashman et al., 2018). A likely explanation for these observations is that other genetic or epigenetic events are required for the induction of ALT in human cancer in concert with ATRX loss. To date, what these events are remains contentious.

ATRX is a chromatin remodelling factor of the Snf2 family (reviewed in (Clynes et al., 2013) which, together with the histone chaperone DAXX, facilitates the incorporation of the histone variant H3.3 into defined genomic sites, including telomeric chromatin, in a replication independent chromatin assembly pathway (Drané et al., 2010; Goldberg et al., 2010; Wong et al., 2010). In the last decade, a number of studies have implicated ATRX in a plethora of roles related to the maintenance of genome stability. One major role of ATRX appears to be the regulation of non-canonical DNA secondary structures, with ATRX null cells displaying increases in both G4 and R-loop structures

(Nguyen et al., 2017a; Wang et al., 2018). ATRX also has multiple reported roles in DNA replication; including the prevention of replication fork stalling, potentiation of fork restart and the prevention of excessive nucleolytic degradation of stalled forks (Clynes et al., 2014; Huh et al., 2012, 2016; Leung et al., 2013a; Watson et al., 2013). Additionally, evidence exists for a role of ATRX in facilitating DNA double strand break (DSB) repair, with roles reported in both the major DSB repair pathways, homologous recombination (HR) (Juhász et al., 2018; Raghunandan et al., 2020) and non-homologous end joining (NHEJ) (Koschmann et al., 2016). Which of these role(s) are required for ATRX to prevent either the induction or maintenance of the ALT pathway is to date unclear.

Two of the major methods to detect the presence of an ALT phenotype look at the quantity of C-circles and ALT associated PML Nuclear Bodies (APB's). C-circles are partially single stranded, circular molecules of C-rich telomeric DNA, the assay to detect these utilises the unique properties of phi29 DNA polymerase to selectively amplify C-circles. APB's are the co-localisation between PML nuclear bodies and telomeres and are thought to be the site of ALT recombination, they can be detected by immunofluorescence and telomere FISH.

Here, I show on an overarching role for ATRX in the suppression of the ALT pathway. Firstly, I demonstrate that ATRX/DAXX is required to prevent ALT in the presence of a variety of genotoxic agents that are known to result in replication fork stalling and reversal. Induction of the ALT phenotype is associated with increases in telomeric DNA damage and single stranded DNA, in addition to a loss of sister chromatid telomere cohesion. Based on this I propose that the induction of ALT in cancer cells

requires two independent events; one involving a mutation (or mutations) in a factor (or factors) that leads to the generation of replicative stress at telomeres, which, if in concert with ATRX loss, leads to both fork collapse and the loss of telomere sister chromatid cohesion. This cumulatively results in out of register BIR and telomere lengthening. I demonstrate one such factor to be the histone methyltransferase SETD2, which is frequently mutated concomitantly with ATRX in high grade gliomas (HGGs), by showing that loss of SETD2 elicits induction of the ALT pathway, specifically in the absence of ATRX, via the generation of telomeric R-loops.

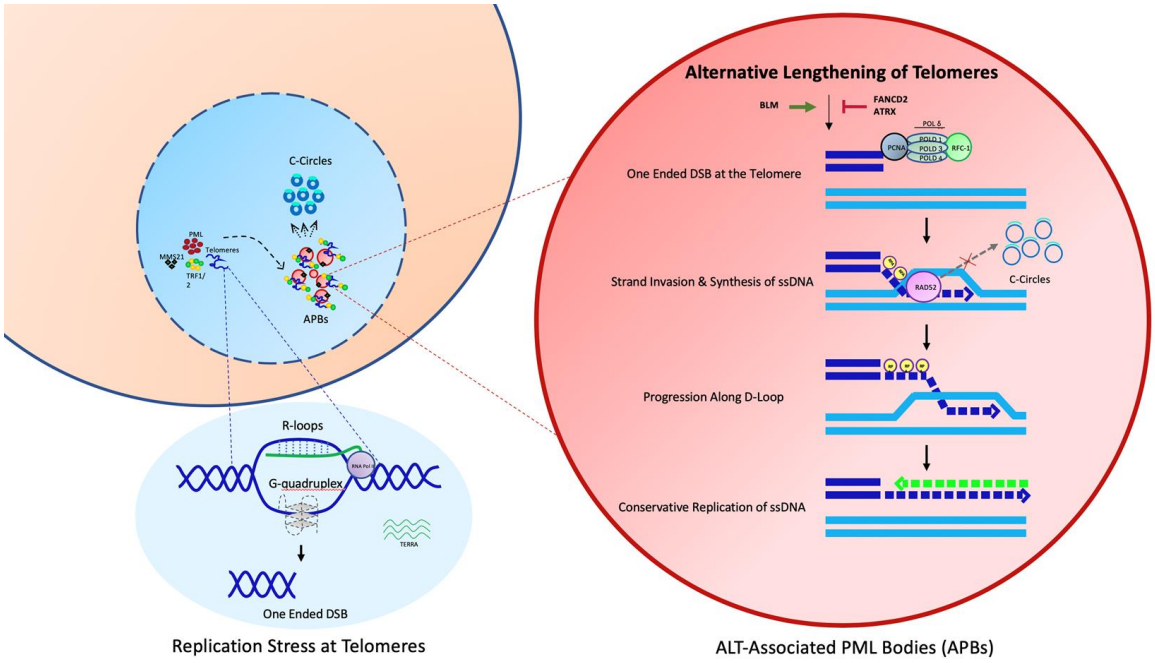

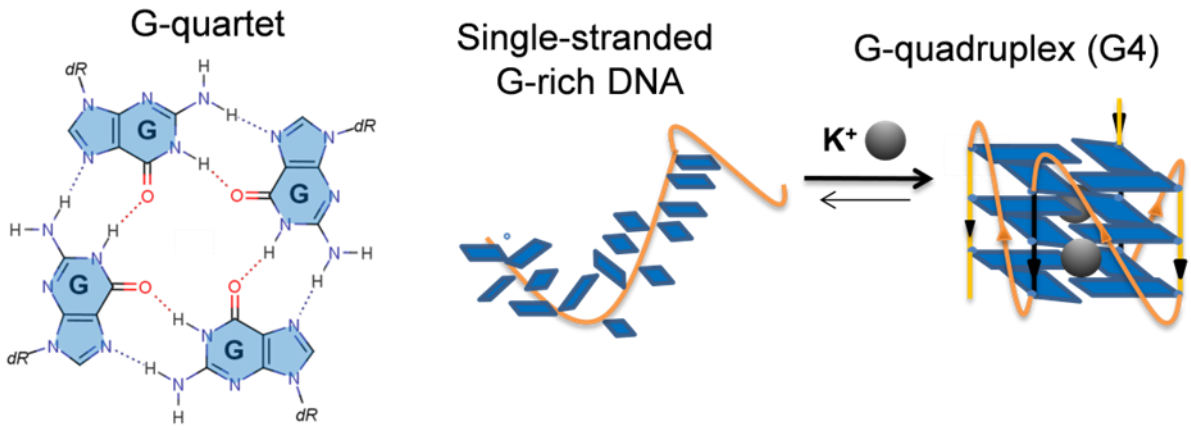

Figure 1. Replication stress at telomeres, one ended double stranded break formation from R-loops and G-quadruplexes, the structure of a G-quadruplex, and the resulting ALT associated homologous recombination.

CHAPTER 2:0: MATERIALS AND METHODS

Cell lines and cell culture conditions

All cell lines were obtained from ATCC with the exception of HeLa LT which was a kind gift from Roderick O'Sullivan. All cells were cultured in standard Dulbecco's Modified Eagle's Medium (DMEM) media supplemented with 10% foetal calf serum, 1% L-glutamine and 1% PenStrep (Gibco). U-2 OSATRX cells were cultured in the presence of 0.4 µg/mL puromycin and 175 µg/mL neomycin. Ectopic ATRX expression was driven through the addition of 0.4 µg/mL doxycycline.

CRISPR-Cas9 KO

CRISPR-Cas9 KO of ATRX was performed using a modified pSpCas9(bb)-2A-GFP tagged Cas9 vector containing sgRNAs targeting exon 16 of ATRX (sgRNA sequence - TOP: 5' caccGTCCAATAACAACCA^AGT 3', BOTTOM: 5' aaacACT^TGGTTGTTATTGGAC 3') with an expected cut site at lysine 1536. Cells were sorted on a BD FACSAria Fusion cell sorter 24 hours after transfection into single wells and grown into clones. KO was determined by western blotting. DAXX KOs were performed using a commercially available DAXX Cas9 plasmid (Santa Cruz, sc-400686-KO-2) and were FACs sorted based on GFP expression. SETD2 Cas9 KO was performed as described in (Pfister et al., 2015). Transfected cells were selected using 0.4 µg/mL puromycin and then sorted into single wells to obtain clones. Combinatorial KOs were made through sequential KO of genes.

Treatment of Cells with Genotoxic Agents

Cells were treated with these genotoxic agents at the following doses for 48 hours prior to downstream analysis with the ALT assays used in this study: PDS at 5 µM, CPT at 50 nM, APH at 0.2 µM and ETO at 0.5 µM.

siRNA Knockdown

Mus81 siRNA experiments were performed using the commercially available ON-TARGETplus Mus81 siRNA SmartPool (Dharmacon, L-016143-01-0005). Cells were reverse transfected when seeding cells to wells or coverslips using Lipofectamine RNAiMAX, to a final concentration of 5 pmol following the manufacturer's instructions. 48 hours after transfection well were forward transfected again to ensure consistent knockdown. For Mus81 experiments, 72 hours after transfection cells were treated with 5 μM PDS and incubated for a further 24 hours before harvesting.

ImmunoFISH

ImmunoFISH experiments were performed with cells seeded onto 13mm #00 thickness coverslips. Briefly, cells were pre-permeabilised with 0.5% Triton-X100 for 1 minute on ice then fixed in 4% paraformaldehyde for 20 minutes. Fixed coverslips were washed in PBS then permeabilised on ice for 6 minutes with 0.5% Triton-X100. Coverslips were blocked in blocking buffer (2% BSA, 0.1% Tween-20 in PBS) for 1 hour and then incubated with the appropriate primary antibody in blocking buffer. Following primary antibody staining, coverslips were washed in PBST (0.5% Tween-20 in PBS) and stained with an appropriate Alexa fluorophore-conjugated secondary antibody. Following further washing, coverslips were post-fixed with 4% PFA for 20 minutes and then a Cy3-[CCCTTA]5 probe was hybridised onto the coverslip in hybridisation buffer (25% formamide, 2xSSC, 200 ng/μL Salmon sperm, 5x Denhardts solution, 50 mM phosphase buffer, 1mM EDTA in water) overnight at 37°C in a humidified chamber. In instances where denatured telomere signals were required, coverslips were incubated in 3.5 N HCl for 13 minutes, then immediately washed with ice cold PBS prior to hybridisation with telomere probes. For analysis of single stranded telomeric DNA the denaturation step was omitted. Coverslips were then washed in 2x SSC before being mounted in VectaShield containing DAPI. Coverslips were then visualised using a DeltaVision widefield microscope. Quantitation was performed using CellProfiler, first all foci in each channel are detected, then any foci overlapping in the respective channels are recorded, additionally foci intensity is also measured.

C-circle Assay

DNA was extracted from approximately 1x106 cells using the QIAGEN Core B kit. Extracted DNA was resuspended in 20 mM Tris-HCl. DNA was quantified and then 30 ng of genomic DNA was amplified in a PCR reaction containing φ29 polymerase, 1% Tween-20, 200 µg/mL BSA and dTTP, dGTP, and dATP, but lacking dCTP for 8 hours at 30°C followed by 20 minutes at 65°C. PCR reactions were run with and without φ29 polymerase to ensure the signal was specific for rolling-circle amplification products. Amplified samples were then blotted onto Zeta-Probe membrane (Bio-Rad) using a slot blotter.

Following fixing of DNA to the membrane with a UVA Stratalinker 2400, membranes were soaked in PerfectHyb Plus (Sigma Aldrich) for 20 minutes at room temperature. A 3' Digitonin (DIG) tagged [CCCATT]5 oligonucleotide was then diluted in PerfectHyb to a final concentration of 40 nM in 20mL hybridisation buffer, and was allowed to hybridise with the membrane in a rolling incubator for 2 hours at 37°C. Following hybridisation, membranes were briefly washed twice with wash buffer (0.1M Maleic acid, 3M NaCl; 0.1% Tween 20 adjusted to pH 7.5), before blocking for 30 minutes and probing with a DIG antibody for 30 minutes. Finally, membranes were vigorously washed 3 times with wash buffer before placing into a cassette with CDP-Star solution. Blots were then developed onto Amersham Hyperfilm ECL film. Quantitation was performed using ImageJ.

Terminal Restriction Fragment (TRF) assay

Terminal restriction fragment assays were performed by first extracting genomic DNA as described above with the QIAGEN Core B kit. Extracted DNA was quantified and at least 2 µg of genomic DNA was digested overnight at 37°C with HinfI and RsaI restriction endonucleases. Following digestion, samples were run on 0.8% agarose gels in 1x TAE at 60 V overnight. Gels were denatured using 1M NaOH and then neutralised and blotted onto Zeta-Probe membrane by upward capillary transfer. Blots were then probed with a DIG-tagged telomere probe as described above. The blots were analysed and quantified using TeloMetric software [(Grant et al., 2001)

Monochrome multiplex qPCR (mm-qPCR)

MM-qPCR was carried out as described in (Cawthon, 2009) with some alterations. Genomic DNA samples were diluted to 5 ng/µL. Primer sets are listed in key resources table. Five concentrations of reference genomic DNA purified from HeLa LT were prepared by 3-fold serial dilution (from 150 ng to 1.85 ng) to generate standard curves for relative quantitation of T/S ratios. For each sample, 20 ng of genomic DNA was mixed with 0.75× PowerUp SYBR Green Master Mix (Thermo Scientific), the primers (300 nM), and water to a final volume of 20 µL per well and analysed using a Thermo Fisher QuantStudio 3 qPCR machine with the following cycle conditions: denaturation for 15 min at 95 °C, followed by two cycles of 15 s at 94 °C/15 s at 49 °C and 32 cycles of 15 s at 94 °C/10 s at 62 °C/15 s at 74 °C with signal acquisition and 10 s at 84 °C/15 s at 88 °C with signal acquisition. Samples were run in triplicate, and analysis was repeated six times using independent runs.

Cohesion FISH

Cohesion FISH was performed using commercially available FISH probe set from Cytocell designed to detect DLEU7 deletion (Cytocell, LPH-043-S) following the manufacturers protocol. Coverslips were then visualised using a DeltaVision widefield microscope.

S9.6 DNA-RNA Immunoprecipitation (DRIP)

R-loop DRIP experiments were performed using the S9.6 antibody as described in (Nguyen et al., 2017a). Eluted DNA was analysed by slot blotting and probing using a DIG-tagged telomere probe as described above.

CellTiterGlo Assay

HeLa-LT cells were seeded on opaque 96-well plate at 100-500 cells in 100 µl of culture media per well. After 6-24 hours, an equal volume of the drug-containing media was added at the desired final concentrations. HU and APH treatment was performed for 72 hours and PDS treatment was performed for 7 days. The cell proliferation was

assessed using CellTiter-Glo 2.0 Reagent (ProMega) according to the manufacturer's instructions. Briefly, the plate and the reagent were equilibrated at room temperature for 5 minutes, the media was removed from the plate, and 100 µl of the diluted reagent (1:5 in PBS) was added to each well. After 10 minutes, the plate was read via the ProMega GloMax Luminometer to assess the quantity of metabolically active cells. The IC50 values were derived by fitting the dose-response data into the curves via GraphPad Prism v8.0.

Triptolide Treatment and Cell Cycle Analysis by PI Staining

ATRX/SETD2 double KO cells were treated with increasing doses of the transcription inhibitor triptolide (25 nM, 50 nM and 100 nM) for 24 hours. gDNA was then extracted and the C-circle assay was performed as described above. To ensure cells were still progressing through the cell cycle, PI staining was utilised. Briefly, cells were harvested, washed in 1x PBS and fixed in 70% ethanol on ice for 30 minutes. Cells were washed again in PBS, treated with 100 µg/ml RNase A and then incubated with 50 µg/ml propidium iodide solution for 10 minutes at room temperature. Samples were then analysed by flow cytometry to estimate the percentage of cells in G1, S and G2 phases of the cell cycle.

RNase H Overexpression

Lentivirus-based constructs for overexpression of wildtype RNase H and the catalytically dead D210N mutant in HeLa cells were generated using InFusion cloning to insert the NLS-RNaseH-V5 sequences from plasmids ppCAG_RNaseH1_WT (Addgene #111906) and ppCAG_RNaseH1_D210N (Addgene #111904) into the pLeGO-C2 backbone (Addgene #27339). The ATRX/SETD2 double KO cells were transduced with the lentivirus and left for 14 days before DNA was harvested and C-circle analysis was carried out as described above. Efficient overexpression was assessed by Western blot.

Quantification and statistical analysis

Each experiment was repeated at least twice, with representative results shown. Statistical analysis was done using GraphPad Prism 9 (GraphPad Software Inc.). Unpaired t tests were used to compare two groups. One-way ANOVA was used to compare more than two groups. Sample sizes and p-values are shown in the figure legends. In all cases ns indicates $p > 0.05$.

CHAPTER 3.0: RESULTS

3.1: Loss of ATRX does not confer activation of the ALT pathway in telomerase positive cell lines

Figure 2A

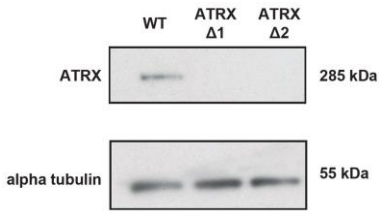

Figure 2B

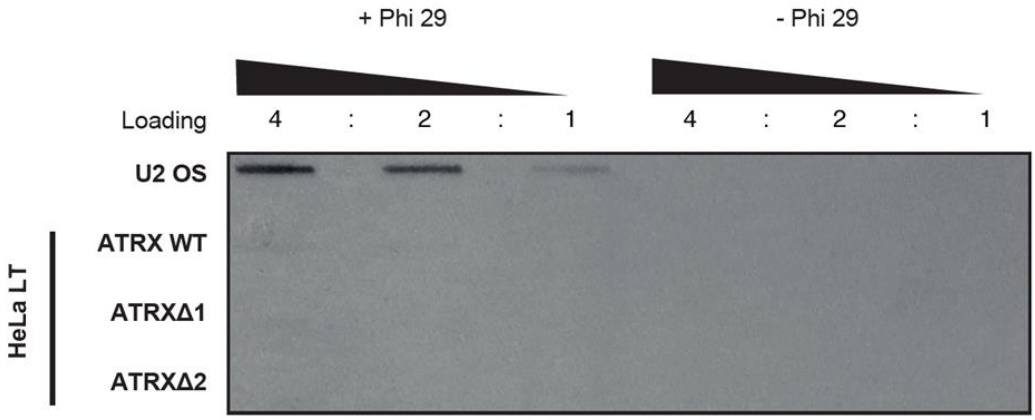

Figure 2C

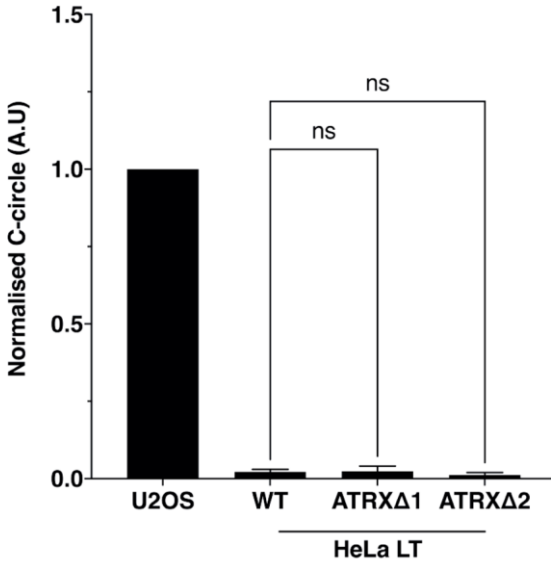

Figure 2D

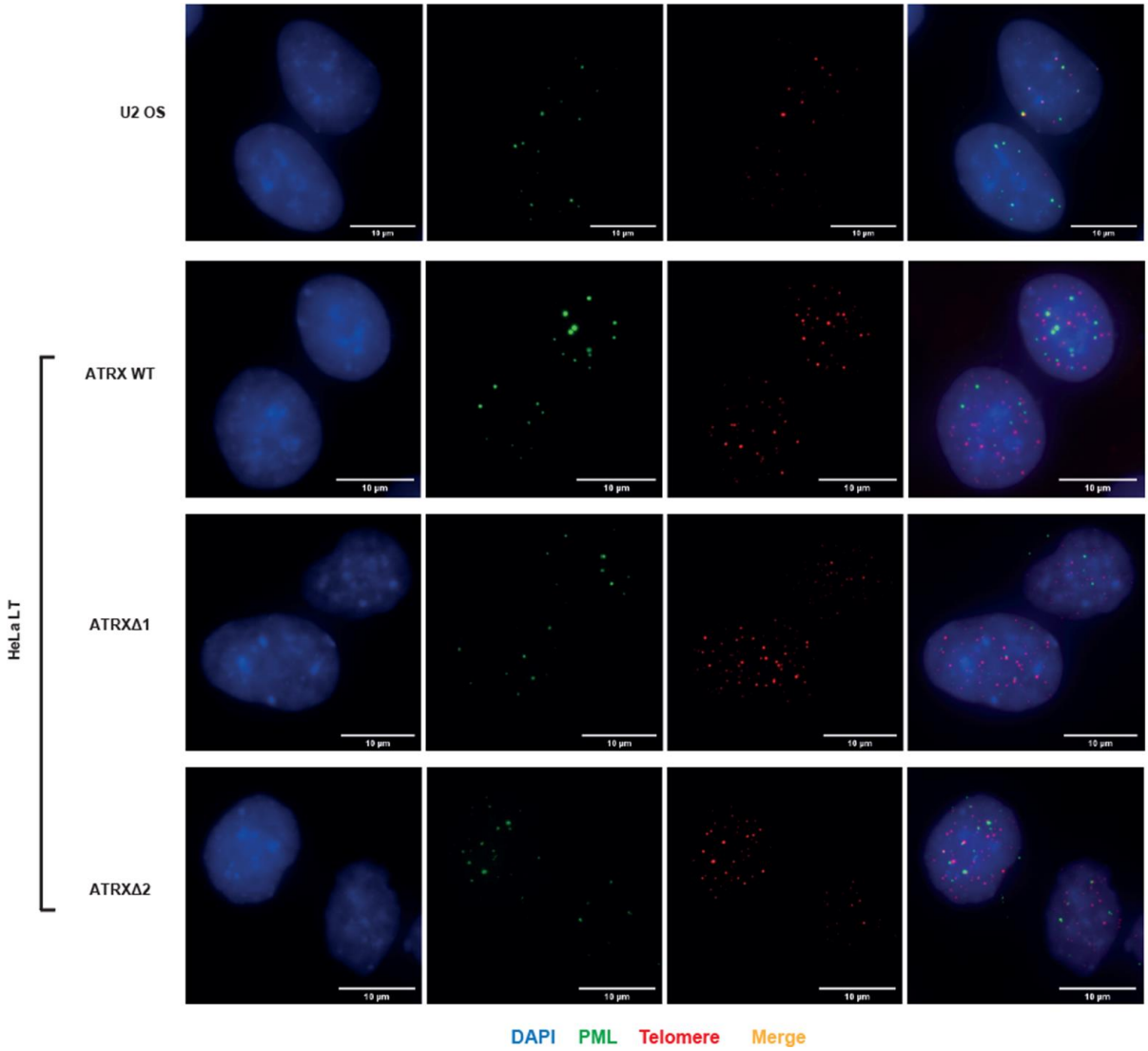

Figure 2E

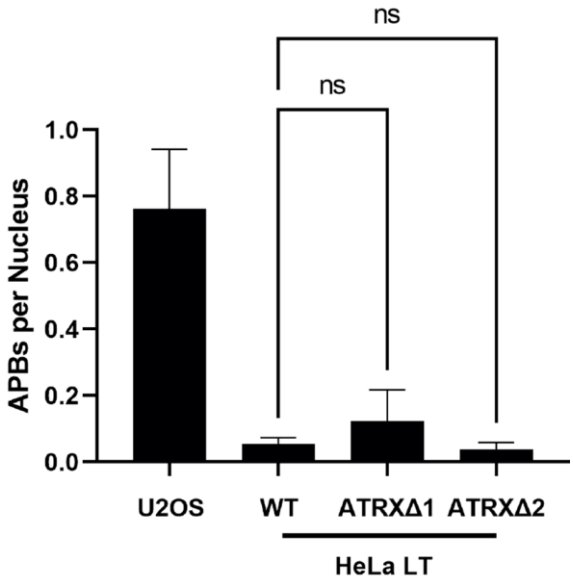

Figure 2F

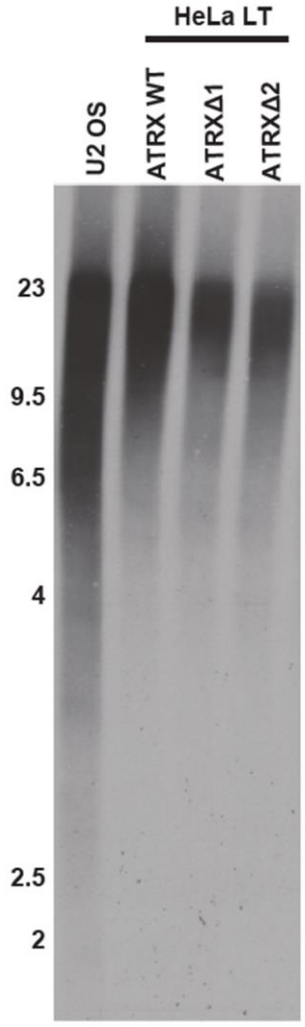

Figure 2G

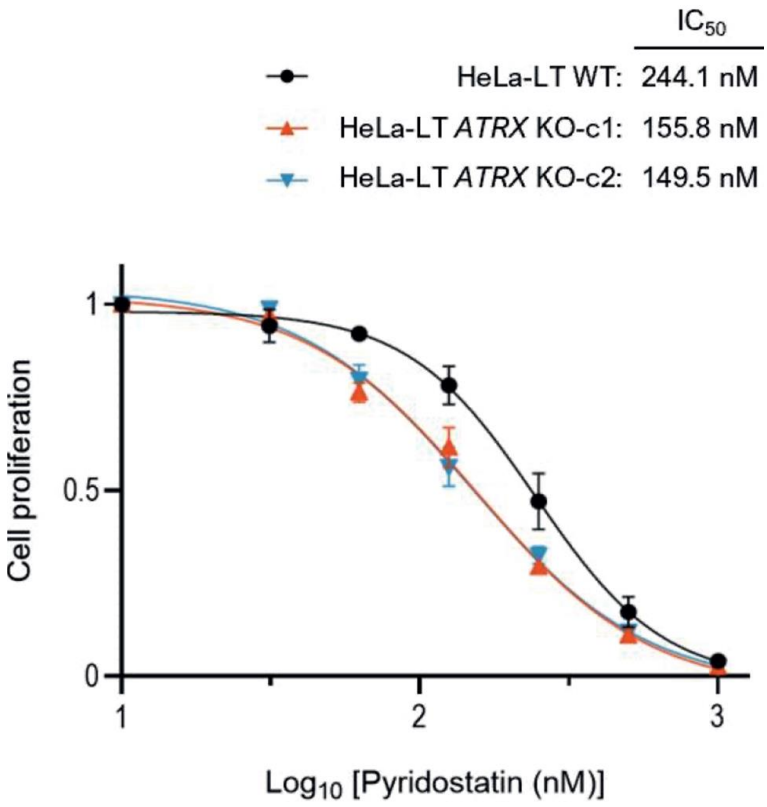

Figure 2H

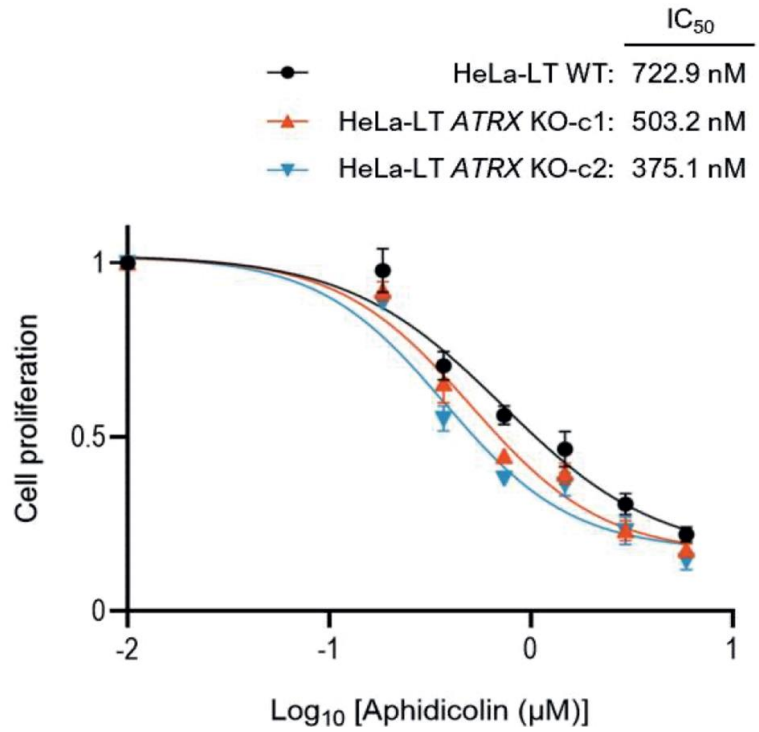

Figure 2I

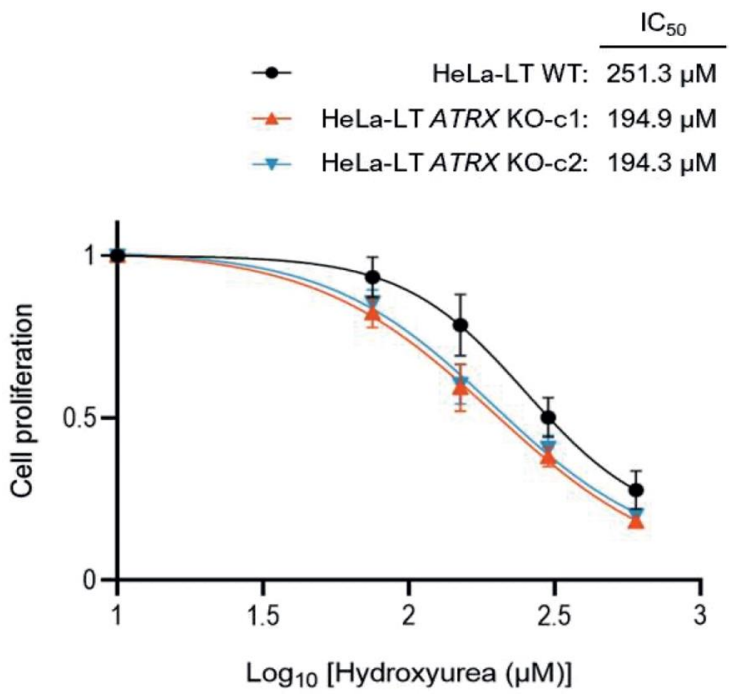

Figure 2. Loss of ATRX alone is insufficient to trigger the ALT pathway. A) Immunoblot confirming CRISPR-Cas9 mediated KO of ATRX in two independent clones of HeLa LT (performed by Siobhan Cunniffe). B-C) C-circle blot and quantification showing that deletion of ATRX in the HeLa LT cell line is insufficient to trigger the accumulation of C-circles, n=3. – Phi 29 is a negative control performed without the addition of the phi29 polymerase. U-2 OS is included as an ALT-positive positive control. D-E) ImmunoFISH detection of APBs both in the presence and absence of ATRX, showing no induction of APB formation upon ATRX loss, >200 nuclei analysed across 3 biological replicates. F) Terminal Restriction Fragment (TRF) analysis of telomere length showing no overt changes in telomere length or heterogeneity upon ATRX deletion (performed by Tomas Goncalves). G-I) Cell proliferation curves in HeLa wild type and two ATRX KO clones with addition of pyridostatin, aphidicolin and

hydroxyurea respectively across 3 biological replicates (performed by Sangwoo Kim). In all panels, ns signifies p > 0.05, determined by one-way ANOVA.

Prior to these experiments, reports show that depletion or knock out of ATRX in telomerase positive or primary cell lines is unable to induce markers of the ALT pathway (Clynes et al., 2014; Eid et al., 2015; Lovejoy et al., 2012; Napier et al., 2015), with the notable exception of some of the glioma cell lines in one study (Brosnan-Cashman et al., 2018). One can therefore assume that the loss of ATRX, while generally a requisite for ALT pathway induction and/or maintenance, must occur in concert with other genomic events within cancer cells that cumulatively lead to telomere lengthening via ALT. This was considered a good place to start for further exploration.

The HeLa long telomere cell line (referred to as HeLa LT throughout) is a subclone of HeLa with long telomeres (~20 kb) which has previously shown to be amenable to ALT induction through depletion of ASF1 (O'Sullivan et al., 2014a). Consistent with previous reports, two independent ATRX CRISPR-Cas9 KO HeLa LT clones (Figure 2A) conferred sensitivity to a variety of genotoxic agents known to induce replicative stress, including the G4 stabilising ligand pyridostatin (PDS), aphidicolin (APH) and hydroxyurea (HU) (Figures 2G-I). Despite these conferred synthetic lethal interactions, neither of the KO clones elicited an increase in cardinal ALT markers, including C-circles (Figures 2B and 2C), ALT-associated PML nuclear bodies (APBs) (Figures 2D and 2E) or telomere length heterogeneity (Figure 2F).

3.2: Treatment with the G-quadruplex stabilising ligand PDS confers activation of the ALT pathway in the absence of ATRX

Figure 3A

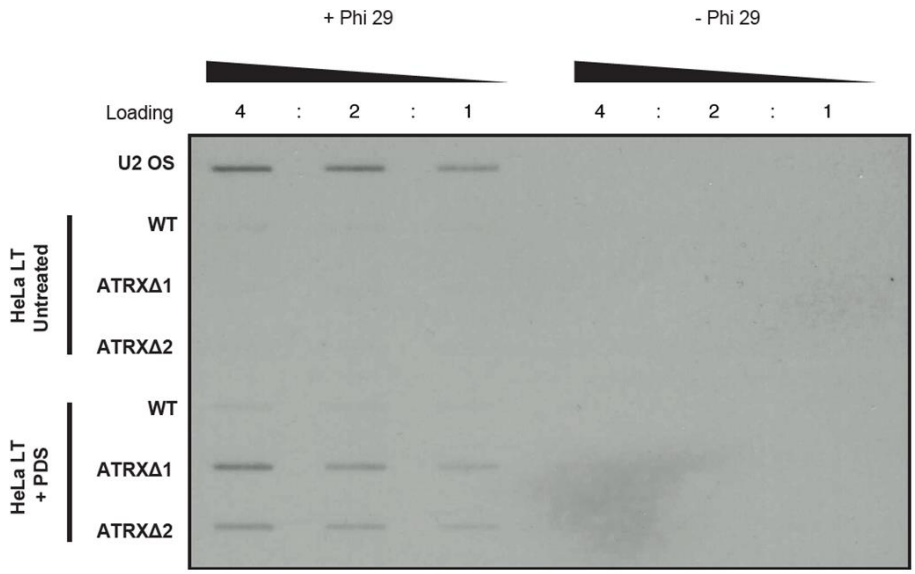

Figure 3B

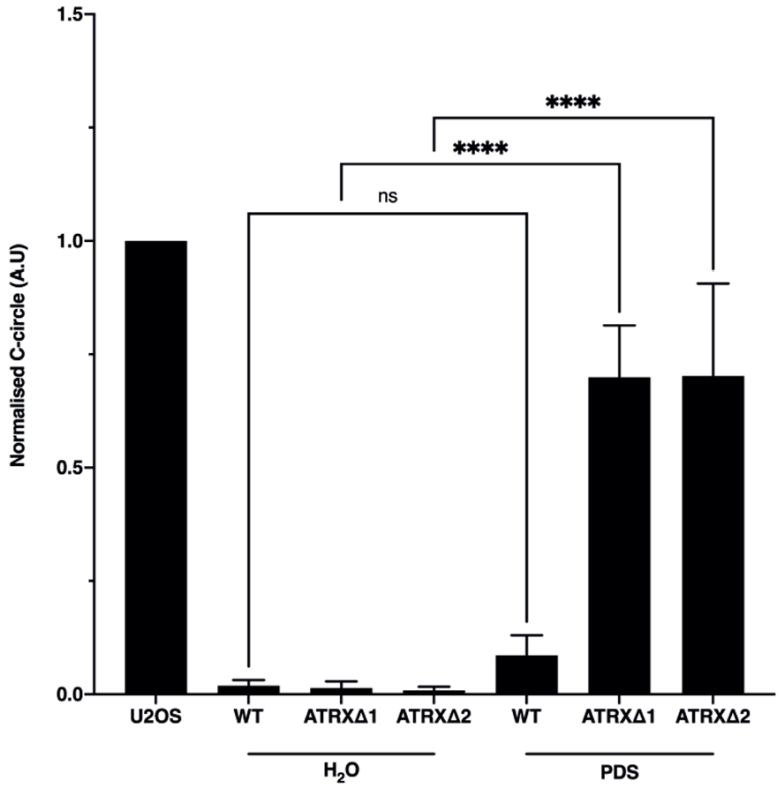

Figure 3C

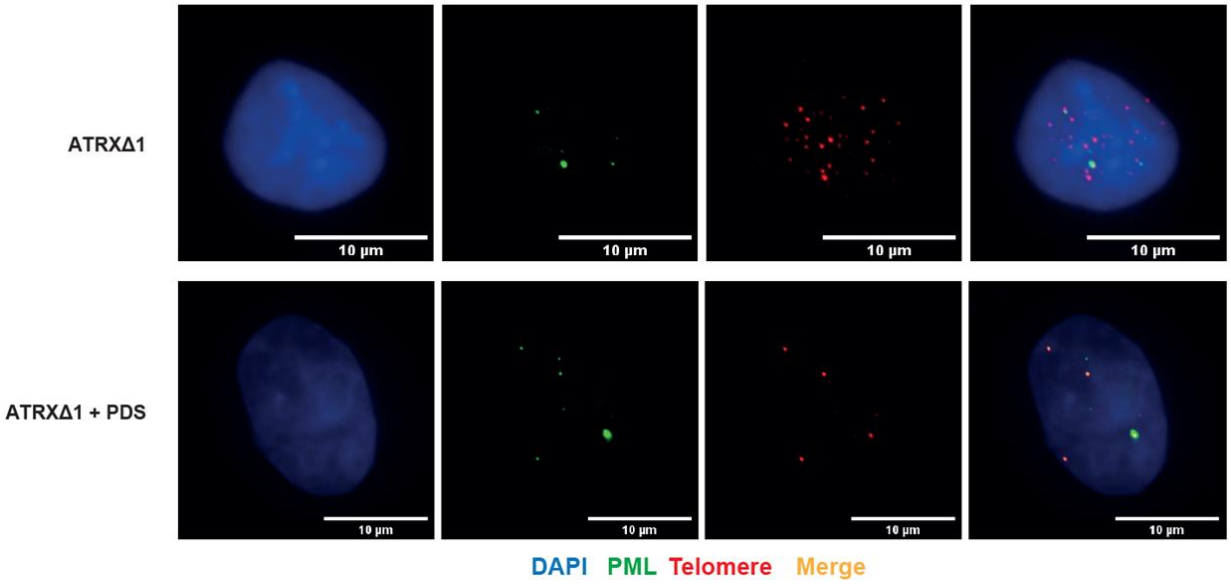

Figure 3D

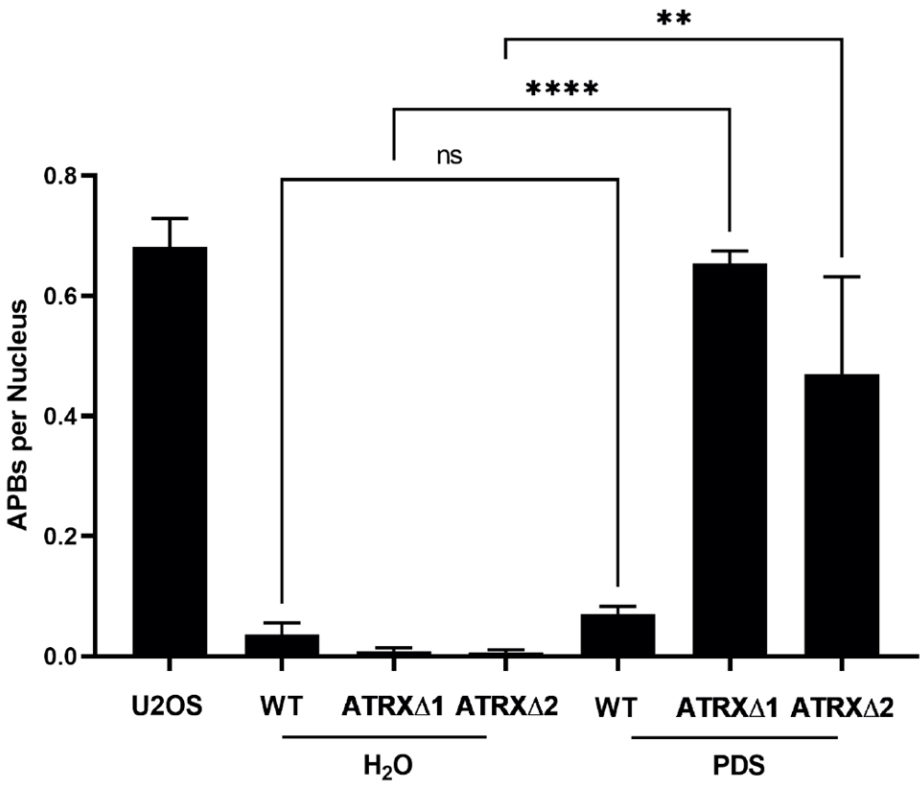

Figure 3E

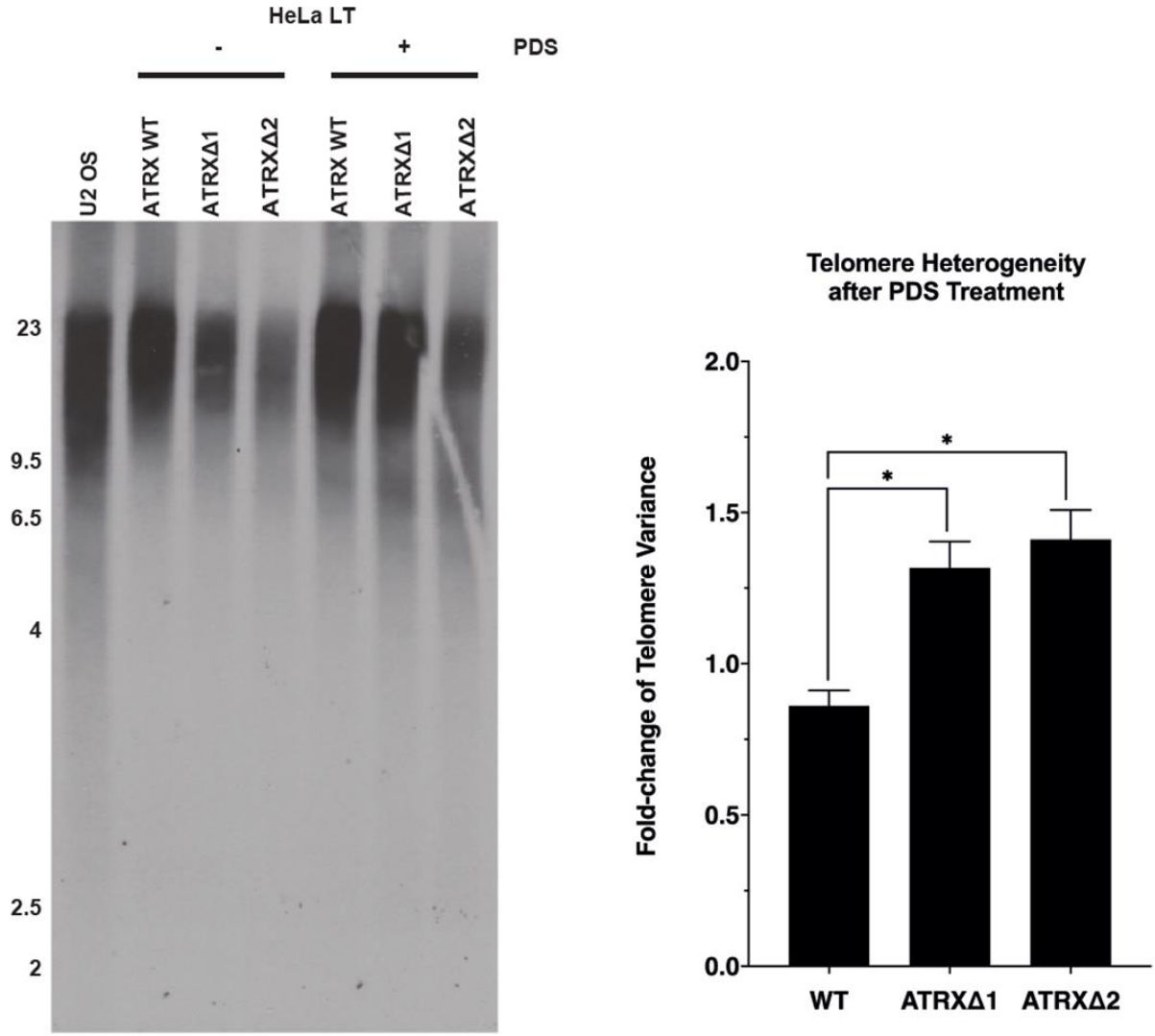

Figure 3F

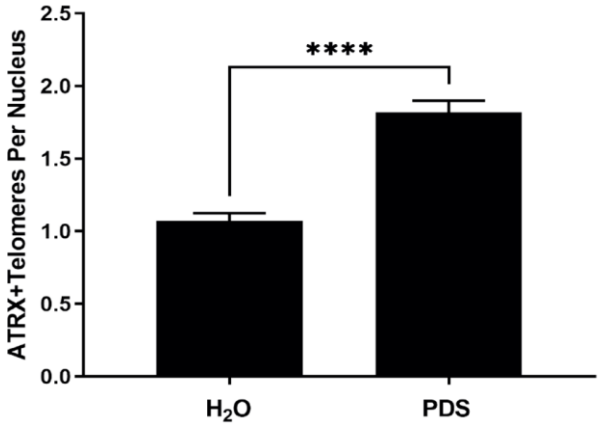

Figure 3G

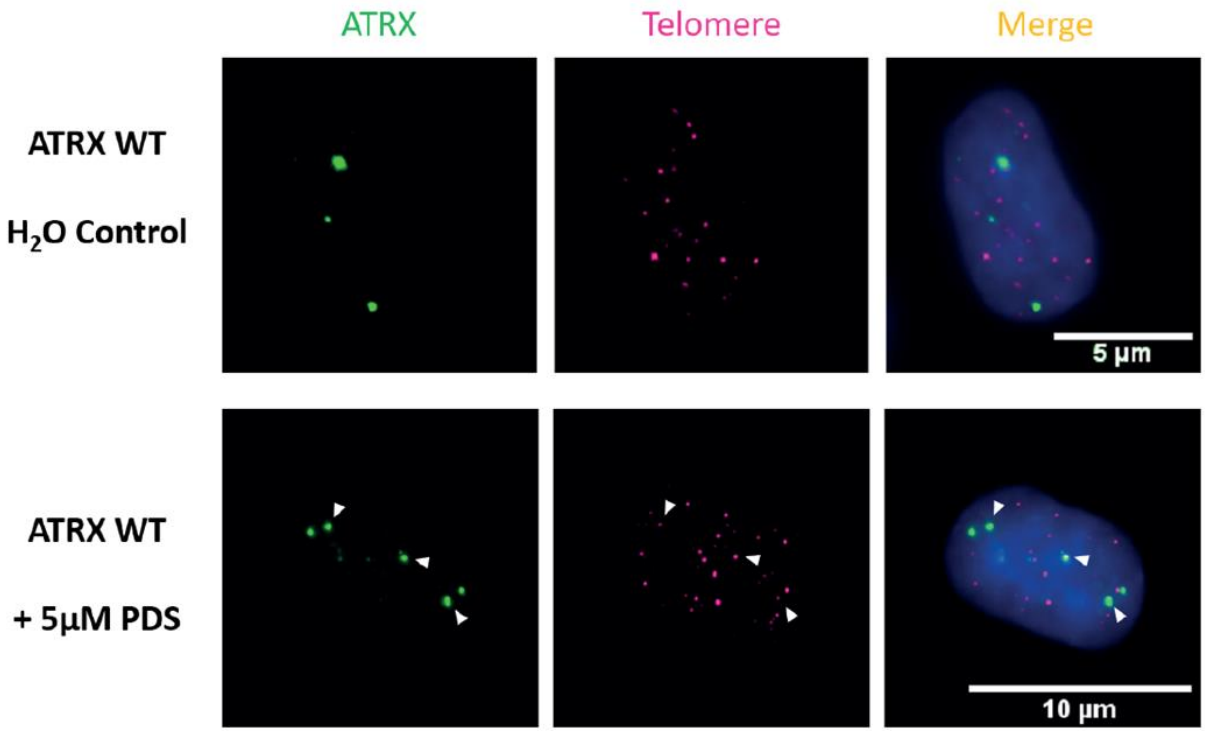

Figure 3H

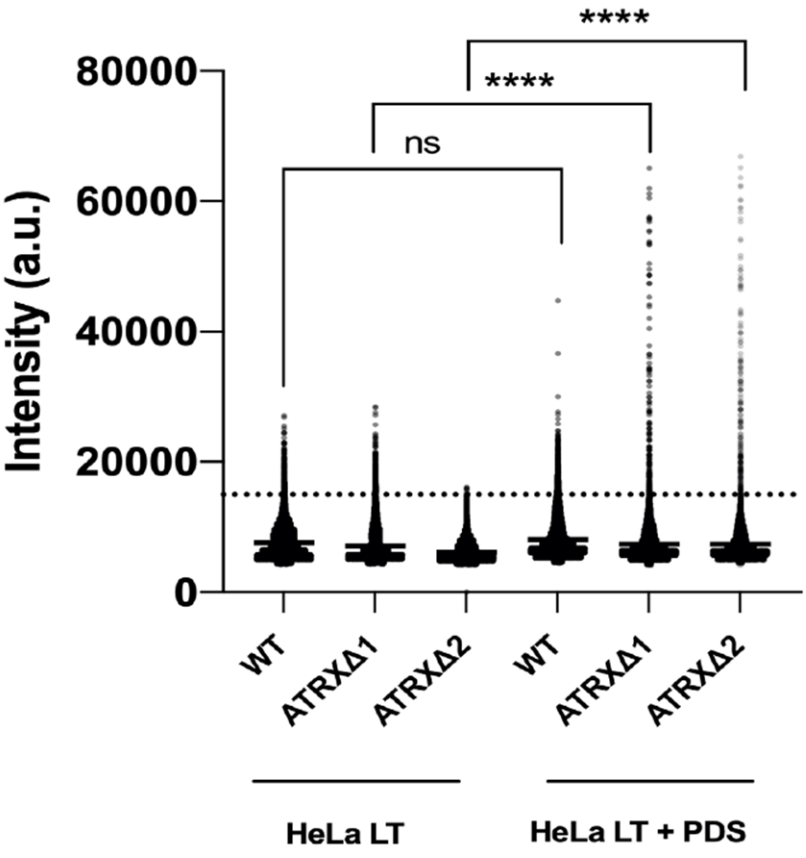

*Figure 3. Treatment with PDS in combination with ATRX loss triggers ALT markers. A-B) C-circle blot and quantification showing C-circle accumulation specifically in ATRX KO clones following 48 hrs treatment with 5μM PDS, n=3. ****p < 0.0001 determined by one-way ANOVA (performed with Tomas Goncalves). C-D) Representative images and quantification of APB induction in HeLa LT ATRX KO clones upon 48 hrs treatment with 5μM PDS, >200 nuclei analysed across 3 biological replicates. **p < 0.001, ****p < 0.0001, determined by one-way ANOVA. E) TRF analysis showing treatment with 5μM PDS for 48 hrs increased telomere length heterogeneity specifically upon depletion of ATRX. Telomere heterogeneity was measured using Telometric software, n=2. *p < 0.05, determined by one-way ANOVA (performed by Tomas Goncalves). F-G) Quantitation and representative images of ATRX and telomere colocalization upon 48 hrs treatment with 5μM PDS, >200 nuclei analysed across 3 biological replicates. ****p < 0.0001, determined by one-way ANOVA (performed by Thomas Kent). H) Telomere intensity indicating telomere clustering and synthesis upon 48 hrs treatment with 5μM PDS, >200 nuclei analysed across 3 biological replicates. ****p < 0.0001, determined by one-way ANOVA.*

A key feature of telomeres is their propensity to adopt non-canonical DNA secondary structures, including the G4 conformation, which has been implicated in both transcriptional dysregulation and DNA damage (Spiegel et al., 2020). ATRX binds widely at sites in the genome predicted to form G4 structures, including telomeres (Law et al., 2010; Wong et al., 2010) and ATRX loss confers sensitivity to various G4 stabilising ligands, including PDS (Figure 2G), suggesting that ATRX protects G4 sites from genome instability (Wang et al., 2018; Watson et al., 2013). In accordance with this, addition of PDS led to an increase in ATRX recruitment to telomeres (Figures 3F

and 3G), suggestive of a putative role for ATRX in protecting telomeric DNA upon the stabilisation of G4s. To explore this possibility further, I treated the two HeLa LT KO clones with PDS and assessed for markers of activation of the ALT pathway. Strikingly, treatment with PDS elicited an increase in many of these cardinal markers, including C-circles (Figures 3A and 3B) and the formation of APBs (Figures 3C and 3D) to levels comparable to the archetypical ALT cell line U-2 OS, whereas no notable increase was observed in the ATRX wildtype cells. Addition of PDS also elicited a decrease in total telomere number and an increase in telomere intensity, consistent with increased telomere clustering and telomere synthesis (Figures 3H). ALT positive cell lines characteristically exhibit long and heterogeneous telomere lengths (Bryan et al., 1995). Consistent with a bona fide induction of the ALT pathway, treatment with PDS led to a characteristic lengthening and spread of telomere lengths in the ATRX KO clones but not in the ATRX wildtype cells (Figure 3E).

3.3: Treatment with the G-quadruplex stabilising ligand PDS confers induction of the replicative stress marker RPA ssTel

Figure 4A

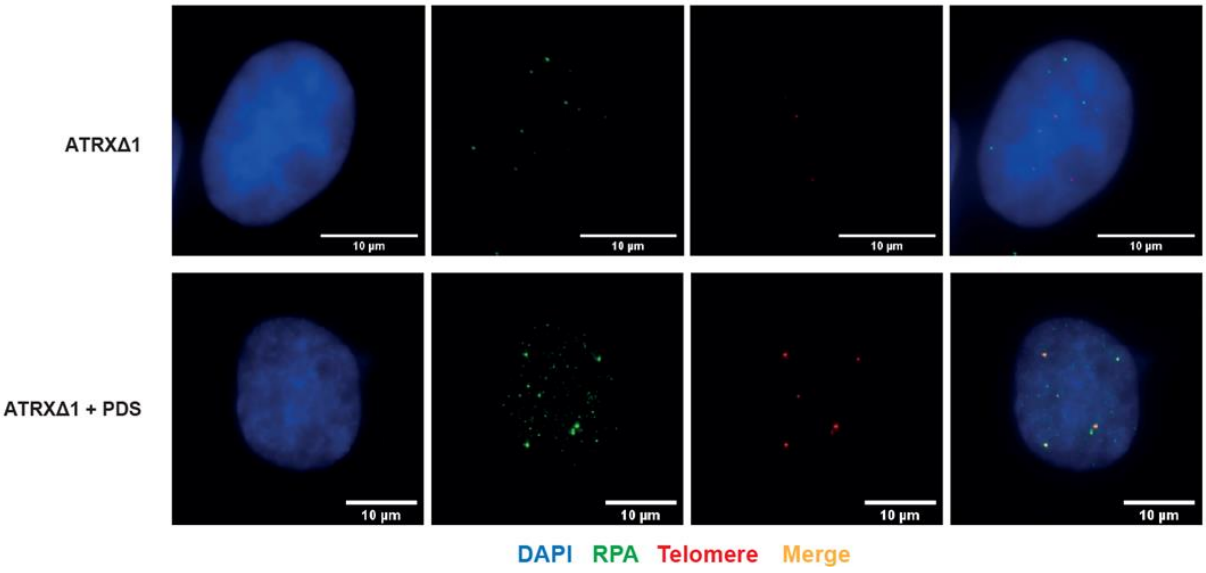

Figure 4B

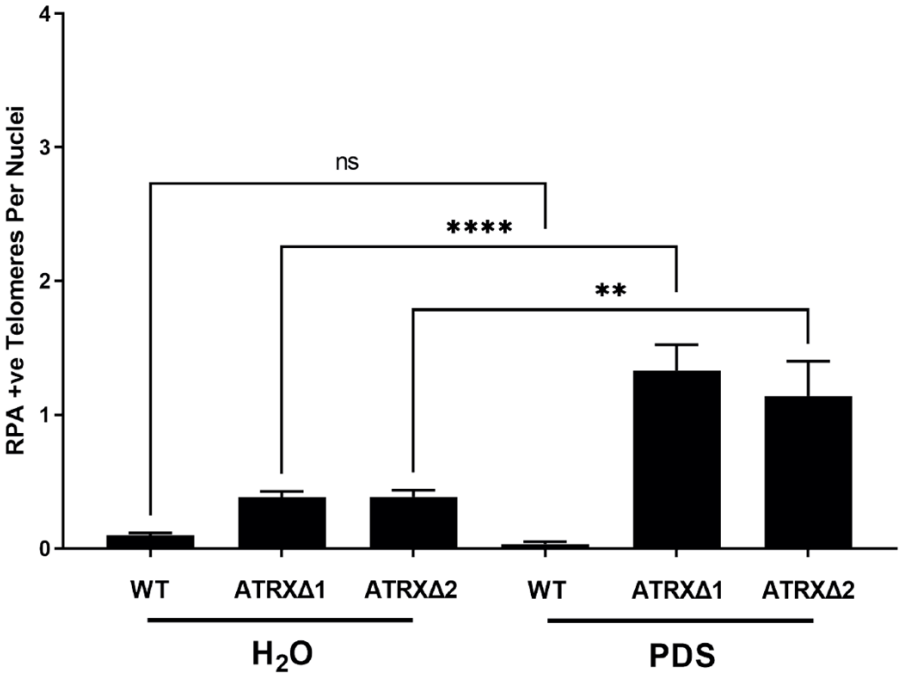

Figure 4C

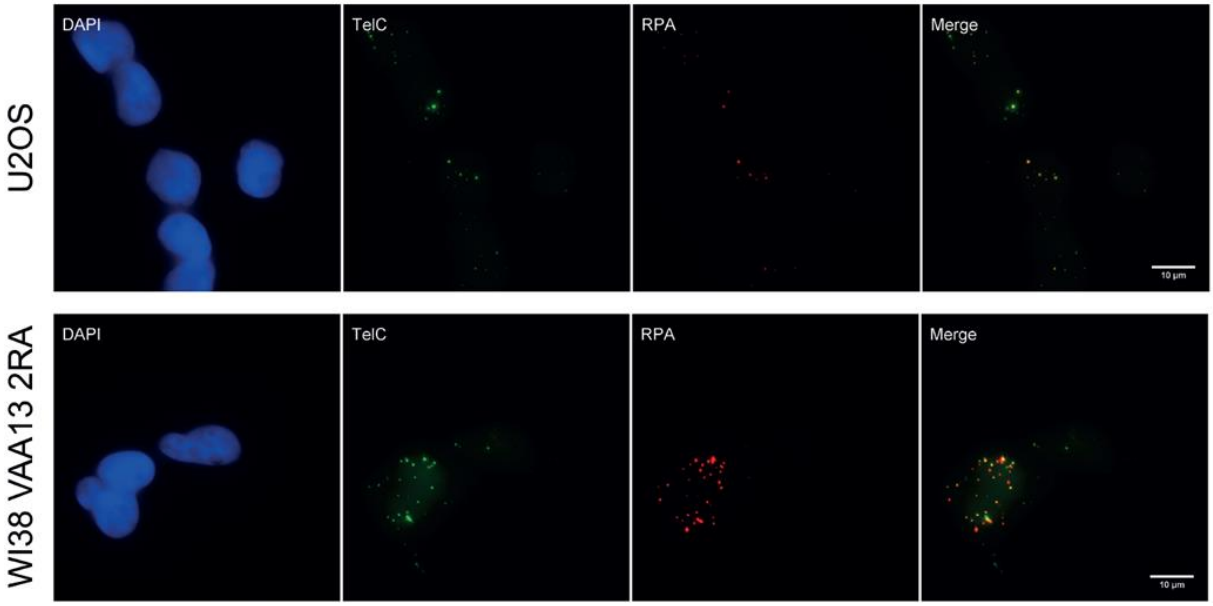

Figure 4D

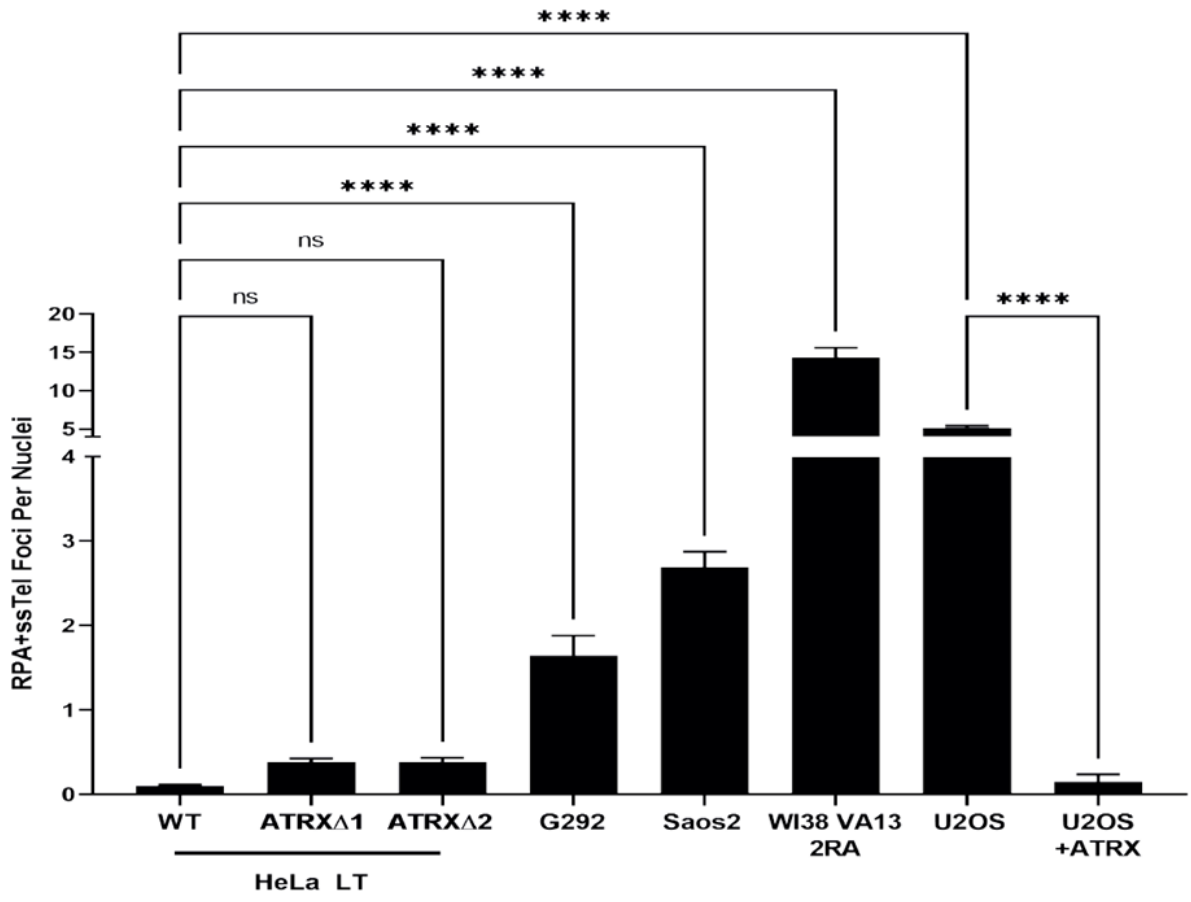

Figure 4E

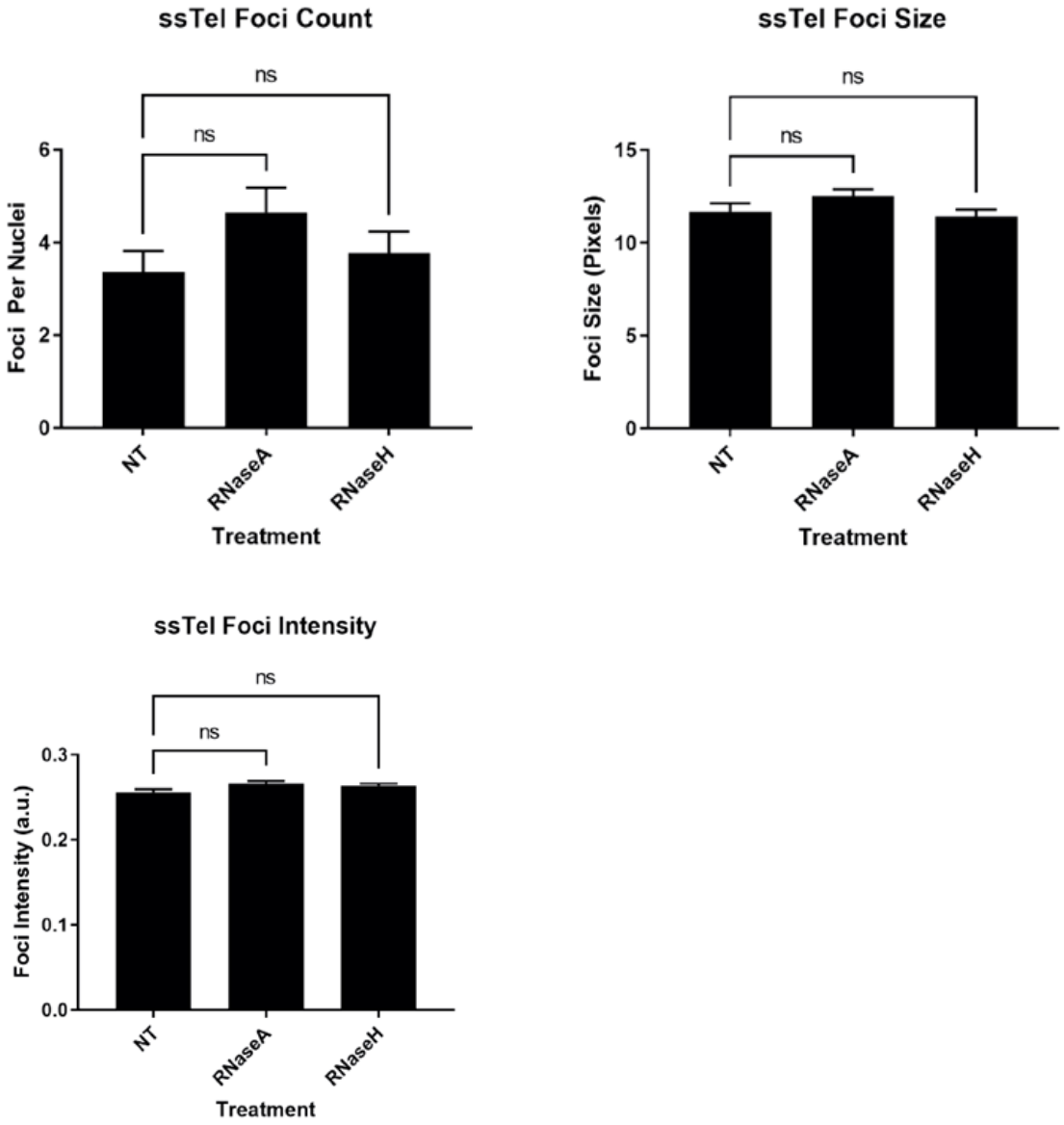
ssTel Foci Count
ns
ns
Foci Per Nuclei
0
2
4
6
NT
RNaseA
RNaseH
Treatment
ssTel Foci Size
ns
ns
Foci Size (Pixels)
0
5
10
15
NT
RNaseA
RNaseH
Treatment
ssTel Foci Intensity
ns
ns
Foci Intensity (a.u.)
0.0
0.1
0.2
0.3
NT
RNaseA
RNaseH
Treatment

Figure 4F

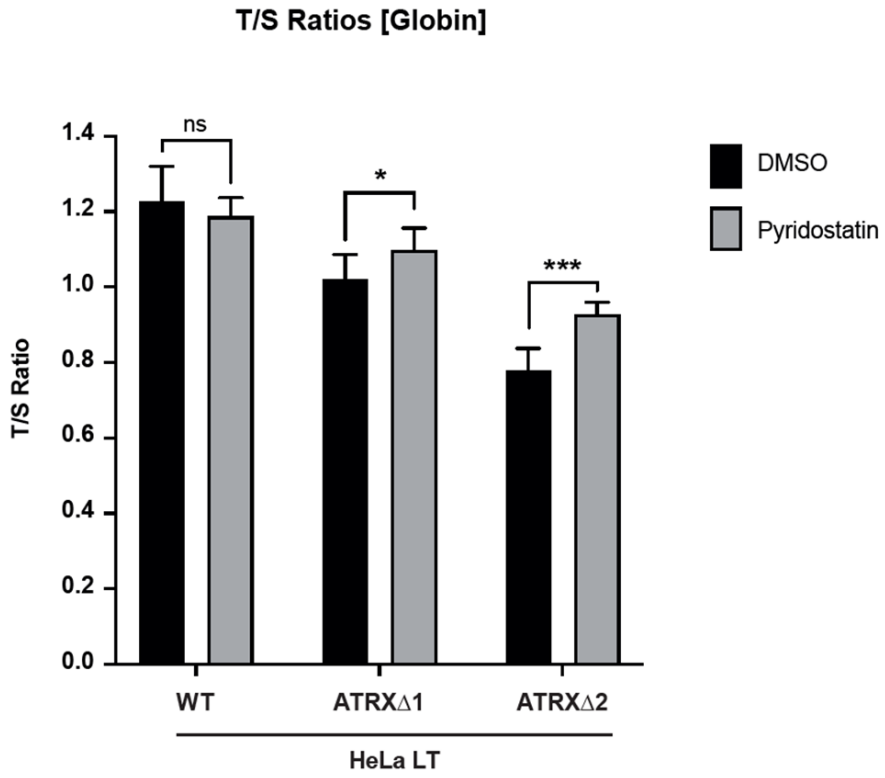

*Figure 4. Treatment with PDS in combination with ATRX loss triggers RPA ssTel. A-B) Representative images and quantification of RPA ssTel in HeLa LT ATRX KO upon treatment with 48 hrs 5μM PDS, >150 nuclei analysed across 3 biological replicates. **p < 0.001, ****p < 0.0001, determined by one-way ANOVA (performed by Thomas Kent). C-D) Representative images and quantification of RPA ssTel across a panel of cell lines. >150 nuclei analysed across 3 biological replicates. ****p < 0.0001, determined by one-way ANOVA (performed by Thomas Kent). E) RNase A and RNase H treatment on U-2 OS to show lack of RNA involvement in the above panel results (performed by Thomas Kent). F) mm-qPCR analysis shows the PDS specific increase in the telomere repeat number normalised to the single copy gene HBB *p < 0.05, ***p < 0.001, determined by one-way ANOVA (performed by Tomas Goncalves).*

ALT has been suggested to be coincident with telomeric replicative stress, with an accumulation of RPA2 at telomeres upon ALT induction (O'Sullivan et al., 2014a) and an increase in single stranded telomeric DNA (ssTel), as detected by non-denaturing telomeric FISH (Loe et al., 2020). Consistent with these findings, an ALT specific co-localisation between RPA and ssTel is clearly detectable across a panel of cell lines (Figures 4C and 4D). This signal was refractory to RNase A and RNase H treatment, confirming that the ssTel signal was detecting telomeric DNA and not TERRA RNA (Figure 4E). Inducible expression of ATRX in ALT positive U-2 OS cells, using the previously characterised U-2 OS^{ATRX} cell line (Clynes et al., 2015b) led to a complete abrogation of RPA ssTel foci, once again confirming RPA/ssTel as a bona-fide ALT marker and suggesting that the signal is a consequence of ATRX loss in ALT cancer cells (Figure 4D). I next asked whether treatment of the Hela LT ATRX KO clones with PDS also induced formation of this novel ALT marker. As expected, addition of PDS significantly increased detectable RPA ssTel foci in both independent ATRX KO clones, with no detectable increase in wildtype ATRX HeLa LT cells (Figures 4A and 4B). I also used monochrome multiplex qPCR (mm-qPCR) analysis to show that the T/S ratio – the telomere repeat number normalised to the single copy gene *HBB* (encoding beta-globin) – significantly increased after PDS treatment in both ATRX KO clones but not in the wildtype cells (Figure 4F), again highly suggestive of a bona fide induction of the ALT pathway and associated telomere synthesis in these cells.

3.4: Induction of ALT in the absence of ATRX upon PDS treatment is dependent on the Mus81 endonuclease

Figure 5A

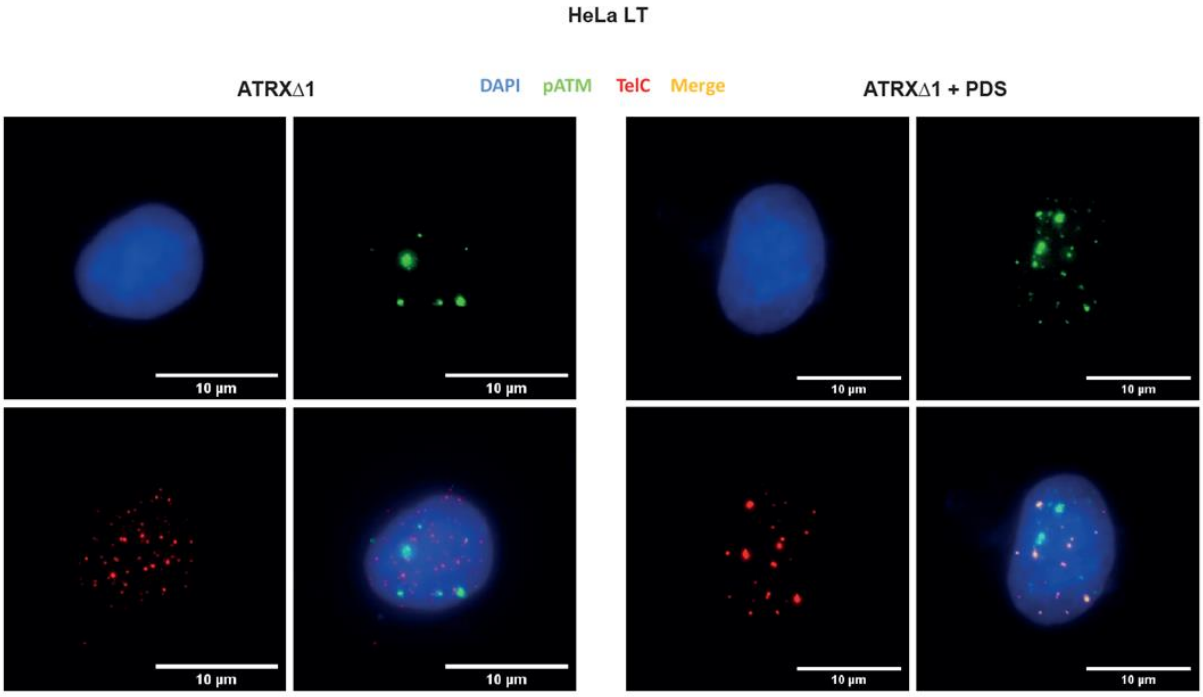

Figure 5B

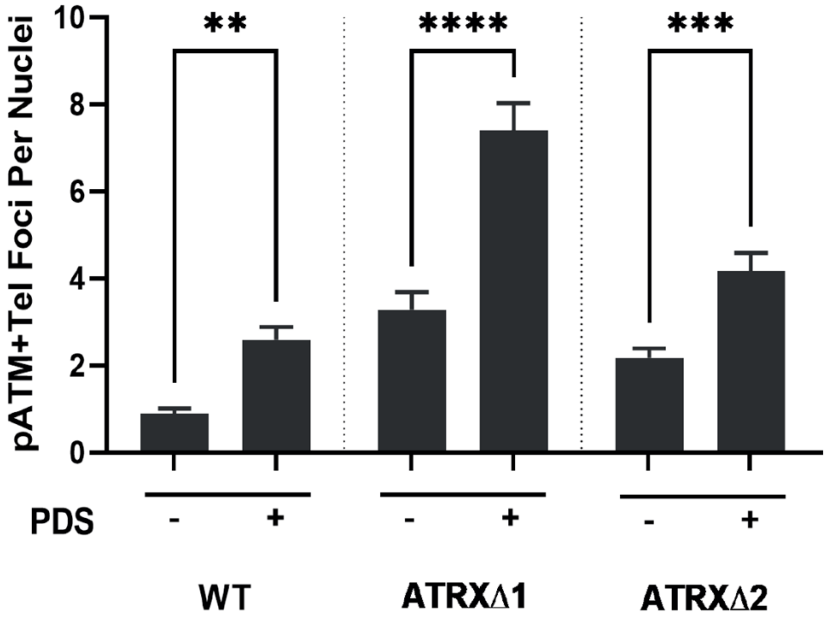

Figure 5C

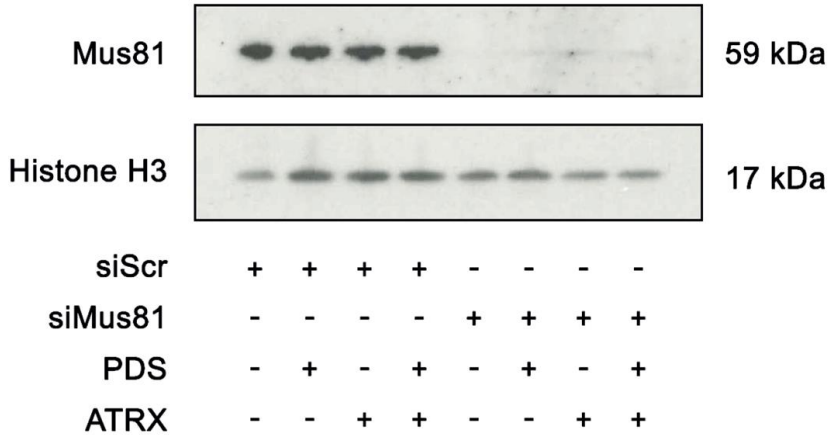

Figure 5D

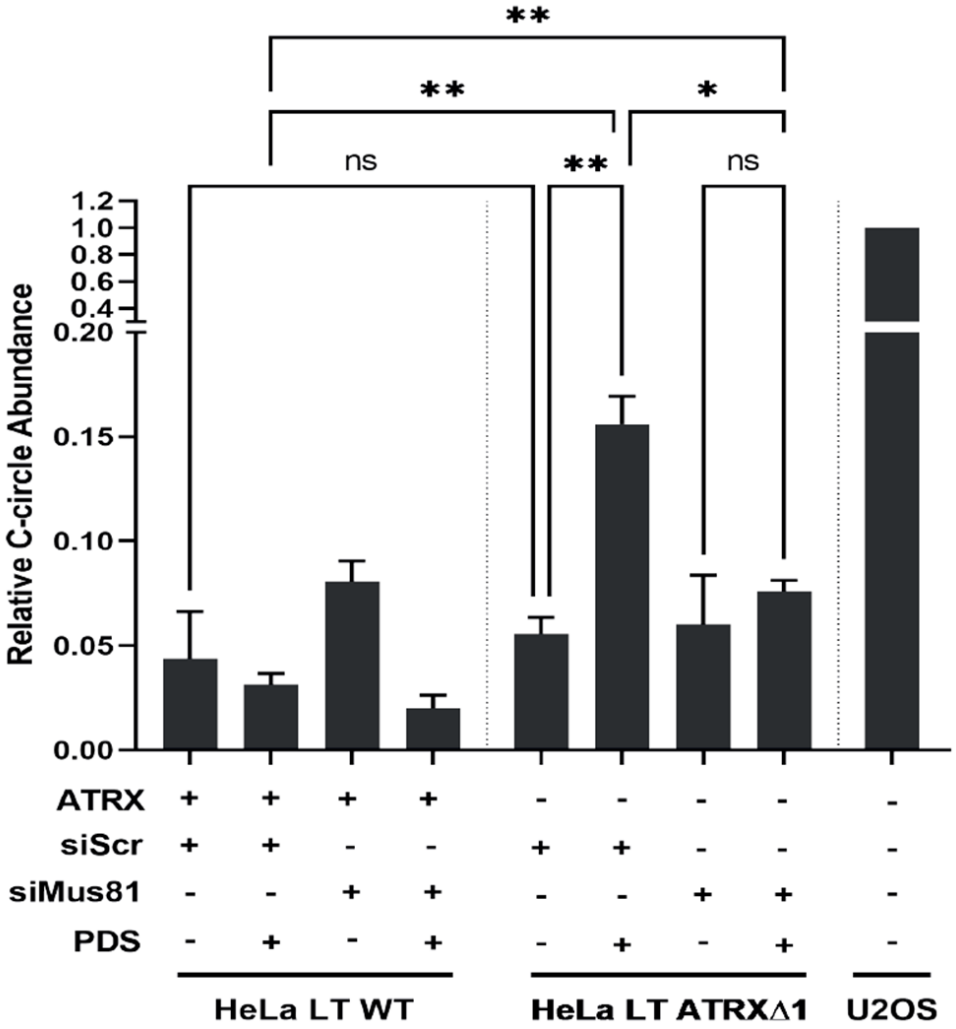

Figure 5E

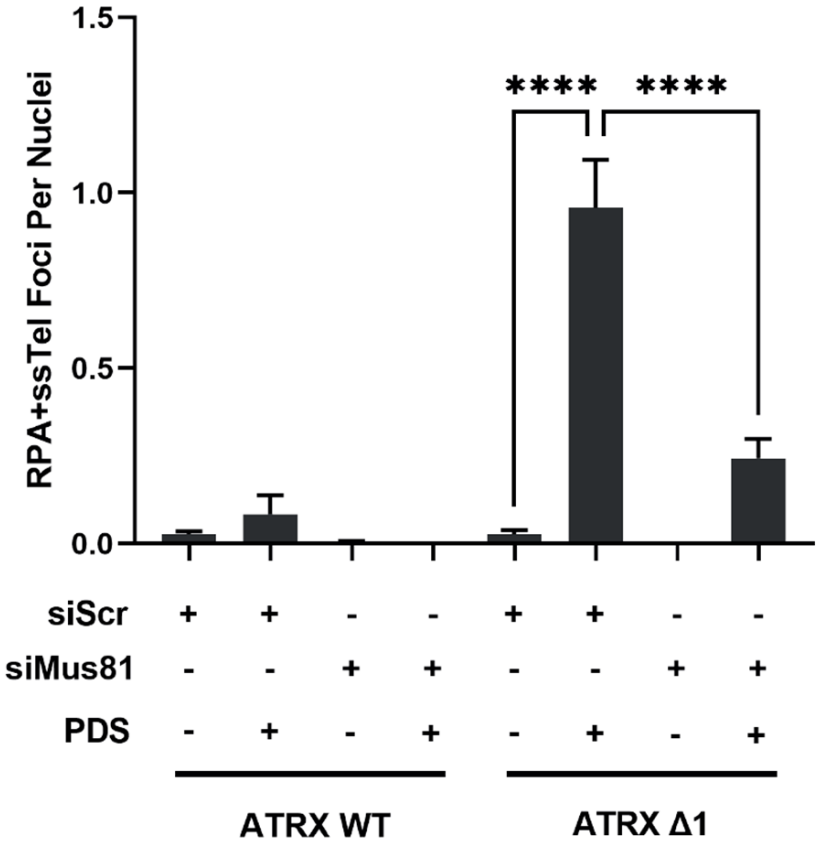
RPA+ssTel Foci Per Nuclei
1.5
1.0
0.5
0.0
****
****
siScr + + - - + + - -
siMus81 - - + + - - + +
PDS - + - + - + - +
ATRX WT
ATRX Δ1

Figure 5F

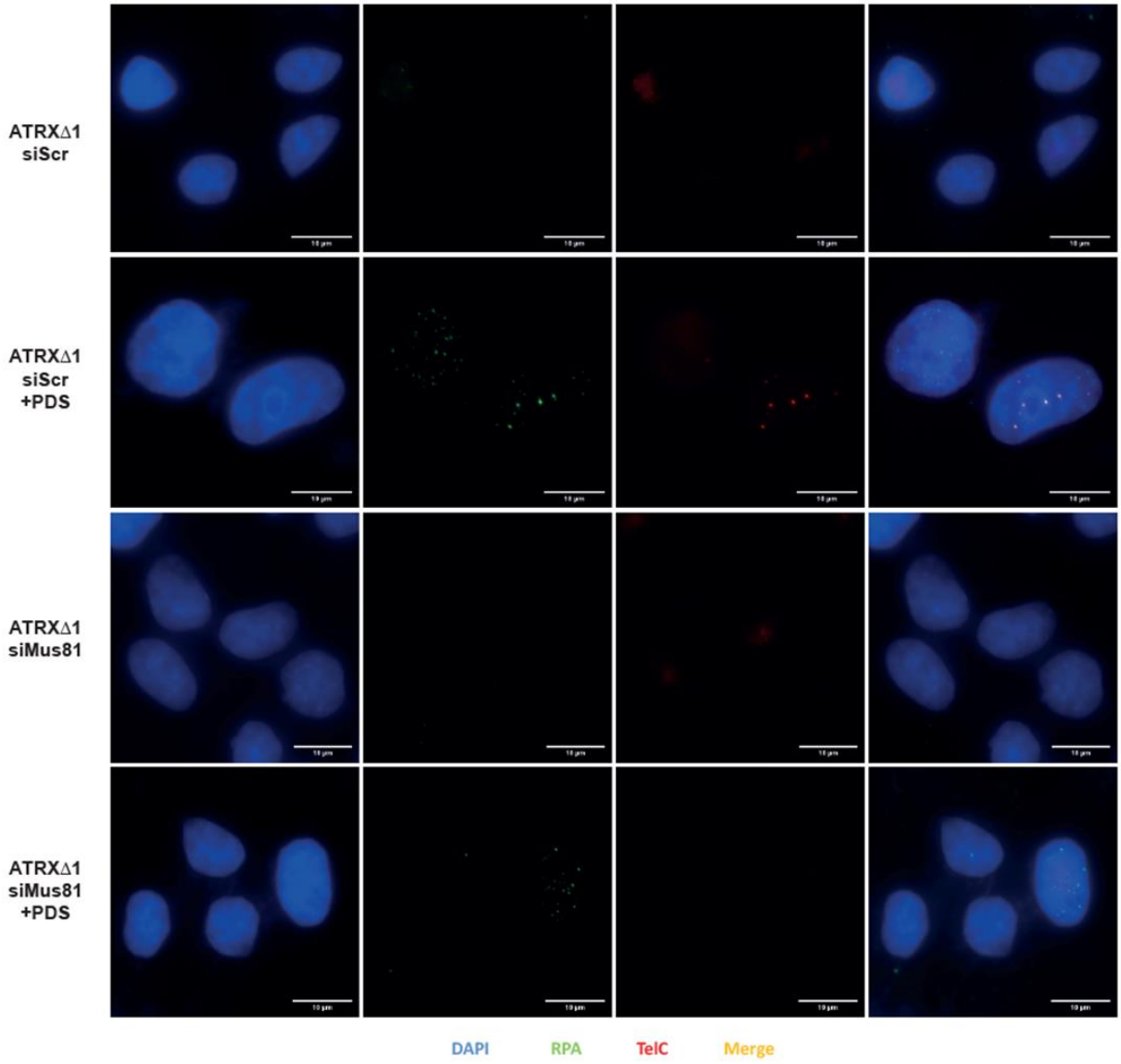

*Figure 5. PDS induced ALT markers require replication fork collapse. A-B) Representative figure and quantification of pATM induction at telomeres upon PDS treatment. >150 nuclei analysed across 3 biological replicates. **p < 0.001, ***p < 0.0001, ****p < 0.0001, determined by one-way ANOVA. C) Immunoblot showing siRNA mediated knockdown of Mus81 in ATRX WT and ATRX KO cells. D) C-circle quantification showing induction of C-circles upon ATRX loss and PDS treatment is dependent on Mus81, n=3. *p < 0.05, **p < 0.001, determined by one-way ANOVA.*

*E-F) Representative images and quantification from ImmunoFISH data showing the induction of RPA ssTel foci upon ATRX loss and PDS treatment is dependent on Mus81, >150 nuclei analysed across 3 biological replicates. ****p < 0.0001, determined by one-way ANOVA. All work in this figure was performed by Thomas Kent.*

It has been hypothesised that ALT emanates from the formation of a DSB within the telomere sequence, likely attributable to the stalling, reversal, and subsequent collapse of replication forks. Consistent with an induction of an ALT like process and fork collapse events, loss of ATRX was associated with a significant increase in telomere-associated ATM, autophosphorylated at serine 1981 (pATM S1981), a marker of ATM activation at DNA DSBs (Bakkenist and Kastan, 2003) (Figures 5A and 5B). The cleavage of stalled forks to generate a DSB is dependent on the activity of the structure-selective endonuclease MUS81-EME2 (Pepe and West, 2014) and, in agreement with a central role for replication fork collapse in the initiation of ALT, MUS81 activity is a requisite for telomere maintenance in ALT cells (Pepe and West, 2014; Zeng et al., 2009). Of note, EME1 and EME2 were not investigated here. I next sought to explore whether the destabilisation and collapse of replication forks was a feature of ALT induction upon the addition of PDS to the ATRX KO cells. Consistent with this requirement, knockdown of Mus81 completely abrogated the increase in C-circles observed in the ATRX KO cells upon PDS treatment (Figures 5C and 5D). Likewise, the depletion of Mus81 was also associated with an attenuation of RPA ssTel foci in the ATRX KO cells (Figures 5E and 5F). Of note, the knockdown of MUS81 did not lead to cell death. Taken together, I conclude that the generation of ALT upon ATRX loss and PDS treatment is likely attributable to an increased

destabilisation and Mus81-dependent processing of replication forks in the absence of ATRX, which in turn generates the DSB substrate for subsequent BIR-mediated lengthening of telomeres.

3.5: Genotoxic agents that cause replicative stress induce markers of ALT in ATRX deficient cells

Figure 6A

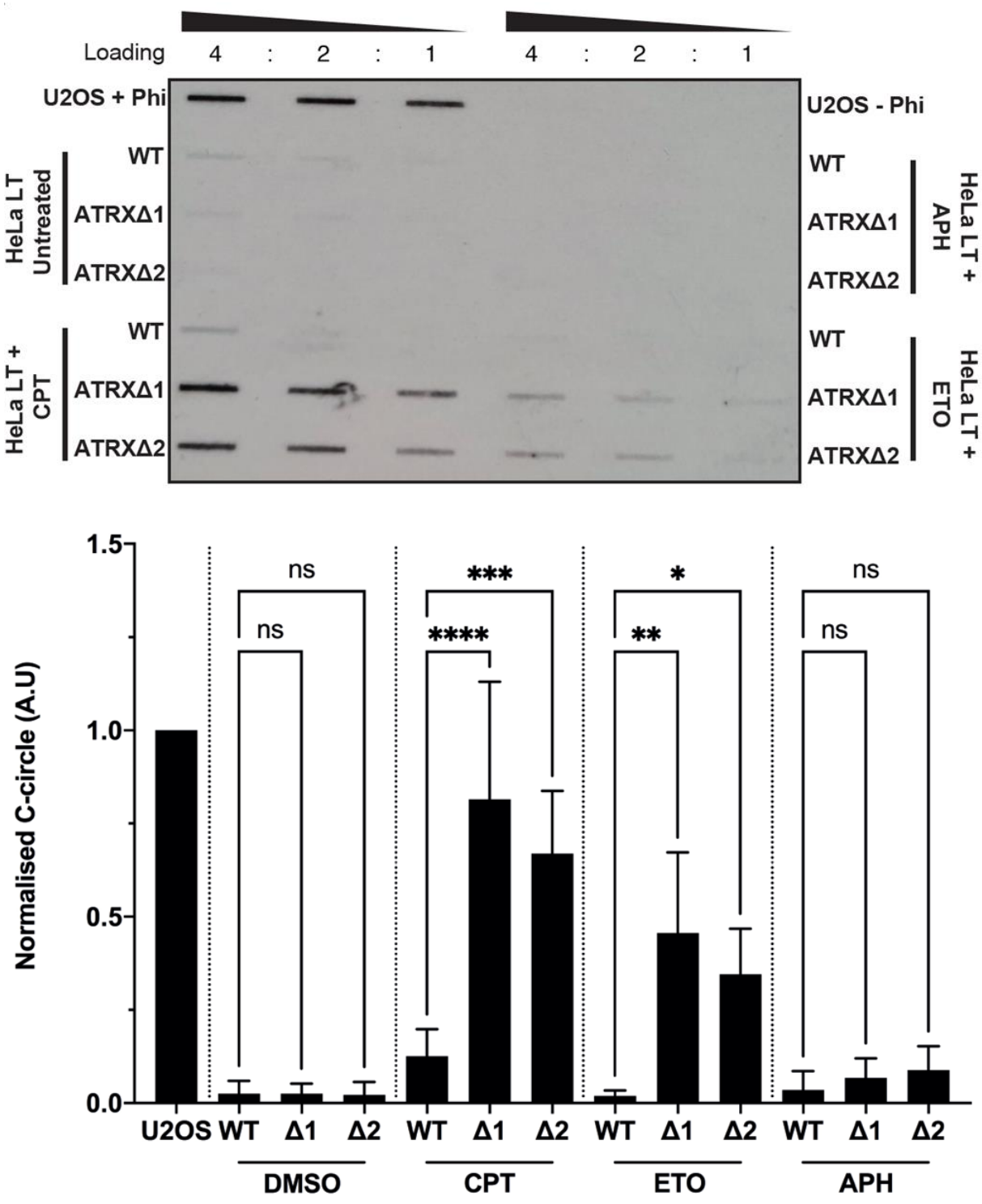

Figure 6B

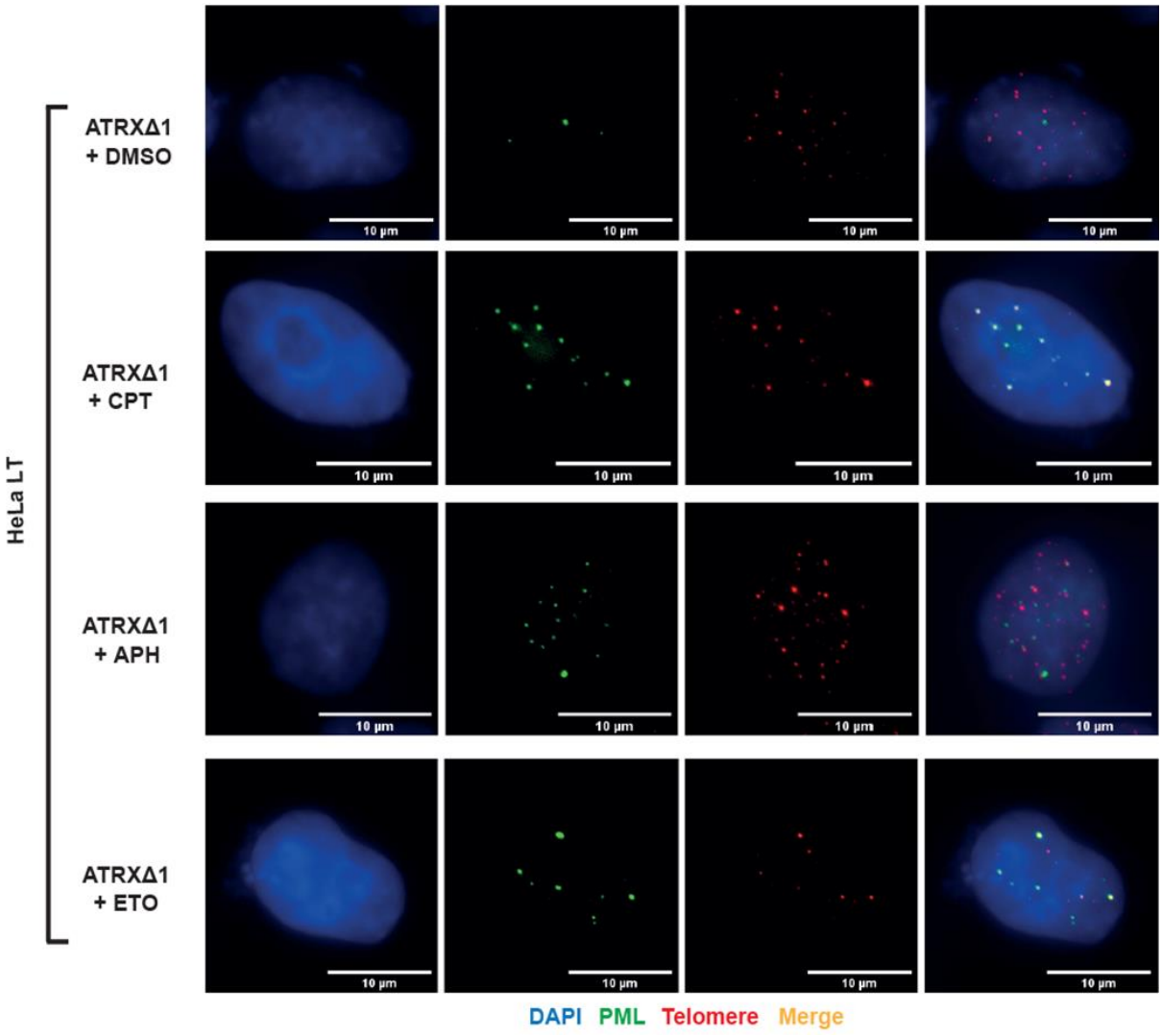
HeLa LT
ATRXΔ1
+ DMSO
ATRXΔ1
+ CPT
ATRXΔ1
+ APH
ATRXΔ1
+ ETO
10 µm
DAPI PML Telomere Merge

Figure 6C

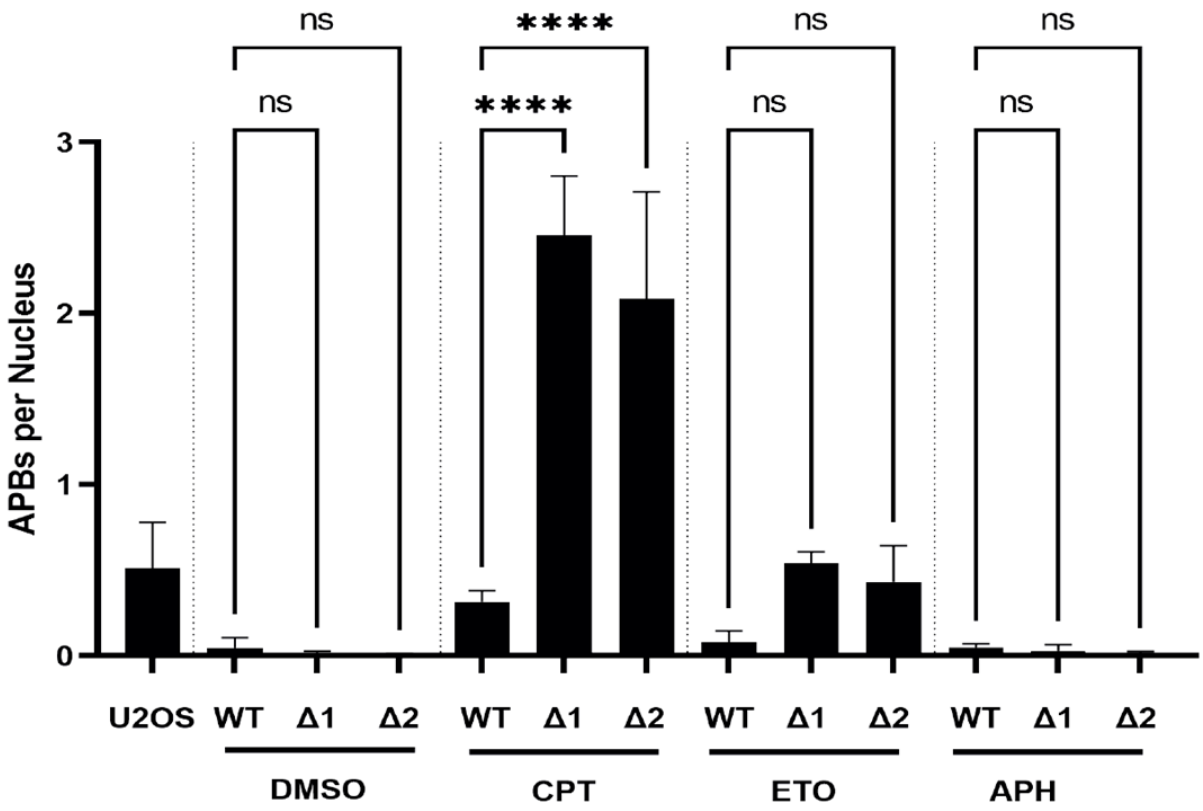
ns
****
ns
ns
ns
****
ns
ns
APBs per Nucleus
3
2
1
0
U2OS
WT
Δ1
Δ2
WT
Δ1
Δ2
WT
Δ1
Δ2
WT
Δ1
Δ2
DMSO
CPT
ETO
APH

Figure 6D

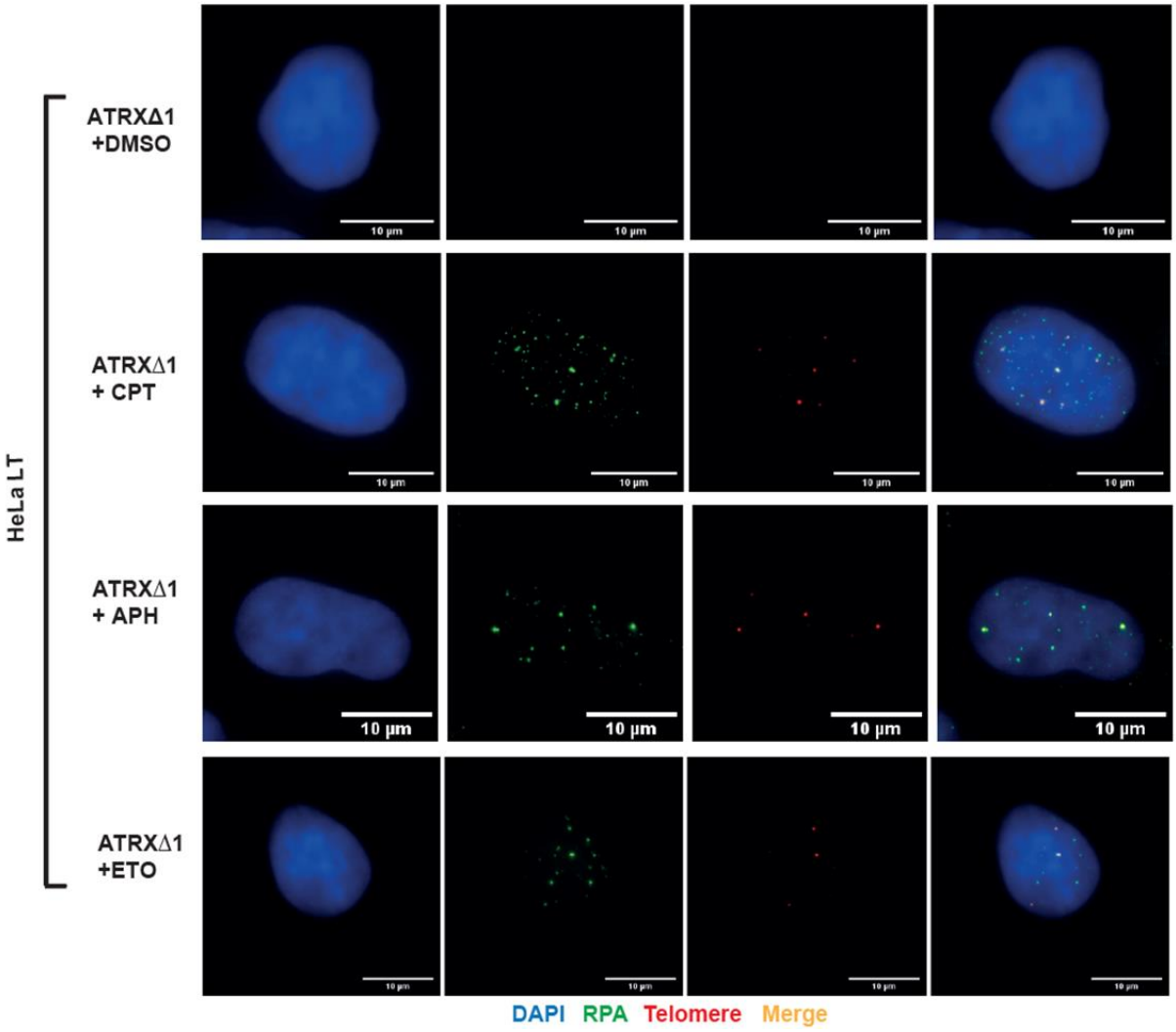
HeLa LT
ATRXΔ1
+DMSO
ATRXΔ1
+ CPT
ATRXΔ1
+ APH
ATRXΔ1
+ETO
10 µm
DAPI RPA Telomere Merge

Figure 6E

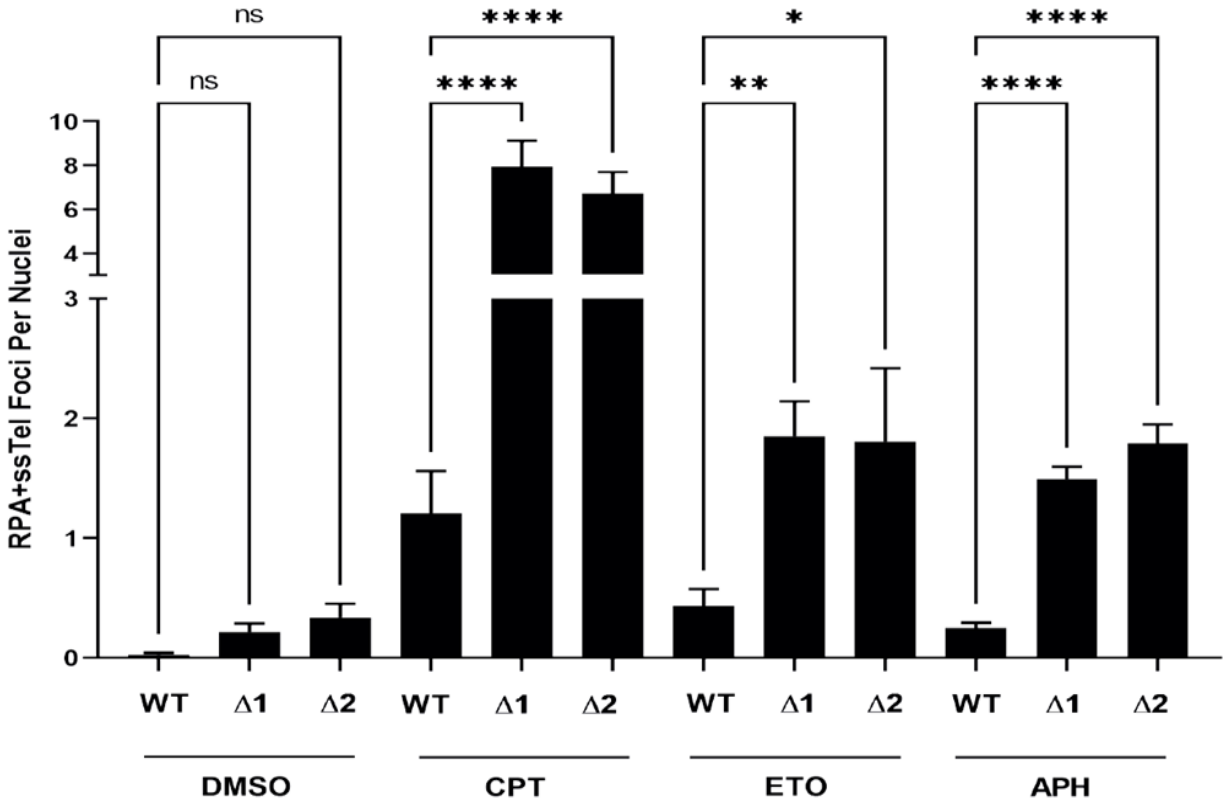
ns
ns
****
****
*
**
****
****
RPA+ssTel Foci Per Nuclei
10
8
6
4
3
2
1
0
WT
Δ1
Δ2
WT
Δ1
Δ2
WT
Δ1
Δ2
WT
Δ1
Δ2
DMSO
CPT
ETO
APH

Figure 6F

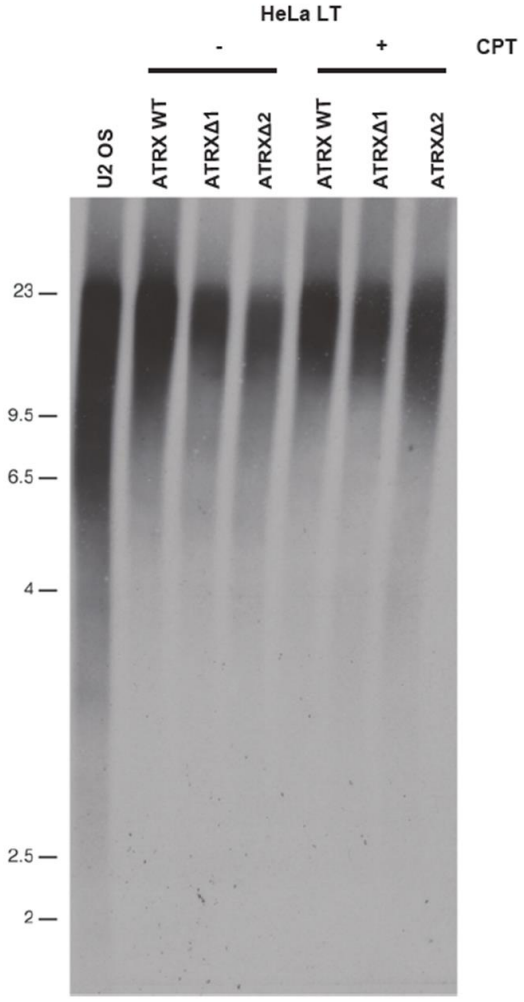

*Figure 6. A variety of genotoxic agents induce markers of ALT in ATRX deficient cells. ALT markers for HeLa LT ATRX KO cells treated with low dose CPT, ETO and APH. A) C-circle blot and quantification, n=3. *p < 0.05, **p < 0.001, ***p < 0.0001, ****p < 0.0001, determined by one-way ANOVA (performed with Tomas Gonclaves and Tomas Kent). B) Representative ImmunoFISH to detect APBs following treatment of ATRX KO cells with CPT, APH and ETO, >200 nuclei analysed across 3 biological replicates. C) Quantification of APBs in treated HeLa LT cells. ****p < 0.0001, determined by one-way ANOVA. D) Representative RPA ssTel immunoFISH images in HeLa LT ATRX KO cells treated with the same panel of genotoxic agents. E)*

*Quantification of RPA ssTel foci, >150 nuclei analysed across 3 biological replicates. *p < 0.05, **p < 0.001, ****p < 0.0001, determined by one-way ANOVA. F) TRF analysis showing treatment with 50nM CPT for 48 hrs increased telomere length heterogeneity specifically upon depletion of ATRX (performed with Thomas Kent).*

Recent work has shown that replication fork uncoupling and reversal is a global response to a plethora of genotoxic agents that can cause adducts or lesions on DNA (Zellweger et al., 2015). Given the reported roles for ATRX in promoting replication fork processivity and stability (Clynes et al., 2014; Huh et al., 2016; Leung et al., 2013b), I considered the possibility that the addition of a panel of genotoxic agents at sublethal doses, which on their own are reported to induce fork remodelling but not collapse, could also specifically elicit ALT in the absence of ATRX. Perturbations in fork processivity and reversal have been extensively reported as a frequent event upon addition of the Topoisomerase I inhibitor camptothecin (CPT) (Ray Chaudhuri et al., 2012). In agreement with the conjecture that ATRX is required to protect telomeres under conditions of replicative stress, addition of a low dose of CPT induced the formation of C-circles to levels almost equivalent to those found in the ALT positive U-2 OS cell line (Figure 6A). Likewise, addition of CPT led to an increase in APBs (Figures 6B and 6C) and RPA ssTel foci (Figures 6D and 6E) as well as a significant increase in telomere length heterogeneity (Figure 6F), specifically in the ATRX KO clones, consistent with a bona fide induction of the ALT pathway. Interfacial inhibition of Topoisomerase II, through addition of etoposide (ETO), elicited a similar response, with preferential increases in C-circles (Figure 6A), APBs (Figures 6B and 6C) and RPA ssTel foci (Figures 6D and 6E) in ATRX deficient cells, albeit to a slightly lesser extent than that observed with CPT. Treatment with low doses of the DNA polymerase

inhibitor APH, which has previously been shown to generate replicative stress at common fragile sites (Sfeir et al., 2009) , elicited only a minimal increase C-circles which failed to reach significance (Figure 6A) and no detectable increase in APBs (Figures 6B and 6C) in the ATRX null cells, but surprisingly did lead to a notable increase in RPA ssTel foci (Figures 6D and 6E). Taken together, this data suggests that it is the formation of a lesion or structure on telomeric DNA, and not replication stress *per se*, that facilitates induction of the ALT pathway in the absence of ATRX.

3.6: Genotoxic agents that cause replicative stress induce markers of ALT in shorter telomere ATRX deficient cells

Figure 7A

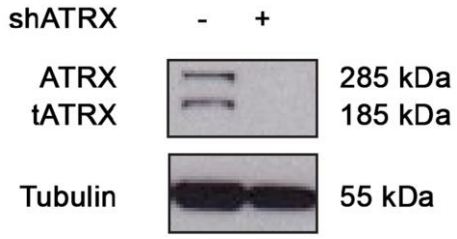

Figure 7B

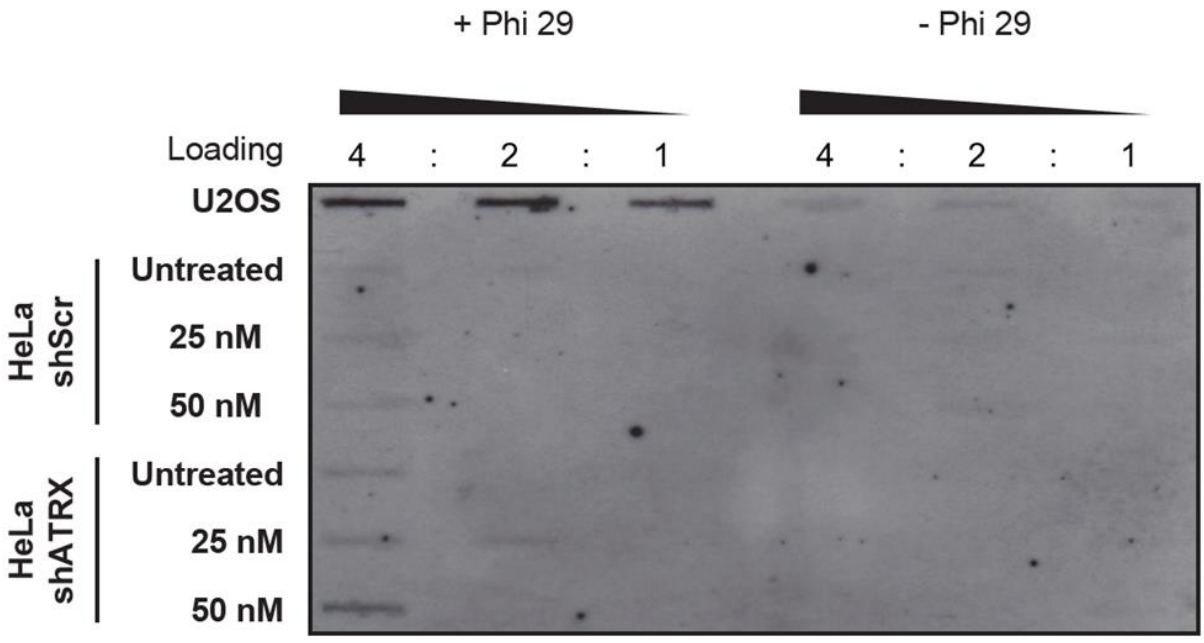

Figure 7C

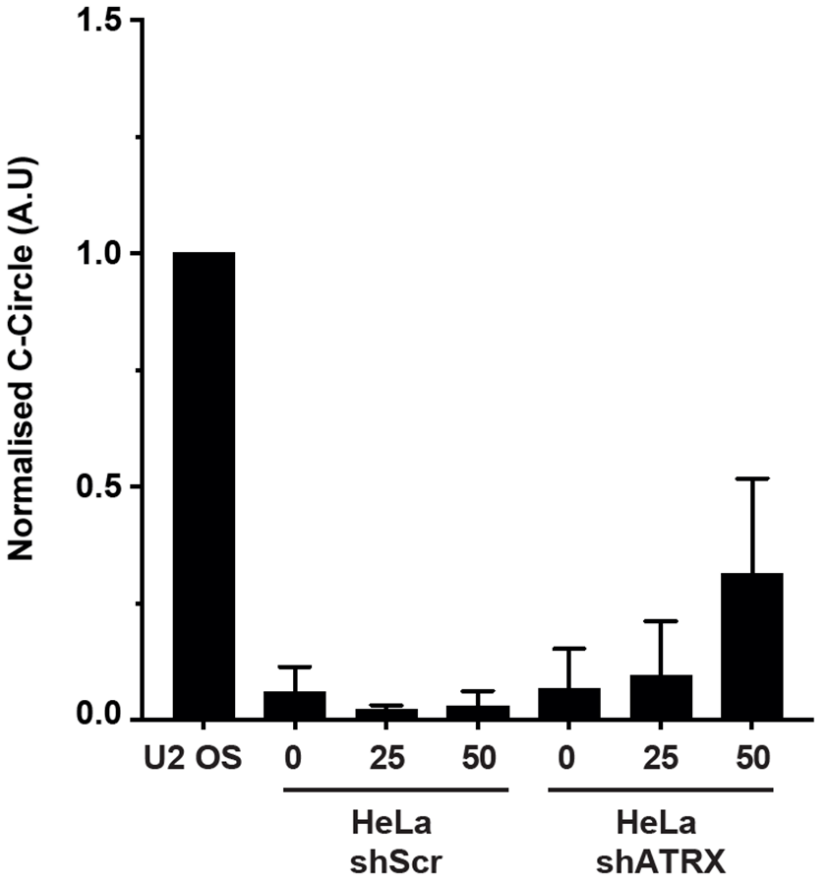

Figure 7D

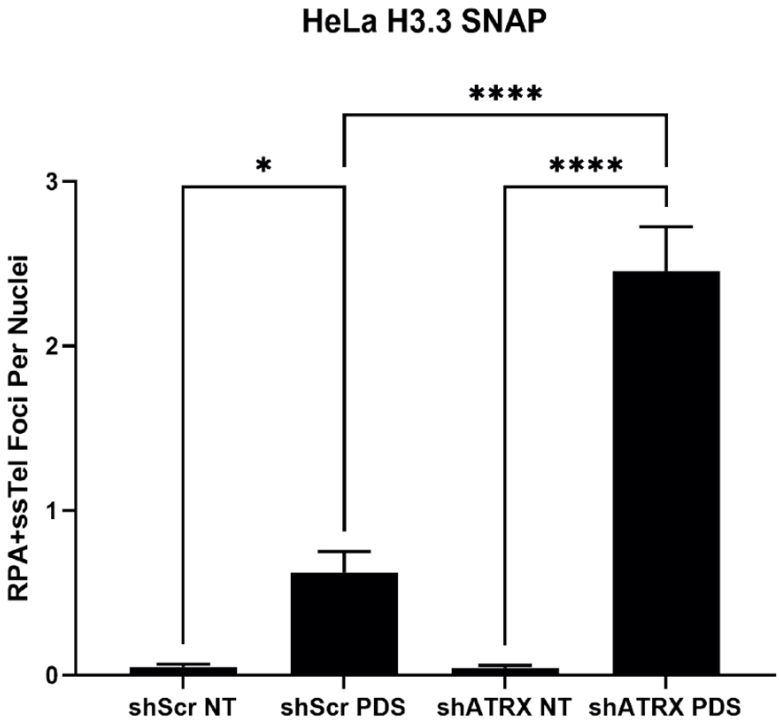

Figure 7E

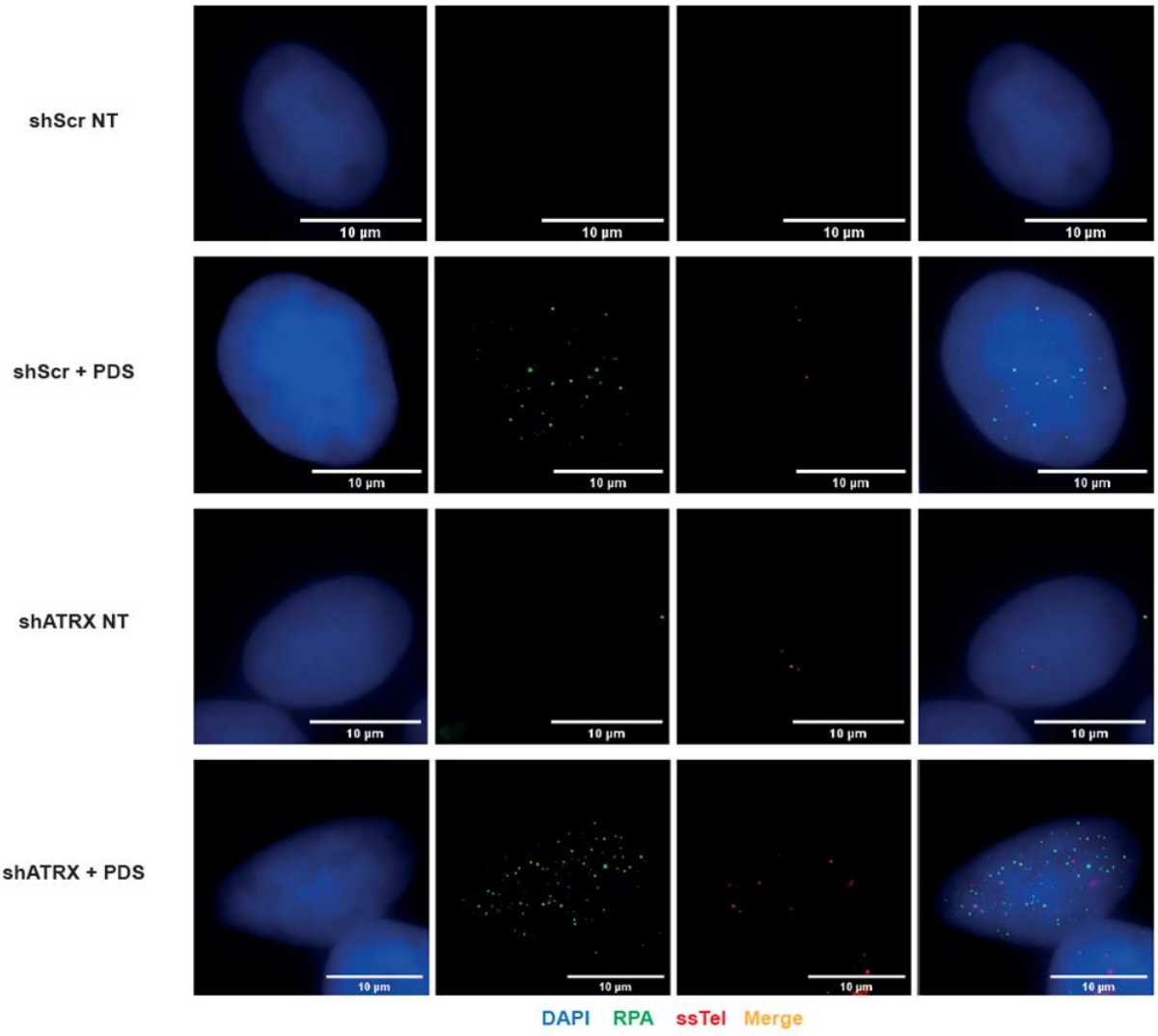

*Figure 7. A variety of genotoxic agents induce markers of ALT in shorter telomere ATRX deficient cells. A) western blot to show shRNA knock down of ATRX. B-C) C circle analysis to show a CPT dose dependent, ATRX loss specific increase in C circles ATRX. J-K) RPA ssTel increases upon shRNA mediated knock down of ATRX. >200 nuclei analysed across 3 biological replicates. *p < 0.5, ****p < 0.0001, determined by one-way ANOVA ATRX. All work in this figure was performed by Tomas Goncalves.*

To assess whether induction of ALT was specific to the HeLa LT cell line upon loss of ATRX, we sought to deplete ATRX via shRNA in a non-LT HeLa cell line with standard length telomeres (HeLa ST) (Figure 7A). Consistent with the previous observations in the HeLa LT cell line, addition of camptothecin (CPT), specifically in ATRX depleted cells, led to a robust augmentation of C-circles (Figures 7B and 7C), albeit to a lesser extent than that observed in the HeLa LT ATRX KO clones. Likewise, we found that addition of PDS led to induction of another of the ALT hallmarks, the RPA ssTel foci, again only in the ATRX depleted cells (Figures 7D and 7E). Taken together, I conclude that the observed induction of ALT is not specific to the HeLa LT cell line, however, the presence of long telomeres does appear to exacerbate the response.

3.7: ATRX and DAXX function epistatically in the suppression of ALT

Figure 8A

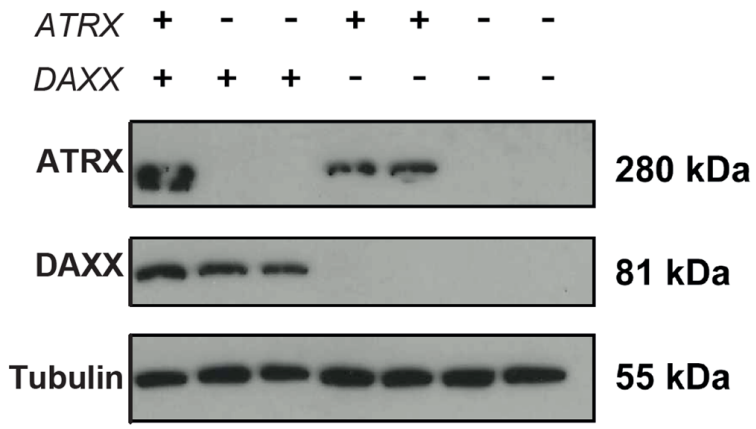

Figure 8B

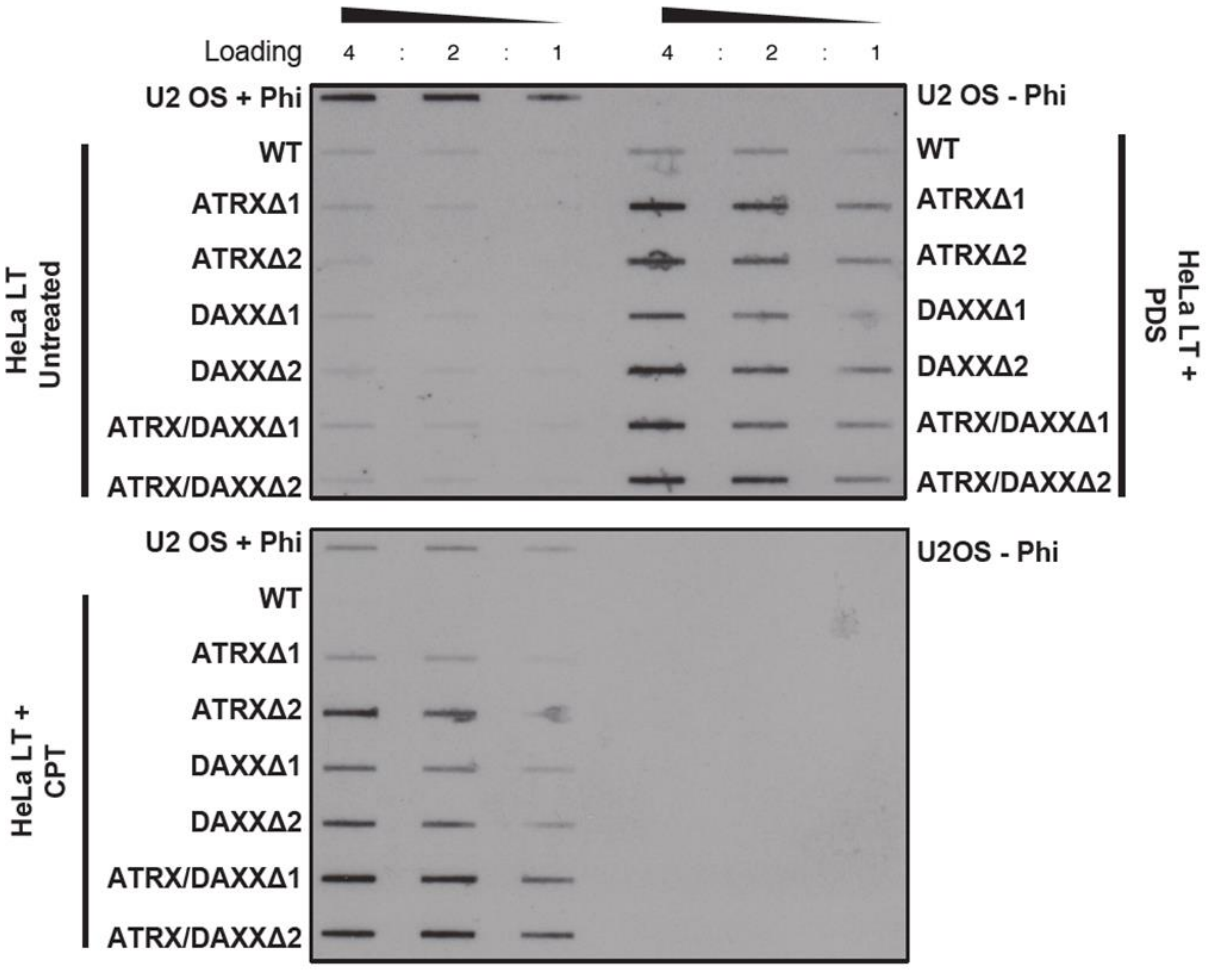

Figure 8C

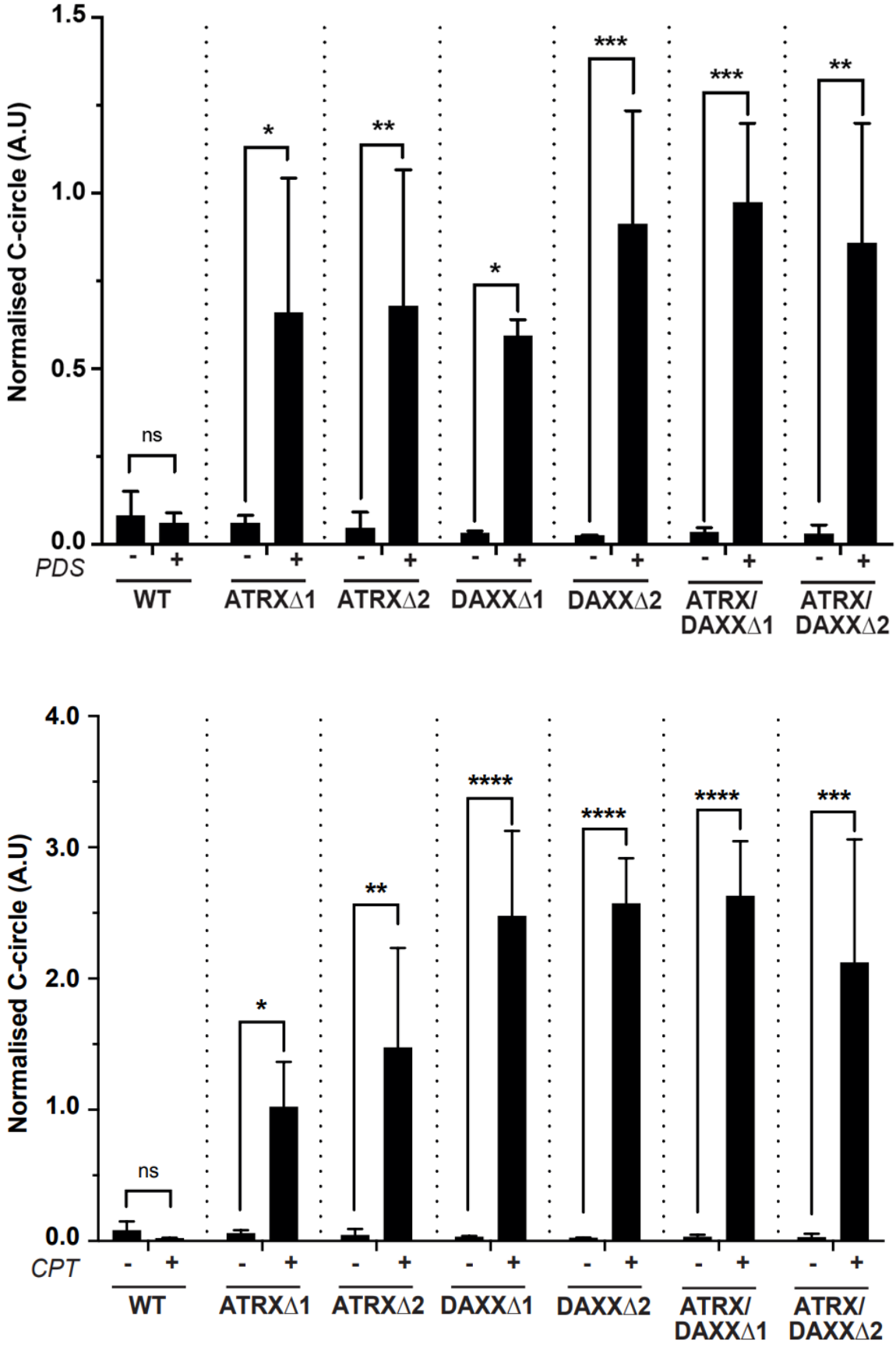
Normalised C-circle (A.U)
1.5
1.0
0.5
0.0
ns
*
**
*
***
***
**
PDS
- + - + - + - + - + - + - +
WT
ATRXΔ1
ATRXΔ2
DAXXΔ1
DAXXΔ2
ATRX/ DAXXΔ1
ATRX/ DAXXΔ2
Normalised C-circle (A.U)
4.0
3.0
2.0
1.0
0.0
ns
*
**
****
****
****
***
CPT
- + - + - + - + - + - + - +
WT
ATRXΔ1
ATRXΔ2
DAXXΔ1
DAXXΔ2
ATRX/ DAXXΔ1
ATRX/ DAXXΔ2

Figure 8D

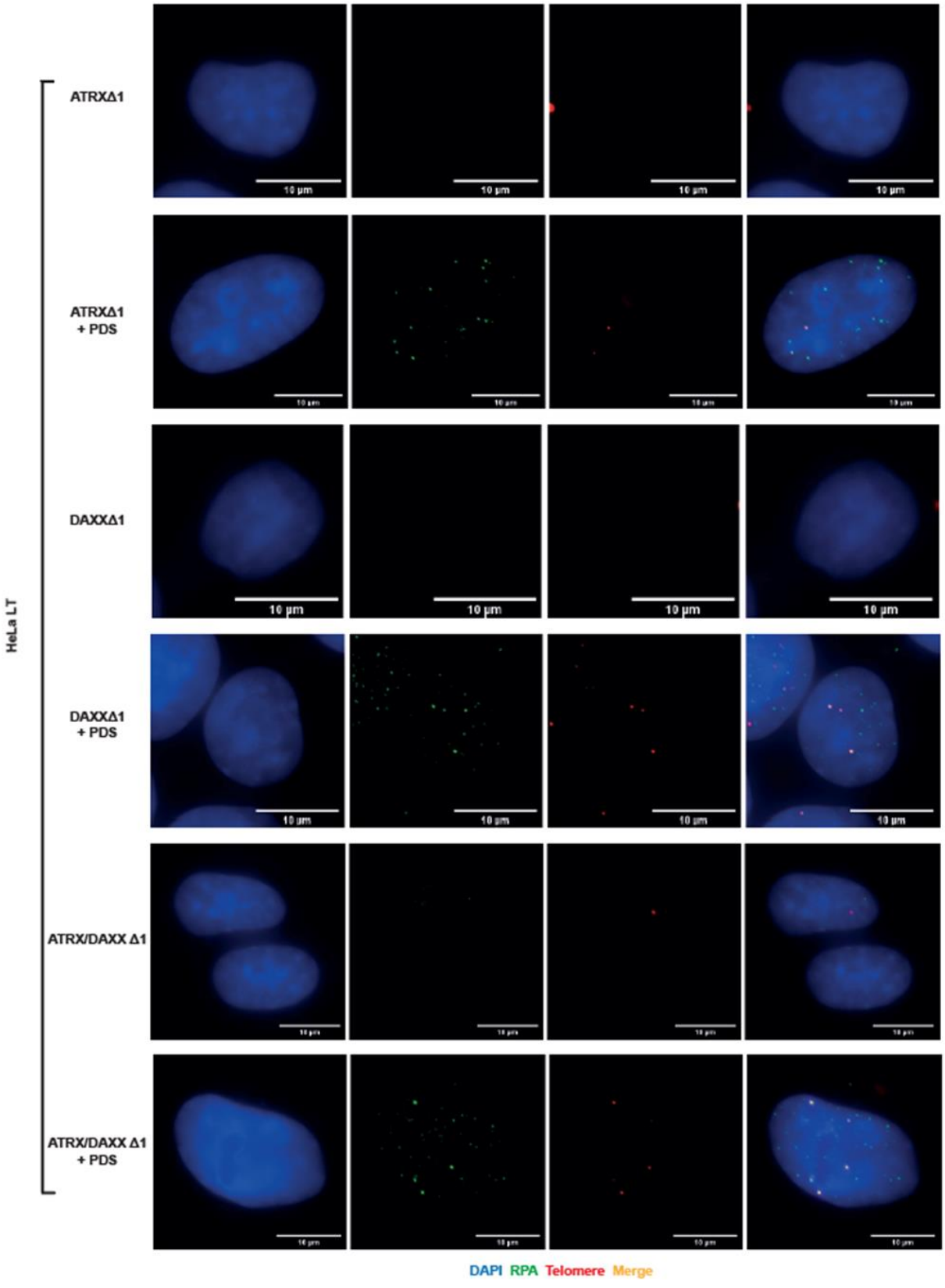
HeLa LT
ATRXΔ1
ATRXΔ1 + PDS
DAXXΔ1
DAXXΔ1 + PDS
ATRX/DAXX Δ1
ATRX/DAXX Δ1 + PDS
10 µm
DAPI RPA Telomere Merge

Figure 8E

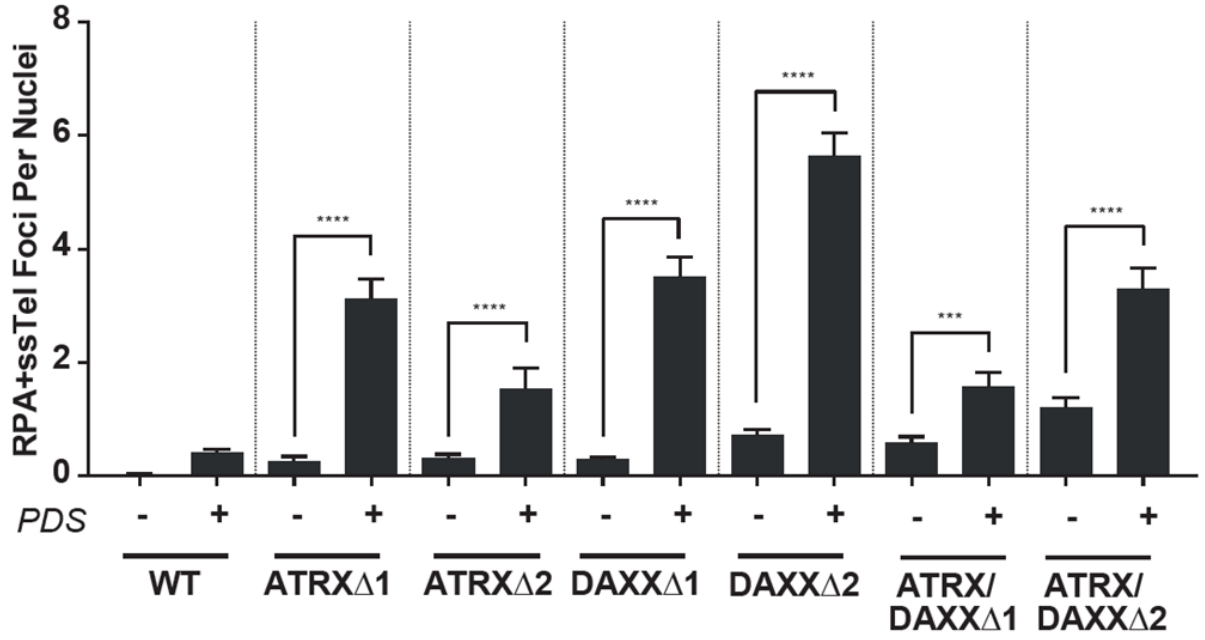

Figure 8F

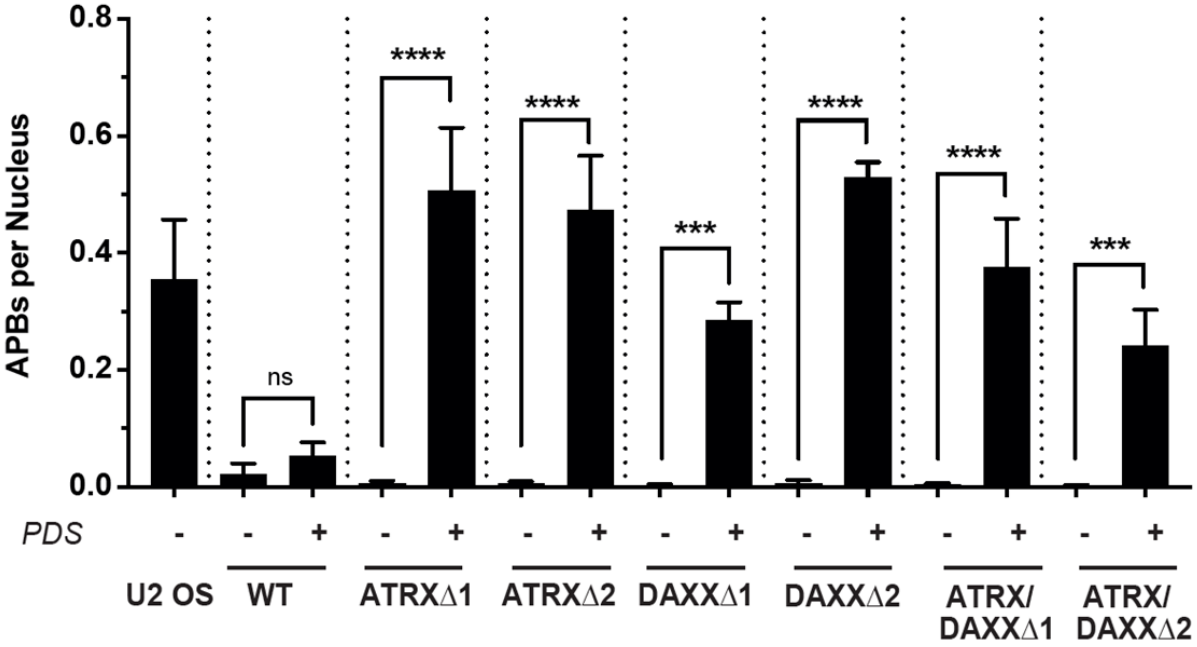

Figure 8G

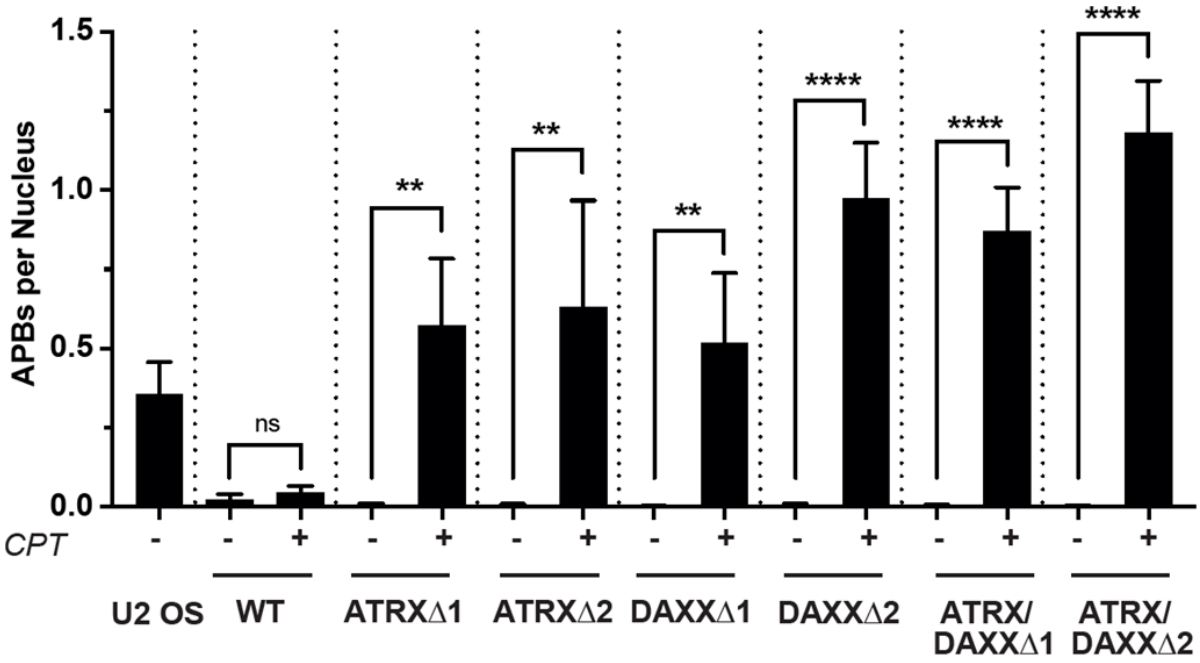

*Figure 8. ATRX and DAXX act epistatically in the suppression of induced ALT. A) Immunoblot of CRISPR-Cas9 mediated DAXX knockouts in HeLa LT ATRX WT and HeLa LT ATRXΔ1 cell lines. B-C) C-circle blot and quantification in DAXX KO clones following treatment with PDS and CPT, n=3. *p < 0.05, **p < 0.001, ***p < 0.0001, ****p < 0.0001, determined by one-way ANOVA (performed with Thomas Kent and Siobhan Cunniffe). D-E) RPA ssTel representative images and quantification in DAXX KO clones following PDS treatment, >200 nuclei analysed across 3 biological replicates. p < 0.0001, ****p < 0.0001, determined by one-way ANOVA (performed by Thomas Kent). F-G) Quantification of APBs following PDS or CPT treatment in ATRX/DAXX KO clones, >200 nuclei analysed across 3 biological replicates. **p < 0.001, ***p < 0.0001, ****p < 0.0001, determined by one-way ANOVA.*

A minority of ALT cancers are characterised by a loss of the histone chaperone protein DAXX which, together with ATRX, forms a complex that can facilitate incorporation of the histone variant H3.3 into ribosomal (Udugama et al., 2018), pericentromeric (Drané et al., 2010) and telomeric (Goldberg et al., 2010; Wong et al., 2010) chromatin. It has been previously reported that the suppression of the ALT pathway through ectopic expression of ATRX is lost upon depletion of DAXX (Clynes et al., 2015a), suggesting that ATRX and DAXX likely work in concert in the suppression of ALT. To further explore the relationship between ATRX and DAXX in the suppression of the ALT pathway, CRISPR-Cas9 mediated DAXX KO clones in the HeLa LT cell line, both in the context of WT ATRX and ATRX KO, were generated (Figure 8A). Consistent with the notion that ATRX/DAXX function as a complex in the suppression of the ALT pathway, the loss of DAXX facilitated the accumulation of C-circles (Figures 8B and 8C), RPA ssTel foci (Figures 8D and 8E) and APBs (Figures 8F and 8G) upon treatment with both PDS and CPT. Importantly, the co-depletion of both ATRX and DAXX failed to confer any cumulative increase in these cardinal ALT markers (Figures 8B-G), strongly suggesting that both ATRX and DAXX are functioning within the same pathway in the suppression of telomeric replicative stress and the ALT pathway.

3.8: SETD2 loss in combination with ATRX loss triggers markers of the ALT pathway

Figure 9A

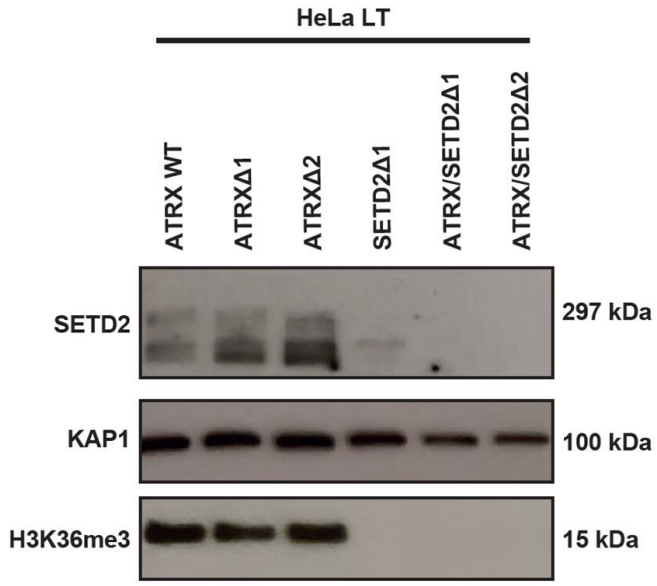

Figure 9B

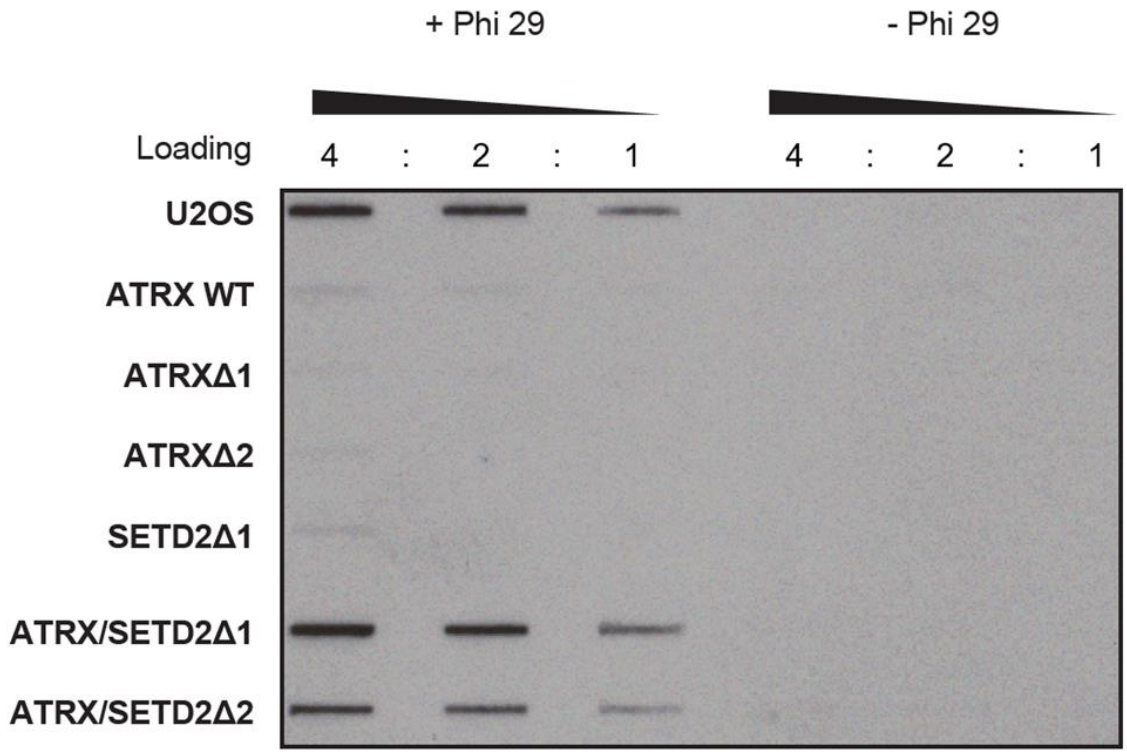

Figure 9C

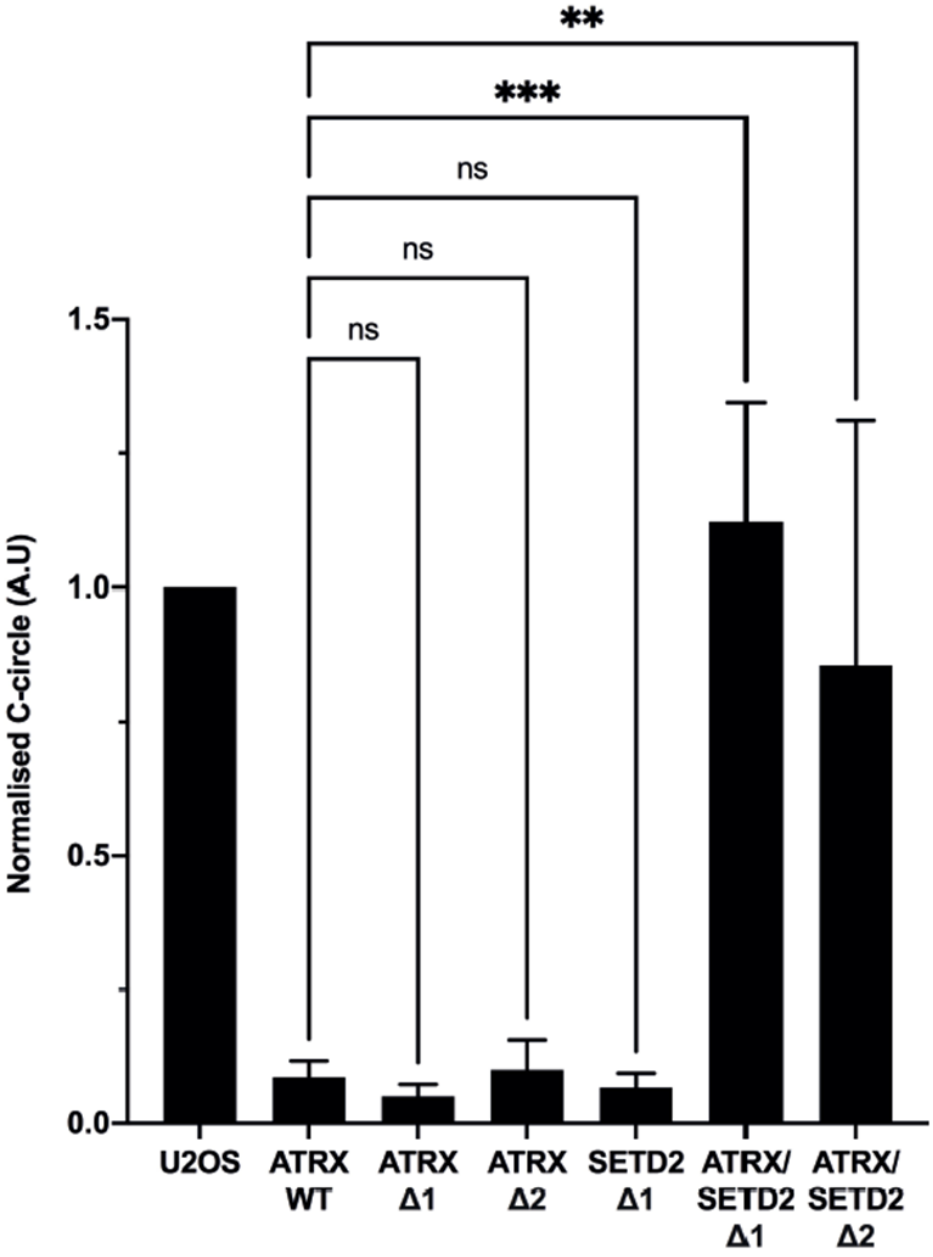
**
***
ns
ns
ns
1.5
1.0
0.5
0.0
Normalised C-circle (A.U)
U2OS
ATRX WT
ATRX Δ1
ATRX Δ2
SETD2 Δ1
ATRX/ SETD2 Δ1
ATRX/ SETD2 Δ2

Figure 9D

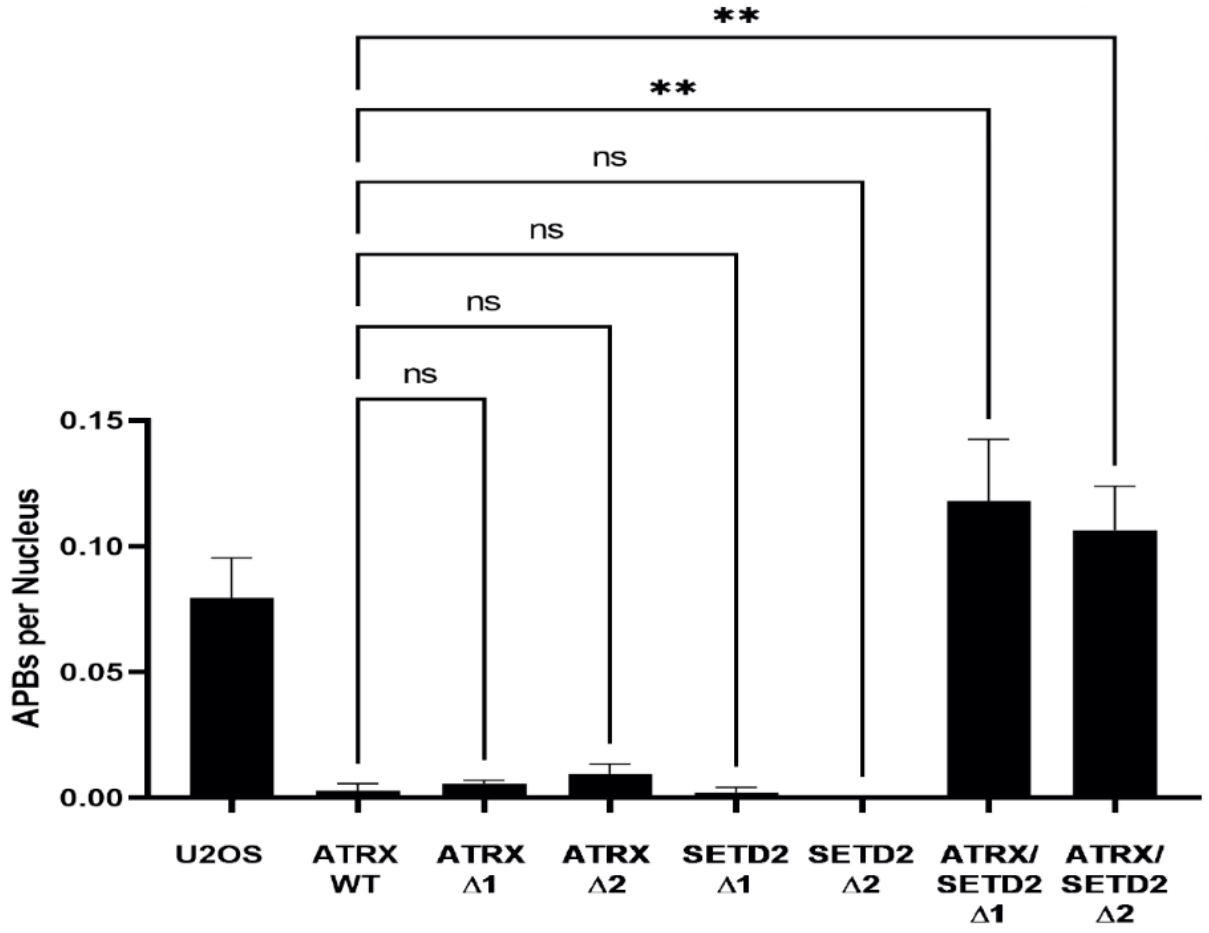

Figure 9E

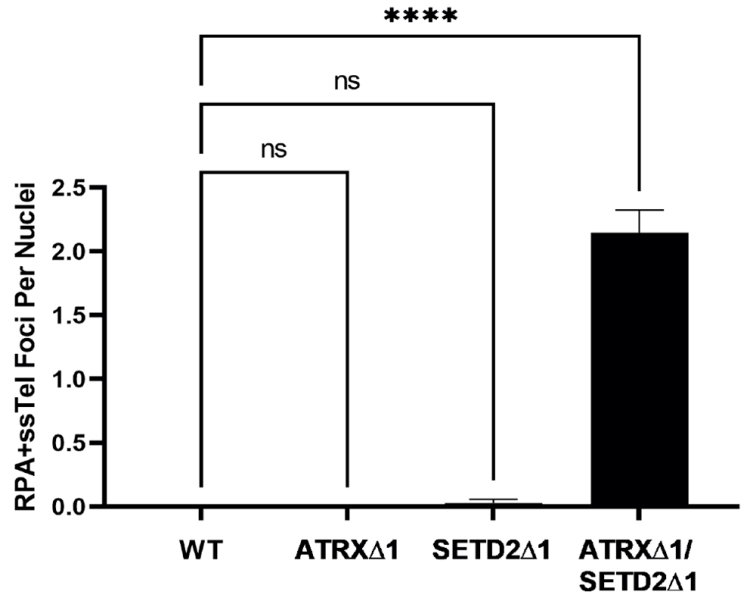

Figure 9F

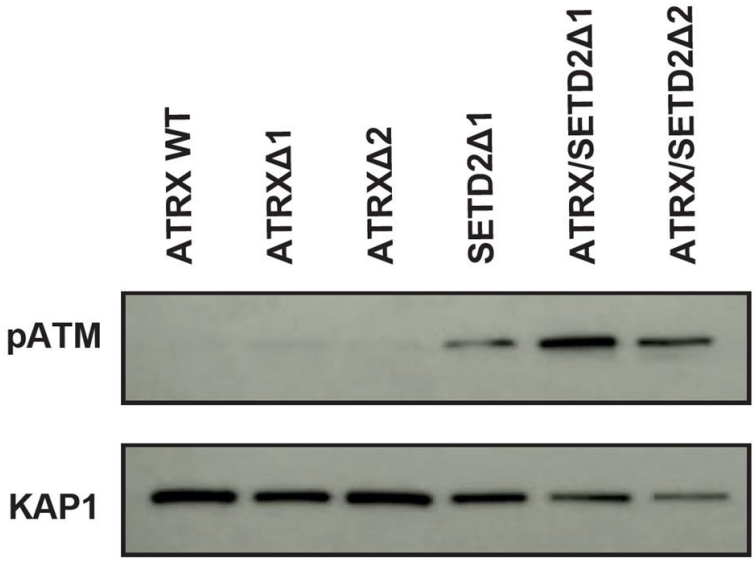

*Figure 9. SETD2 loss in combination with ATRX loss triggers markers of the ALT pathway. A) Immunoblot showing loss of H3 K36me3 upon CRISPR-Cas9 mediated deletion of SETD2. B-C) C-circle blot and quantification showing accumulation of C-circles specifically upon co-deletion of both ATRX and SETD2 in HeLa LT cells, n=3. **p < 0.001, ***p < 0.0001, determined by one-way ANOVA. D) APB analysis showing accumulation of APBs specifically upon co-depletion of ATRX and SETD2, >100 nuclei analysed across 3 biological replicates. **p < 0.001, determined by one-way ANOVA. E) Quantification of RPA ssTel positive telomeres upon co-depletion of ATRX and SETD2, >150 nuclei analysed across 2 biological replicates. ****p < 0.0001, determined by one-way ANOVA (performed by Thomas Kent). F) Immunoblot showing combined loss of ATRX and SETD2 leads to DNA damage (performed by Tomas Goncalves).*

It is likely that induction of ALT in cancer cells in fact requires two independent events, involving mutations or factors that generate a telomeric structure or lesion, which, if in concert with ATRX loss, leads to fork collapse. This thereby provides the substrate and means for BIR and subsequent telomere lengthening. Recurrent mutations in genes that disrupt the post-translational modification of histone H3 at H3 K36, including mutations in H3.3 G34R/V or the histone methyl transferase SETD2, are also frequently found in paediatric HGGs and are highly co-incident with mutations in ATRX (Fontebasso et al., 2013). Of note, mutations in SETD2 have recently been linked to the generation of replicative stress (Kanu et al., 2015). To explore the possibility that loss of ATRX, in the context of SETD2 loss, is sufficient to drive the ALT pathway, I generated SETD2 KO clones both in the context of wildtype ATRX and ATRX loss. Loss of SETD2 activity in the resulting clones was confirmed by a global loss of histone H3 K36me3 (Figure 9A). Loss of SETD2 alone was insufficient to elicit markers of ALT, however strikingly, the combination of both ATRX and SETD2 loss induced an accumulation of C-circles (Figures 9B and 9C), APBs (Figure 9D) and RPA ssTel foci (Figure 9E) akin to those observed in U-2 OS cells. The loss of SETD2 was associated with increases in DNA damage markers, including pATM, which were further exacerbated upon the combined KO of both SETD2 and ATRX (Figure 9F).

3.9: Effect of triptolide on ATRX/SETD2 double knock outs

Figure 10A

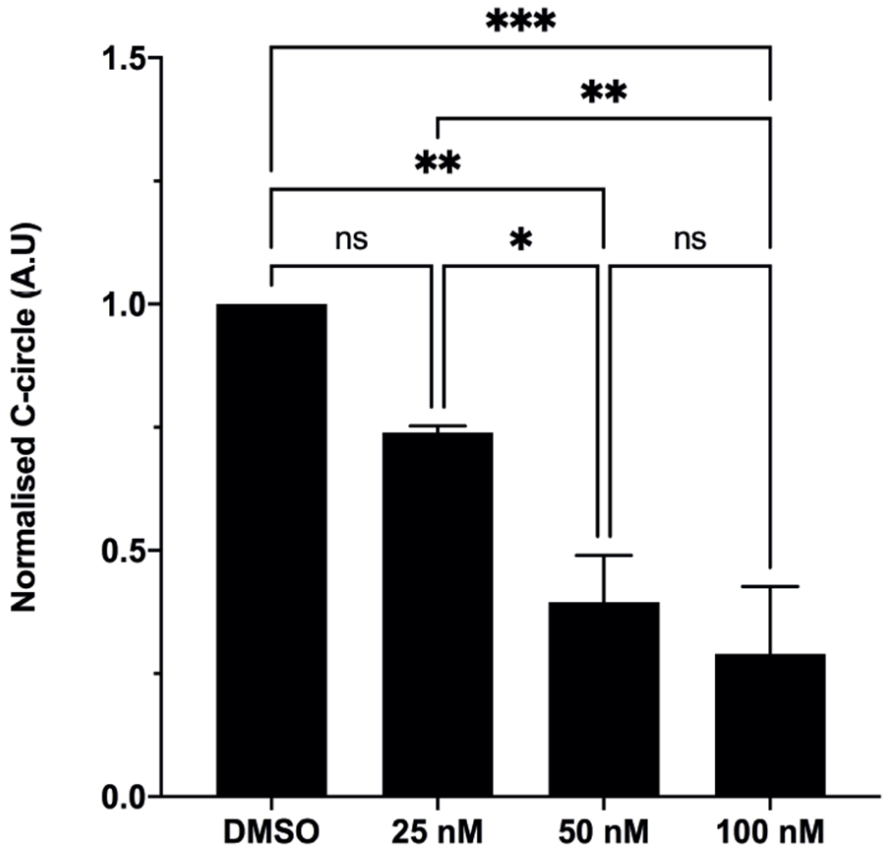

Figure 10B

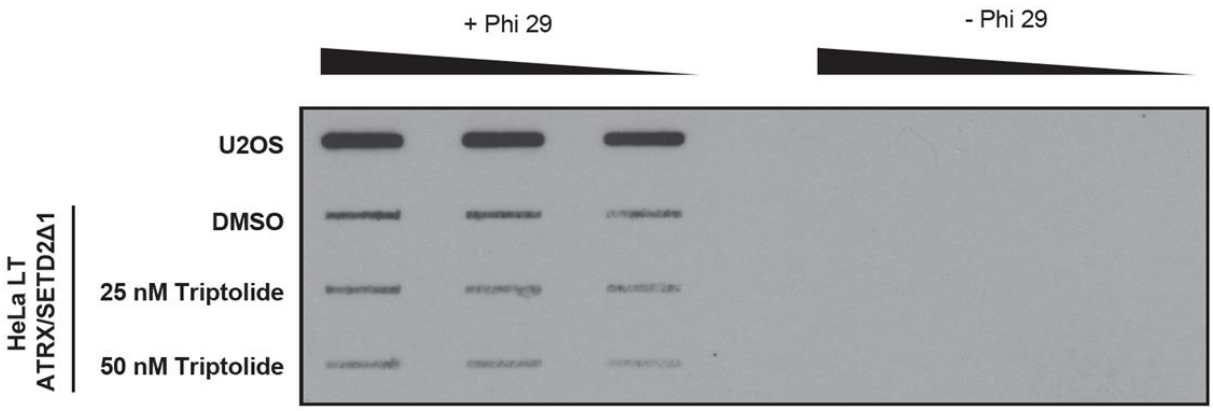

Figure 10C

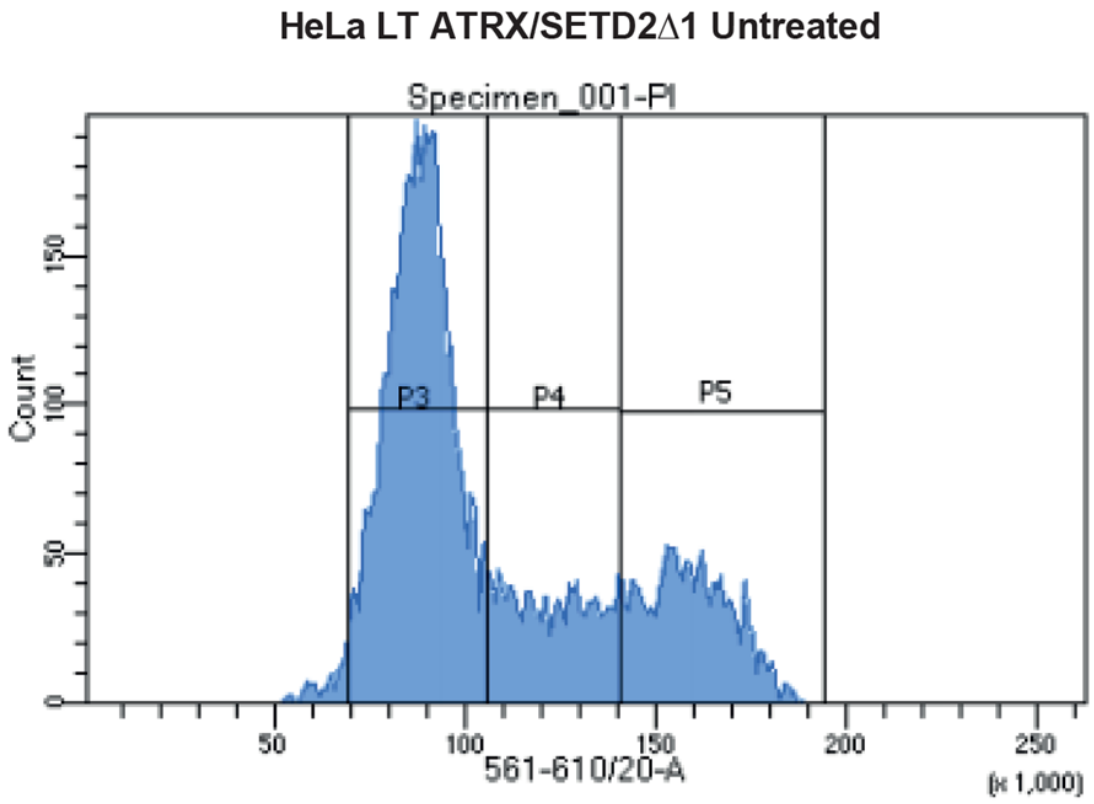

Figure 10D

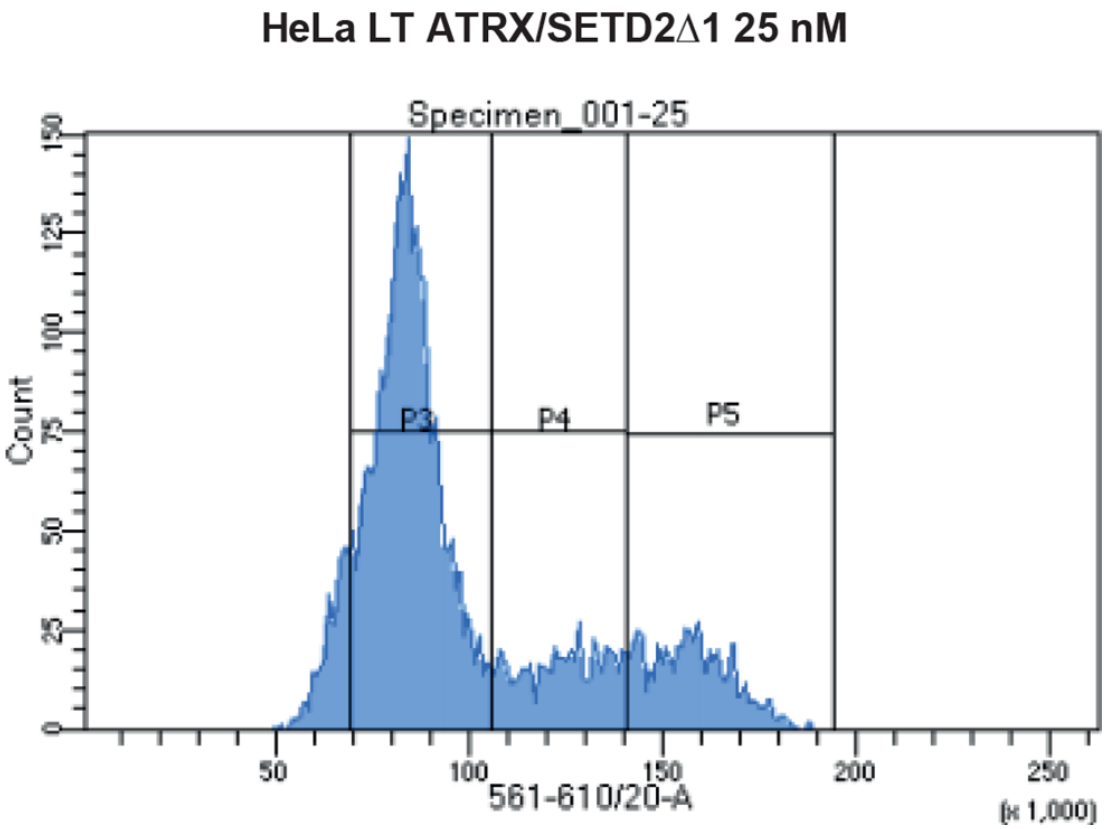

Figure 10E

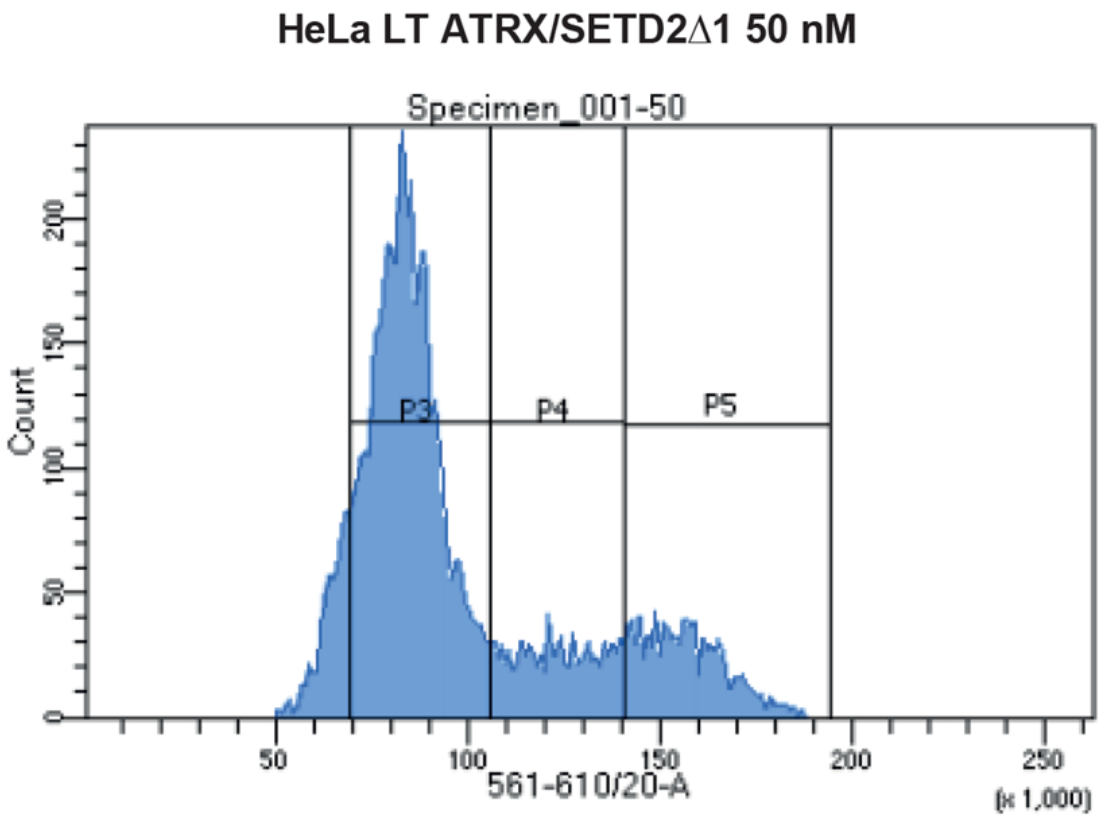

Figure 10F

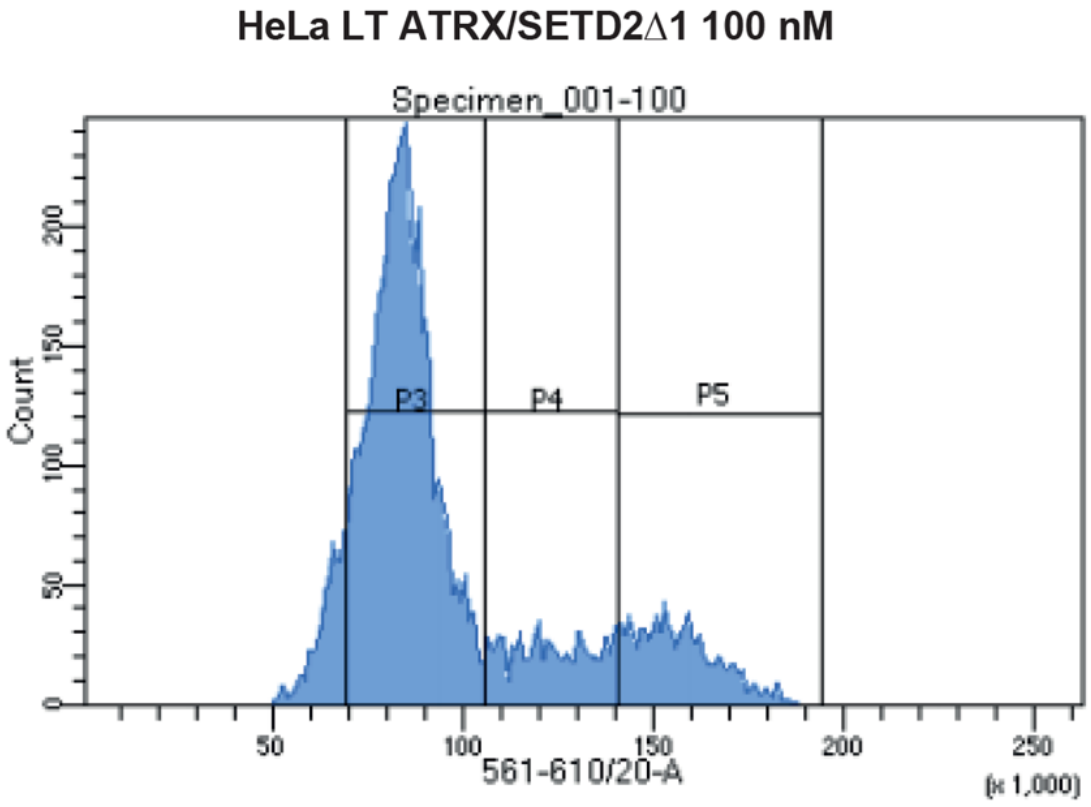

Figure 10G

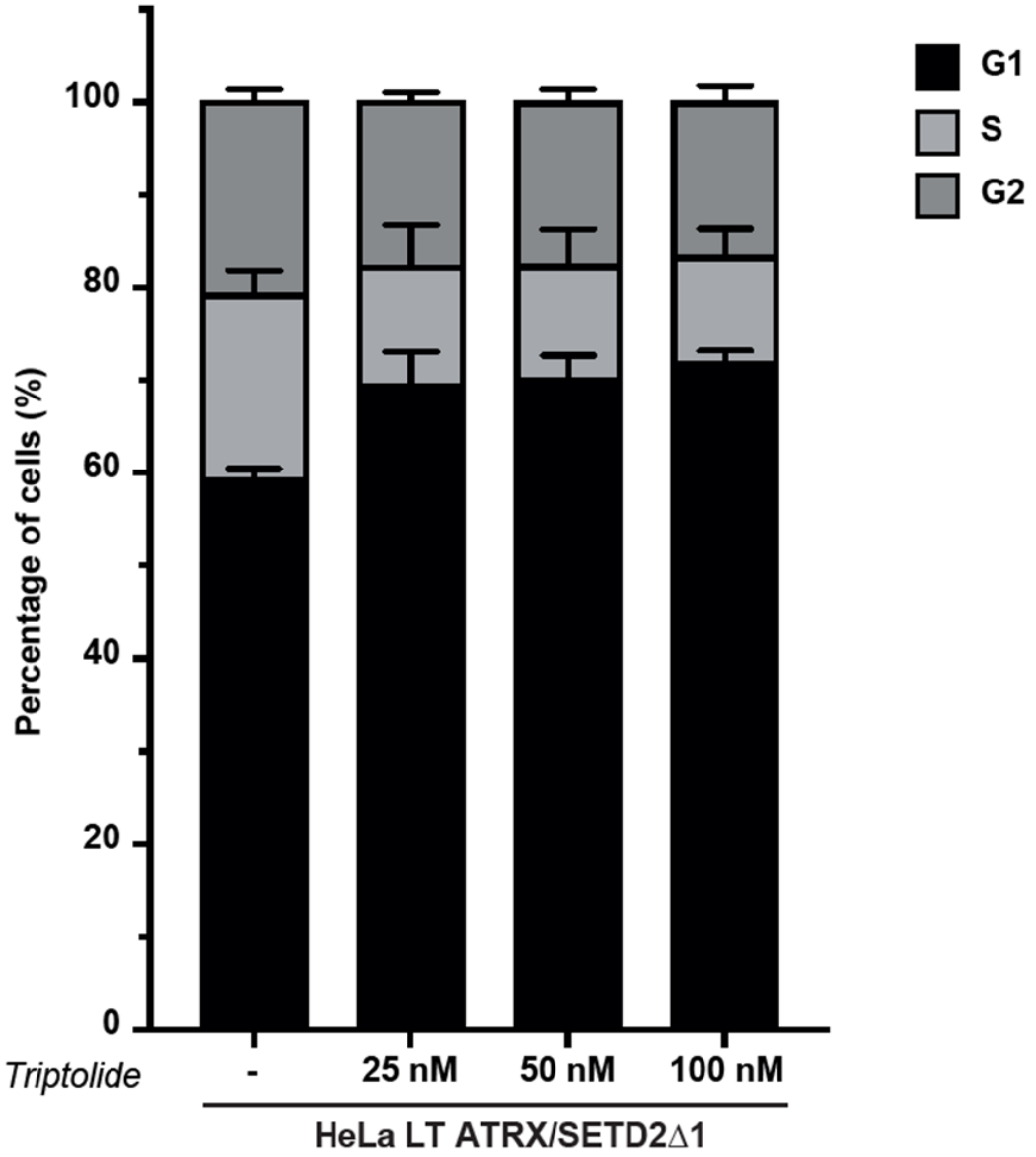

*Figure 10. Triptolide and the cell cycle, effect on C-circles. A) C-circle assay quantification in ATRX/SETD knockout cells treated with triptolide at indicated concentrations, n=2. *p < 0.05, **p < 0.001, ***p < 0.0001, determined by one-way ANOVA. B) dose dependent reduction of the transcription inhibitor triptolide on ATRX/SETD2 combined loss induced C circle generation. C-G) change in cell cycle distribution after triptolide of the ATRX SETD2 double knock out. All work in this figure was performed by Thomas Kent and Tomas Goncalves.*

Strikingly, the accumulation of C-circles in ATRX/SETD2 double knock outs was dramatically reduced upon treatment with the transcription inhibitor triptolide in a dose dependent manner (Figures 10A and 10B). Treatment with triptolide elicited a minor effect on cell cycle distribution, with a slight increase in the percentage of cells in G1, however, in contrast to the dose dependency observed with the loss of C-circles, treatment with all 3 doses of triptolide elicited an identical change to the cell cycle distribution (Figures 10C-G). Taken together, it is therefore unlikely that the reduction in C-circles is an indirect consequence of changes to the cell cycle. It is Important to note however, that triptolide has a range of targets within a cell, and experiments to determine any mentioned effects have not been performed.

3.10: Potential for R-loops to induce ALT in ATRX/SETD2 double knock outs

Figure 11A

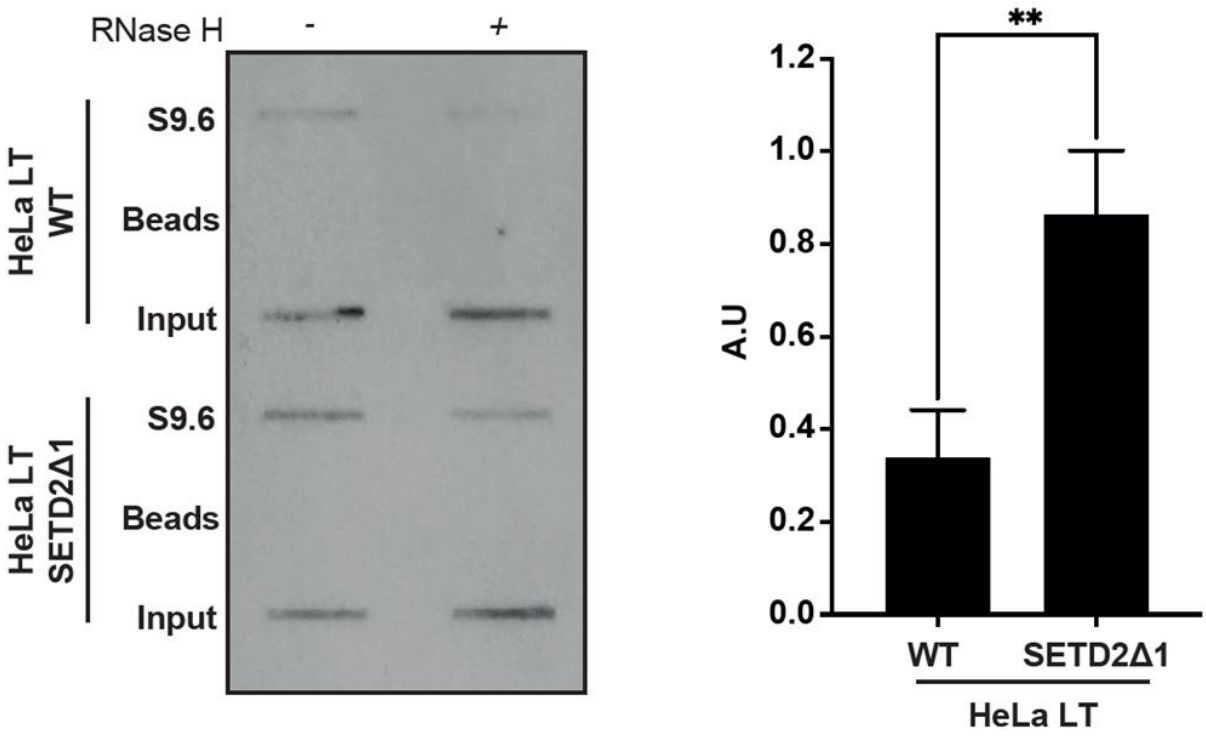

Figure 11B

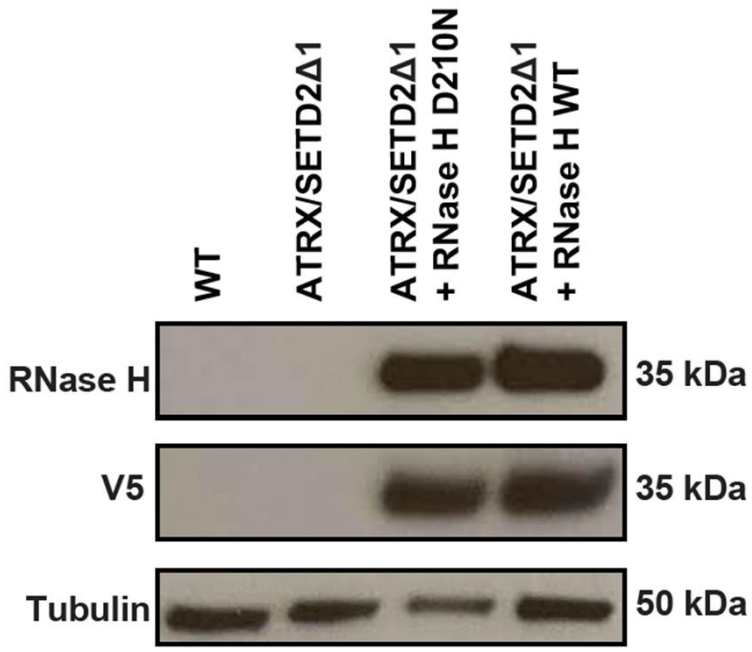

Figure 11C

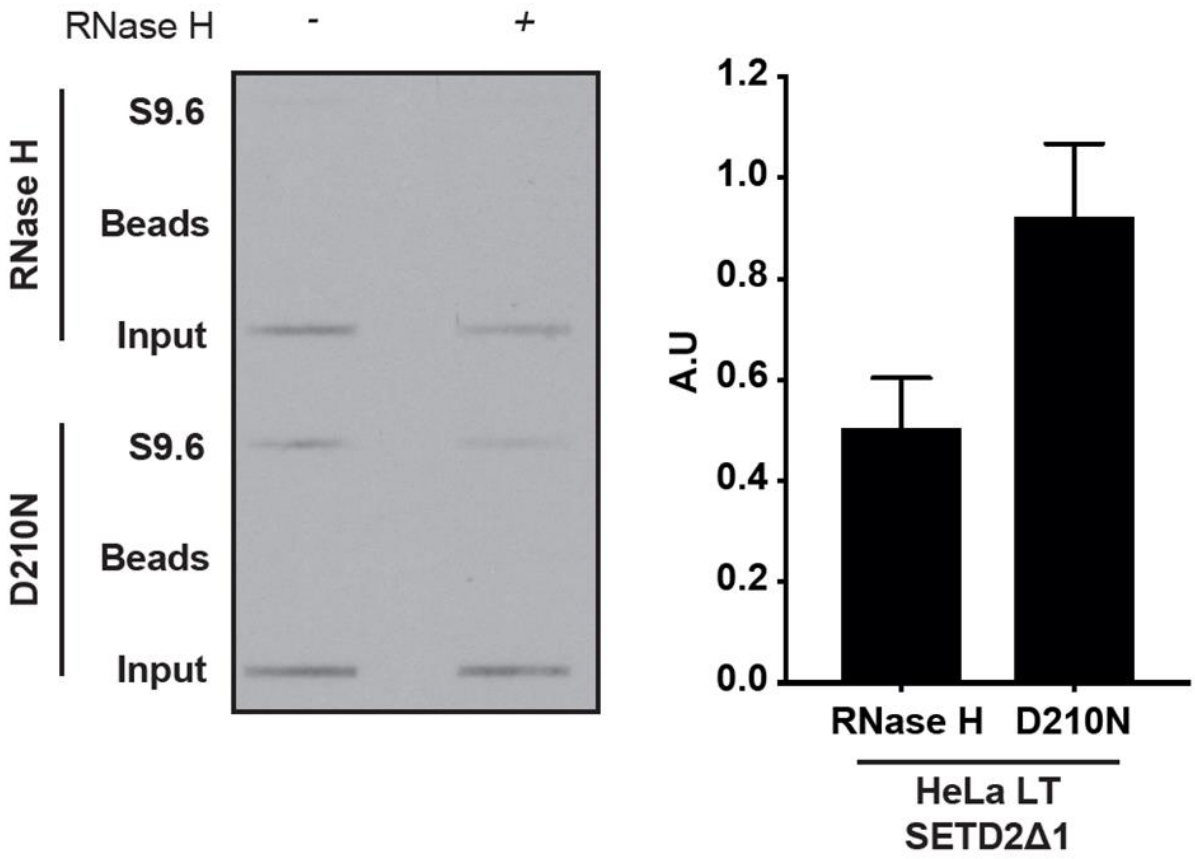

Figure 11D

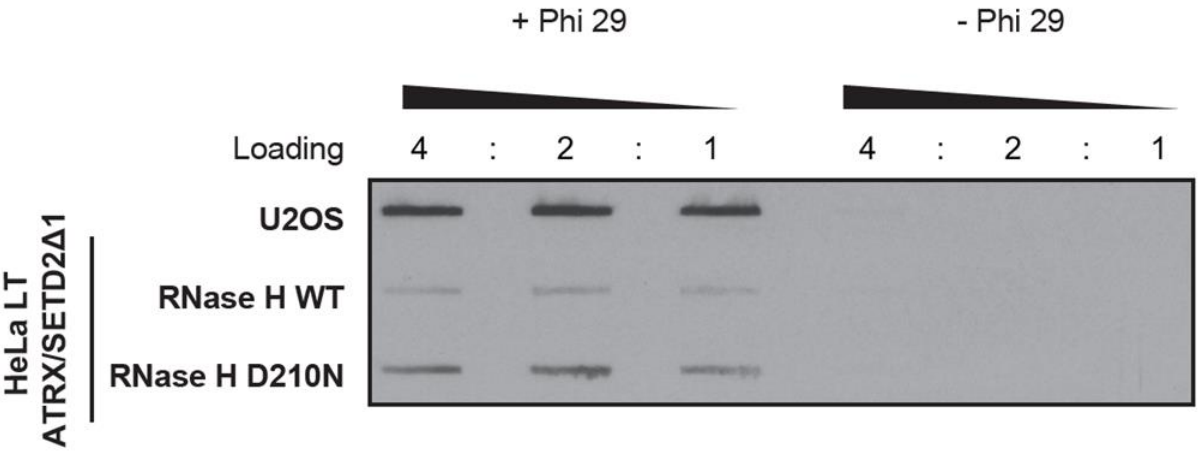

Figure 11E

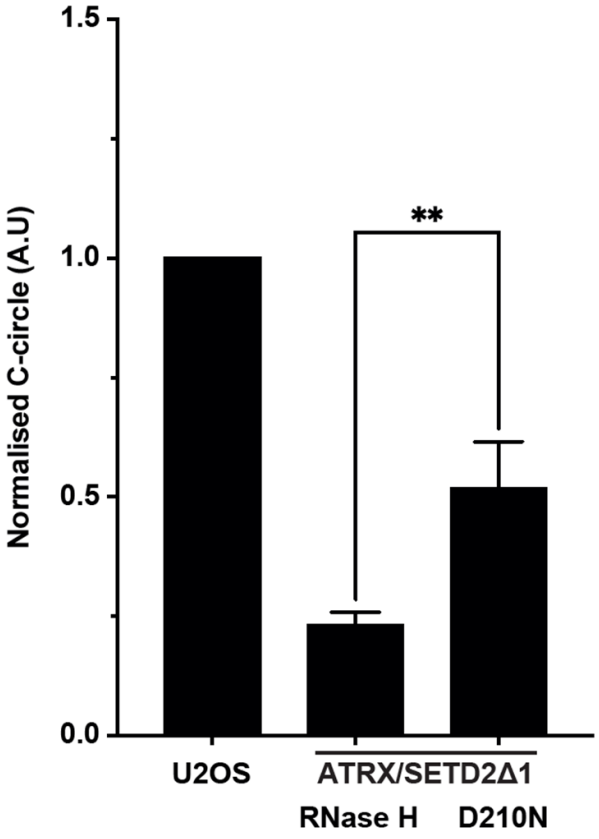

*Figure 11. Using RNase H to investigate effect of R-loops on ATRX/SETD2 double knock out induced ALT. A) S9.6 DRIP slot blot and quantification showing increased levels of R loops at telomeres upon SETD2 loss, n=3. **p < 0.001, determined by unpaired Student's t test. B) Immunoblot showing overexpression of RNase H WT and the catalytically dead D210N mutant in the HeLa LT ATRX/SETD2Δ1 14 days after lentiviral transduction. C) S9.6 DRIP slot blot and quantification showing loss of telomeric R-loops upon ectopic expression of RNase H WT but not the D210N mutant, n=2. D-E) C-circle blot and quantification of ATRX/SETD2Δ1 cells overexpressing RNase H WT or the D210N mutant 14 days following transfection, n=3. **p < 0.001, determined by unpaired Student's t test. All work in this figure was performed by Thomas Kent and Tomas Goncalves.*

Given this dependence on transcription and previous findings that the ALT pathway is potentiated through the formation of telomeric R-loops (Arora et al., 2014; Lu et al., 2019b; Pan et al., 2017a, 2017b; Silva et al., 2019), I asked whether the depletion of SETD2 was associated with an increase in telomeric R-loops. Immunoprecipitation using an antibody which can recognise RNA-DNA hybrids (S9.6) showed a marked accumulation of telomeric signal upon loss of SETD2 (Figure 11A). The results from Smolka *et al*. (2021) do however show that this signal may not be R-loops and so the R-loop related results shown here could be pervasive artifacts. When cells were pre-treated with RNase H prior to immunoprecipitation, the signal was decreased, suggesting that the signal could be specific to the DNA-RNA hybrids (Figure 11A). I next sought to determine whether the possible accumulation of telomeric R-loops observed upon SETD2 loss was responsible for facilitating the accumulation of ALT markers in the combined ATRX SETD2 KO cells. To this end, I overexpressed the RNA-DNA endonuclease RNase H1 in HeLa LT SETD2 KO cells (Figure 11B) which led to a marked decrease in telomeric S9.6 signal (Figure 11C). Moreover, overexpression of RNase H1 in the ATRX SETD2 KO cells resulted in a reduction of C-circles that was not observed upon overexpression of a catalytically dead mutant of RNase H1 (D210N) (Figure 11D-E). Taken together, this data could support a model whereby loss of SETD2 leads to the accumulation of telomeric R-loops which triggers the ALT pathway, specifically in the absence of ATRX.

3.11: ATRX is required for telomere sister chromatid cohesion

Figure 12A

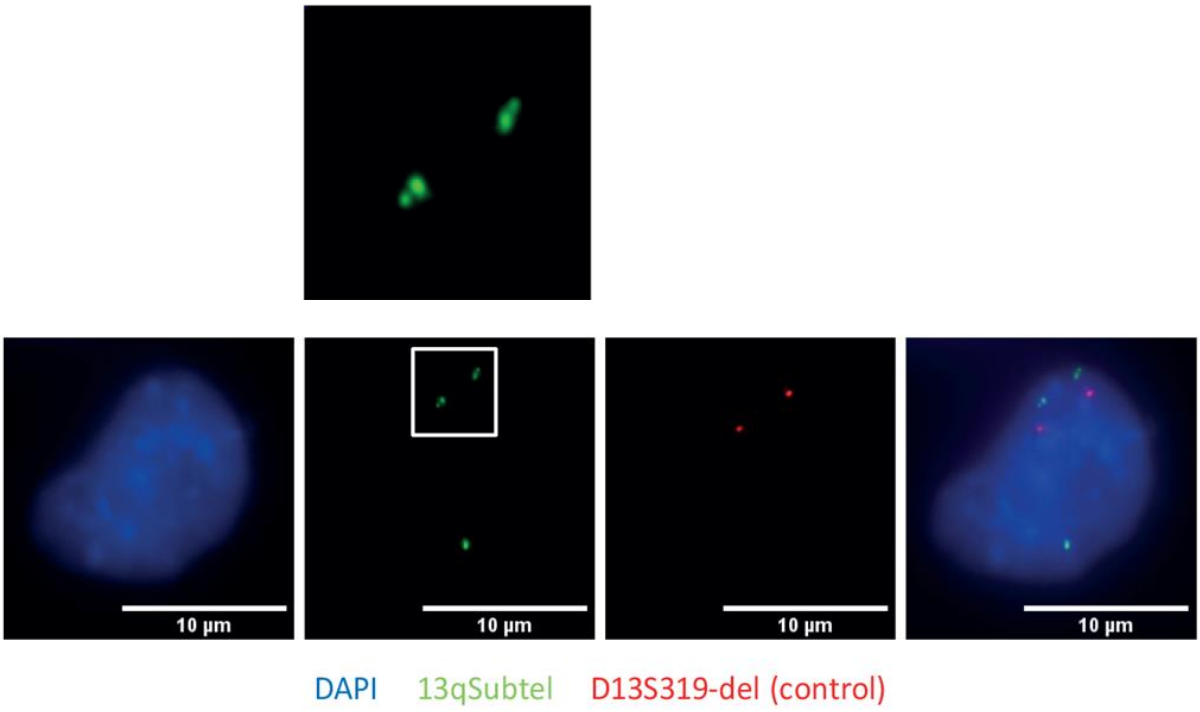

Figure 12B

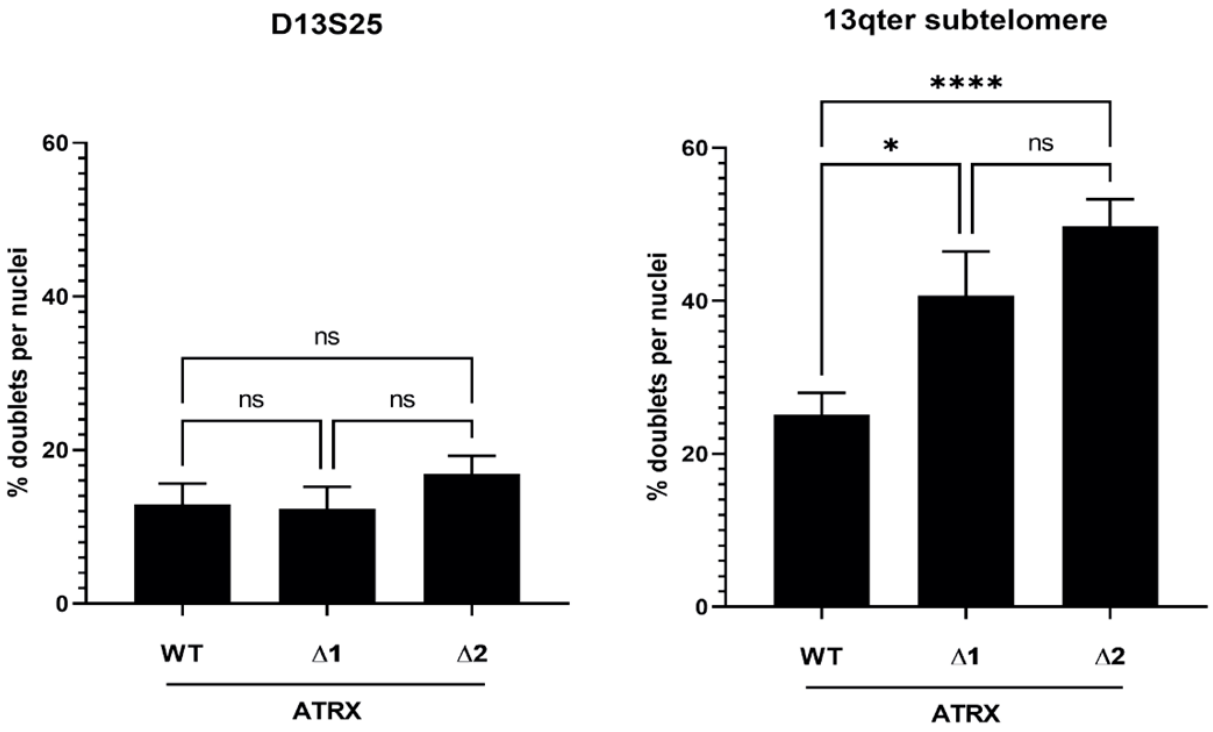

Figure 12C

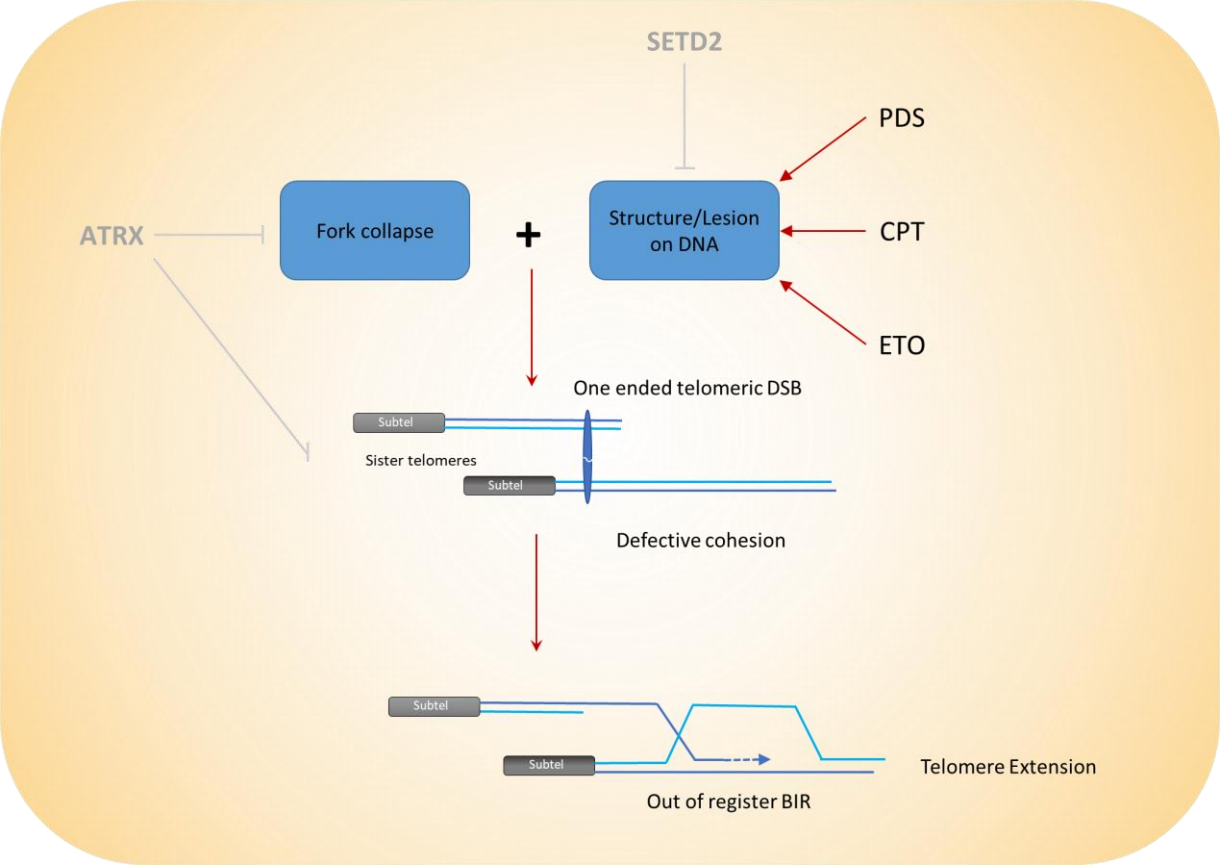

*Figure 12. Loss of ATRX induces loss of telomere sister chromatid cohesion. A) FISH of 156 kb region of chromosome 13 covering the D3S319-del genetic marker (red) and 13qter subtelomeric probe (green). Loss of sister chromatid cohesion is observed as a doublet, >50 nuclei analysed across 2 biological replicates. B) Quantification of doublet formation using the 13qter subtelomeric probe. *p < 0.05, ****p < 0.00001, determined by one-way ANOVA. C) Proposed model for suppression of the ALT pathway by the chromatin remodelling factor ATRX. All work in this figure was performed by David Clynes.*

The repair of telomeric DNA DSBs by BIR is not exclusive to cancer cells dependent on the ALT pathway (Dilley et al., 2016; Yang et al., 2020) and the use of a sister telomere as an in-register template will not result in a net elongation of telomeres. Prior reports have suggested that loss of ATRX leads to a diminution of telomere cohesion (Eid et al., 2015; Lovejoy et al., 2020), suggesting that ATRX may have an additional major role in the suppression of the ALT pathway, by ensuring the correct register of telomeric BIR. To this end, I sought to determine whether loss of ATRX in the HeLa LT cell line elicited a loss of telomeric cohesion using a FISH probe specific to the subtelomeric q arm of chromosome 13 (and an internal control probe mapping to 13q14). A loss of telomere cohesion was then scored in interphase cells as the appearance of a doublet as opposed to a single focus, with doublets indicative of a separation of sister telomeres. Strikingly, loss of ATRX resulted in a significant increase in the proportion of doublets, consistent with a premature loss of telomere sister chromatid cohesion in the absence of ATRX (Figures 12A and 12B). No significant changes were observed when using a FISH probe targeting an internal region of chromosome 13, suggesting that defective sister chromatid cohesion in the absence of ATRX was confined to telomeres (Figures 12A and 12B).

CHAPTER 4.0: DISCUSSION

Loss of ATRX or its functional interaction partner DAXX are hallmarks of the vast majority of ALT cancer cells but, despite ectopic expression of ATRX being sufficient to suppress the pathway in ALT cells (Clynes et al., 2015a; Napier et al., 2015), the loss of ATRX is generally insufficient to induce markers of the ALT pathway (Clynes et al., 2014; Eid et al., 2015; Lovejoy et al., 2012; Napier et al., 2015). Of note, recent work has shown that CRISPR-Cas9 mediated depletion of ATRX induces canonical markers of ALT in two specific glioma cell lines (U-251 and UW479) and a prostate cancer cell line (LAPC-4) (Brosnan-Cashman et al., 2018; Graham et al., 2019). Given that this induction was specific to these cell lines, it is likely that additional genetic or epigenetic events occur alongside ATRX loss to facilitate induction of ALT in human cancer. Consistent with this prediction, I show here that the loss of ATRX in HeLa cells failed to induce the canonical markers of ALT. It has been suggested that the presence of telomeric replicative stress drives the ALT pathway, with the stalling and collapse of replication forks at telomeres leading to the generation of a one ended DSB which is subsequently repaired by BIR in G2 or mitosis (MiDAS) (Min et al., 2017; Zhang et al., 2019b). Loss of ATRX has previously been linked to the generation of replicative stress (Clynes et al., 2014; Huh et al., 2012, 2016; Leung et al., 2013b; Watson et al., 2013), however, given that loss of ATRX is generally insufficient to induce ALT, I reasoned that the parallel induction of telomeric replicative stress, which would normally be tolerated through the activity of ATRX/DAXX, could trigger the ALT pathway only when in concert with ATRX loss. In concordance with this notion, I show here that the treatment of ATRX deplete cells with genotoxic agents known to induce structures/lesions on DNA triggers multiple canonical markers of an active ALT

pathway, specifically in the absence of ATRX and/or DAXX. Genotoxic agents that were found to induce ALT included the G4 stabilising ligand PDS, and the topoisomerase inhibitors ETO and CPT, both of which are frequently used in cancer therapy. Despite their different mechanisms, treatment with relatively mild doses of these drugs has been linked to fork slowing and reversal in the absence of chromosomal breakage (Zellweger et al., 2015), implying that under these conditions fork collapse is facilitated only upon ATRX and/or DAXX loss. In line with this, telomeric S1981 phosphorylated ATM was dramatically enriched at telomeres upon PDS treatment in ATRX null cells and the generation of ALT markers was dependent on the MUS81 endonuclease, suggesting that forks are cleaved and collapsed in the absence of ATRX upon PDS treatment. Importantly, I found that low dose APH treatment did not elicit the same response, implying that it is not replicative stress *per se* that elicits ALT in the absence of ATRX and/or DAXX, but more likely the presence of a 'lesion' or 'secondary structure' on telomeric DNA. Indeed, G4 structures have been proposed to form a barrier to the replisome, although in the case of telomeres the G4 structure would form on the lagging strand, which presumably constitutes less of a hindrance to the fork. In line with this, it has been reported that a block in lagging strand replication does not result in fork arrest *in vitro*, but rather is bypassed via re-priming by Polα/Primase allowing the fork to progress (Taylor and Yeeles, 2018). One potential explanation for the findings is that the stabilisation of G4 structures via PDS treatment has also been shown to result in a further potential barrier to replication fork processivity in the form of R-loops, with both PDS-mediated DNA damage and micronuclei formation abrogated upon the overexpression of RNase H1 (de Magis et al., 2019). Consistent with an important role for R-loops in facilitating ALT, overexpression of RNase H1 in ALT cells has been shown to abrogate ALT markers,

whereas the loss of RNase H1 or FANCM (a factor also linked to the prevention of R-loop formation), have the opposite effect (Arora et al., 2014; Lu et al., 2019a; Pan et al., 2019; Silva et al., 2019).

Recent work has also suggested that PDS induced cytotoxicity is dependent on TOP2 (Olivieri et al., 2020), inferring that the formation of G4 and/or R-loop structures leads to trapping of topoisomerases which, in turn, may block replication fork progression (Tammaro et al., 2013). I show here that, analogous to PDS, treatment with the TOP2 poison ETO elicited markers of ALT specifically in ATRX depleted cells. I note the largest induction of ALT markers manifested following treatment with the TOP1 inhibitor CPT. Interestingly, poisoning of TOP1 by camptothecins also effectively leads to the formation of R-loops (Marinello et al., 2013; Sordet et al., 2009). I show here that the induction of C-circles in ATRX null cells upon CPT treatment is most pronounced in the HeLa LT cell line, which harbthes very long telomeres of ~20 kb in length. This is consistent with previous findings that the induction of ALT was most robust in this cell line upon co-depletion of ASF1a and ASF1b (O'Sullivan et al., 2014b). The most likely explanation for this is that longer telomeres inherently provide more opportunity for aberrant structures and/or genotoxic lesions to form. Indeed, each telomeric repeat has been shown to represent a potential TOP1 cleavage site (Kang et al., 2004).

The combined depletion of ATRX and the histone H3 K36me3 methyltransferase SETD2 triggers a dramatic induction of ALT pathway markers, akin to that observed upon CPT treatment. Mutations in SETD2 have been identified in ~15% of paediatric HGGs and are highly coincident with ATRX loss (Fontebasso et al., 2013). Here, I

show that depletion of SETD2 possibly leads to an enrichment of R-loops at telomeres, which in turn facilitates the ALT pathway in the absence of ATRX. This raises the interesting question as to how SETD2 normally modulates the formation of telomeric R-loops. Histone H3 K36me3 is known to recruit a variety of chromatin associated proteins, many with defined roles in reshaping chromatin accessibility following transcription, including MRG15 (a component of the Rpd3S/Sin3S histone deacetylase complex) (Kumar et al., 2012), SPT16 (a component of the FACT complex) (Carvalho et al., 2013) and PHF1/19 (a component of the polycomb repressive complex 2 (PRC2)) (Ballaré et al., 2012; Cai et al., 2013). One possibility therefore is that a more open telomeric chromatin structure upon SETD2 loss is more permissive to the formation of R-loop and/or G-loop structures. In line with this hypothesis, loss of FACT has previously been linked to increases in R-loop formation (Herrera-Moyano et al., 2014). Histone H3 K36me3 has also been shown to recruit the DNA methyltransferase DNMT3b, loss of which has been shown to induce hypomethylation at sub-telomeres and the accumulation of telomeric R-loops in patients with ICF (Immunodeficiency, Centromeric instability and Facial anomalies) syndrome (Sagie et al., 2017). Taken together, the data I present here suggests that it is the combination of increased telomeric R-loops upon SETD2 disruption, in concert with ATRX loss, that triggers the ALT pathway in this cohort of paediatric HGG.

Mutations in histone H3.3 at glycine 34 to arginine or valine (G34R/V) are also highly co-incident with ATRX loss in HGG and tend to be mutually exclusive with SETD2 mutations (Fontebasso et al., 2013; Schwartzentruber et al., 2012b). Indeed, these mutations are thought to impede the ability of SETD2 to methylate the H3 tail, suggesting that in all likelihood the mechanism of ALT induction in tumors with this

mutational signature phenocopies that of a SETD2 mutant, with the accumulation of telomeric R-loops. H3.3 G34R/V has, however, only been shown to obstruct SETD2 activity in *cis* (Lewis et al., 2013; Weinberg et al., 2017) and this conjecture is therefore dependent on the mutant histone being incorporated into telomeric chromatin. In support of this possibility, recent work has shown that in the absence ATRX/DAXX, the histone H3.3 chaperone HIRA is enriched at ALT telomeres as an adaptive response to allow the deposition of histone H3.3 at telomeres (Hoang et al., 2020). A second mutation in histone H3.3 at lysine 27 to methionine (K27M) is also highly coincident with ATRX loss and inhibits the catalytic activity of PRC2 (Fontebasso et al., 2013; Lewis et al., 2013; Schwartzentruber et al., 2012b). It will therefore be of interest to ascertain whether the inhibition of PRC2 also elicits ALT markers when combined with ATRX/DAXX loss and, if so, whether loss of PRC2 function leads to the accumulation of aberrant secondary structures on telomeric DNA.

ATRX has previously been implicated with multiple roles at the replication fork which could explain the data I present here, including roles in both the protection of stalled forks from nucleolytic degradation (Huh et al., 2016) and the restart of stalled replication forks (Leung et al., 2013a; Raghunandan et al., 2020). Of note, ATRX has been proposed to interact with factors known to modulate both fork restart and protection. ATRX has been shown to interact and cooperate with FANCD2 to recruit CtIP to stalled replication forks and promote MRE11 dependent fork restart. ATRX itself has also been shown to interact with components of the MRN complex, raising the intriguing possibility that ATRX constitutes a component of a fork restart complex (Clynes et al., 2014; Leung et al., 2013a; Raghunandan et al., 2020). Understanding how these interactions are regulated will likely give important insights as to how ATRX

facilitates progressive DNA replication through genotoxic lesions and/or aberrant DNA secondary structures.

A second implication of the data presented here is that ATRX/DAXX may have a direct role in the clearing or resolution of structures or genotoxic lesions on telomeric DNA. Of note, ATRX possesses a translocase activity (Xue et al., 2003) which could potentially resolve R-loops via branch migration. Indeed, loss of ATRX has been shown to lead to an increase in telomeric R-loops at a highly transcribed ectopic telomeric repeat (Nguyen et al., 2017b), consistent with a role for ATRX in clearing R-loops once they have been triggered. R-loops have also been suggested to be excised by the nucleotide excision repair (NER) nucleases XPG and XPF, resulting in the formation of a single strand break, which could then ultimately trigger fork collapse in S-phase (Sollier et al., 2014). Interestingly, histone H3.3 deficient chicken DT40 cells have recently been shown to exhibit a likely defect in NER (Frey et al., 2014), raising the interesting possibility that ATRX/DAXX may be the histone H3.3 chaperone facilitating the completion of this process. In line with this notion, the nicking of telomeric DNA to form single stand breaks using the CRISPR-Cas9 system has been shown to induce the formation of C-circles in ATRX proficient cells (Zhang et al., 2019c).

Finally, the KO of ATRX in HeLa LT cells is associated with a marked loss of telomere sister chromatid cohesion, consistent with a recent report in mouse cells, published during the preparation of this manuscript (Lovejoy et al., 2020). How ATRX normally maintains telomere cohesion remains an interesting question, nonetheless this observation likely accounts for the net gain in telomere length observed as a result of

the BIR-like pathway in ALT cancer cells by facilitating the use of an out of register telomere template. Taken together, work presented here suggests that ATRX has a multi-faceted role in the suppression of the ALT pathway, accounting for its role as a near universal tumour suppressor in these cancers. Firstly, ATRX protects replication forks from collapse in the presence of telomeric lesions including R-loop structures. Secondly, ATRX maintains cohesion between sister telomeres, ensuring the faithful use of BIR without aberrant increases in telomere length. Finally, I provide evidence that the induction of ALT requires two independent cellular events; the loss of ATRX/DAXX in conjunction with the loss of another factor or factors that lead to the formation of lesions or structures at telomeres. An interesting avenue to further investigate is the contribution of protein trapping to this phenomenon.

REFERENCES

Aguilera, A., and García-Muse, T. (2012). R Loops: From Transcription Byproducts to Threats to Genome Stability. Molecular Cell *46*, 115–124.

Arora, R., Lee, Y., Wischnewski, H., Brun, C.M., Schwarz, T., and Azzalin, C.M. (2014). RNaseH1 regulates TERRA-telomeric DNA hybrids and telomere maintenance in ALT tumour cells. Nature Communications *5*.

Bakkenist, C.J., and Kastan, M.B. (2003). DNA damage activates ATM through intermolecular autophosphorylation and dimer dissociation.

Ballaré, C., Lange, M., Lapinaite, A., Martin, G.M., Morey, L., Pascual, G., Liefke, R., Simon, B., Shi, Y., Gozani, O., et al. (2012). Phf19 links methylated Lys36 of histone H3 to regulation of Polycomb activity. Nature Structural and Molecular Biology *19*, 1257–1265.

Brosnan-Cashman, J.A., Yuan, M., Graham, M.K., Rizzo, A.J., Myers, K.M., Davis, C., Zhang, R., Esopi, D.M., Raabe, E.H., Eberhart, C.G., et al. (2018). ATRX loss induces multiple hallmarks of the alternative lengthening of telomeres (ALT) phenotype in human glioma cell lines in a cell line-specific manner. PLoS ONE *13*.

Bryan, T.M., Englezou, A., Gupta, J., Bacchetti, S., and Reddel, R.R. (1995). Telomere elongation in immortal human cells without detectable telomerase activity. EMBO Jthenal *14*, 4240–4248.

Cai, L., Rothbart, S.B., Lu, R., Xu, B., Chen, W.Y., Tripathy, A., Rockowitz, S., Zheng, D., Patel, D.J., Allis, C.D., et al. (2013). An H3K36 Methylation-Engaging Tudor Motif of Polycomb-like Proteins Mediates PRC2 Complex Targeting. Molecular Cell *49*, 571–582.

Carvalho, S., Raposo, A.C., Martins, F.B., Grosso, A.R., Sridhara, S.C., Rino, J., Carmo-Fonseca, M., and de Almeida, S.F. (2013). Histone methyltransferase SETD2 coordinates FACT recruitment with nucleosome dynamics during transcription. Nucleic Acids Research *41*, 2881–2893.

Cawthon, R.M. (2009). Telomere length measurement by a novel monochrome multiplex quantitative PCR method. Nucleic Acids Research *37*.

Cho, N.W., Dilley, R.L., Lampson, M.A., and Greenberg, R.A. (2014). Interchromosomal homology searches drive directional ALT telomere movement and synapsis. Cell *159*, 108–121.

Clynes, D., Higgs, D.R., and Gibbons, R.J. (2013). The chromatin remodeller ATRX: A repeat offender in human disease. Trends in Biochemical Sciences *38*, 461–466.

Clynes, D., Jelinska, C., Xella, B., Ayyub, H., Taylor, S., Mitson, M., Bachrati, C.Z., Higgs, D.R., and Gibbons, R.J. (2014). ATRX dysfunction induces replication defects in primary mouse cells. PLoS ONE *9*.

Clynes, D., Jelinska, C., Xella, B., Ayyub, H., Scott, C., Mitson, M., Taylor, S., Higgs, D.R., and Gibbons, R.J. (2015a). Suppression of the alternative lengthening of telomere pathway by the chromatin remodelling factor ATRX. Nature Communications *6*.

Clynes, D., Jelinska, C., Xella, B., Ayyub, H., Scott, C., Mitson, M., Taylor, S., Higgs, D.R., and Gibbons, R.J. (2015b). Suppression of the alternative lengthening of telomere pathway by the chromatin remodelling factor ATRX. Nature Communications *6*.

Dilley, R.L., Verma, P., Cho, N.W., Winters, H.D., Wondisford, A.R., and Greenberg, R.A. (2016). Break-induced telomere synthesis underlies alternative telomere maintenance. Nature *539*, 54–58.

Drané, P., Ouararhni, K., Depaux, A., Shuaib, M., and Hamiche, A. (2010). The death-associated protein DAXX is a novel histone chaperone involved in the replication-independent deposition of H3.3. Genes and Development *24*, 1253–1265.
Eid, R., Demattei, M.-V., Episkopou, H., Augé-Gouillou, C., Decottignies, A., Grandin, N., and Charbonneau, M. (2015). Genetic Inactivation of ATRX Leads to a Decrease in the Amount of Telomeric Cohesin and Level of Telomere Transcription in Human Glioma Cells . Molecular and Cellular Biology *35*, 2818–2830.
Fontebasso, A.M., Schwartzentruber, J., Khuong-Quang, D.A., Liu, X.Y., Sturm, D., Korshunov, A., Jones, D.T.W., Witt, H., Kool, M., Albrecht, S., et al. (2013). Mutations in SETD2 and genes affecting histone H3K36 methylation target hemispheric high-grade gliomas. Acta Neuropathologica *125*, 659–669.
Frey, A., Listovsky, T., Guilbaud, G., Sarkies, P., and Sale, J.E. (2014). Histone H3.3 is required to maintain replication fork progression after UV damage. Current Biology *24*, 2195–2201.
Goldberg, A.D., Banaszynski, L.A., Noh, K.M., Lewis, P.W., Elsaesser, S.J., Stadler, S., Dewell, S., Law, M., Guo, X., Li, X., et al. (2010). Distinct Factors Control Histone Variant H3.3 Localization at Specific Genomic Regions. Cell *140*, 678–691.
Graham, M.K., Kim, J., Da, J., Brosnan-Cashman, J.A., Rizzo, A., del Valle, J.A.B., Chia, L., Rubenstein, M., Davis, C., Zheng, Q., et al. (2019). Functional loss of ATRX and TERC activates Alternative Lengthening of Telomeres (ALT) in LAPC4 prostate cancer cells. Molecular Cancer Research *17*, 2480–2491.
Grant, J.D., Broccoli, D., Muquit, M., Manion, F.J., Tisdall, J., and Ochs, M.F. (2001). Telometric: A Tool Providing Simplified, Reproducible Measurements of Telomeric DNA from Constant Field Agarose Gels. BioTechniques *31*, 1314–1318.
Heaphy, C.M., Subhawong, A.P., Hong, S.M., Goggins, M.G., Montgomery, E.A., Gabrielson, E., Netto, G.J., Epstein, J.I., Lotan, T.L., Westra, W.H., et al. (2011). Prevalence of the alternative lengthening of telomeres telomere maintenance mechanism in human cancer subtypes. American Jthenal of Pathology *179*, 1608–1615.
Herrera-Moyano, E., Mergui, X., García-Rubio, M.L., Barroso, S., and Aguilera, A. (2014). The yeast and human FACT chromatinreorganizing complexes solve R-loopmediated transcription-replication conflicts. Genes and Development *28*, 735–748.
Hoang, S.M., Kaminski, N., Bhargava, R., Barroso-González, J., Lynskey, M.L., García-Expósito, L., Roncaioli, J.L., Wondisford, A.R., Wallace, C.T., Watkins, S.C., et al. (2020). Regulation of ALT-associated homology-directed repair by polyADP-ribosylation. Nature Structural and Molecular Biology.
Huh, M.S., O'Dea, T.P., Ouazia, D., McKay, B.C., Parise, G., Parks, R.J., Rudnicki, M.A., and Picketts, D.J. (2012). Compromised genomic integrity impedes muscle growth after Atrx inactivation. Jthenal of Clinical Investigation *122*, 4412–4423.
Huh, M.S., Ivanochko, D., Hashem, L.E., Curtin, M., Delorme, M., Goodall, E., Yan, K., and Picketts, D.J. (2016). Stalled replication forks within heterochromatin require ATRX for protection. Cell Death and Disease *7*.
Juhász, S., Elbakry, A., Mathes, A., and Löbrich, M. (2018). ATRX Promotes DNA Repair Synthesis and Sister Chromatid Exchange during Homologous Recombination. Molecular Cell *71*, 11-24.e7.
Kang, M.R., Muller, M.T., and Chung, I.K. (2004). Telomeric DNA damage by topoisomerase I: A possible mechanism for cell killing by camptothecin. Jthenal of Biological Chemistry *279*, 12535–12541.

Kanu, N., Grönroos, E., Martinez, P., Burrell, R.A., Yi Goh, X., Bartkova, J., Maya-Mendoza, A., Mistrík, M., Rowan, A.J., Patel, H., et al. (2015). SETD2 loss-of-function promotes renal cancer branched evolution through replication stress and impaired DNA repair. Oncogene *34*, 5699–5708.
Koschmann, C., Calinescu, A.-A., Nunez, F.J., Mackay, A., Fazal-Salom, J., Thomas, D., Mendez, F., Kamran, N., Dzaman, M., Mulpuri, L., et al. (2016). C A N C E R ATRX loss promotes tumor growth and impairs nonhomologous end joining DNA repair in glioma. Science Translational Medicine *8*, undefined.
Kumar, G.S., Chang, W., Xie, T., Patel, A., Zhang, Y., Wang, G.G., David, G., and Radhakrishnan, I. (2012). Sequence requirements for combinatorial recognition of histone H3 by the MRG15 and Pf1 subunits of the Rpd3S/Sin3S corepressor complex. Jthenal of Molecular Biology *422*, 519–531.
de Lange, T. (2018). Shelterin-Mediated Telomere Protection.
Law, M.J., Lower, K.M., Voon, H.P.J., Hughes, J.R., Garrick, D., Viprakasit, V., Mitson, M., de Gobbi, M., Marra, M., Morris, A., et al. (2010). ATR-X syndrome protein targets tandem repeats and influences allele-specific expression in a size-dependent manner. Cell *143*, 367–378.
Leung, J.W.C., Ghosal, G., Wang, W., Shen, X., Wang, J., Li, L., and Chen, J. (2013a). Alpha thalassemia/mental retardation syndrome X-linked gene product ATRX is required for proper replication restart and cellular resistance to replication stress. Jthenal of Biological Chemistry *288*, 6342–6350.
Leung, J.W.C., Ghosal, G., Wang, W., Shen, X., Wang, J., Li, L., and Chen, J. (2013b). Alpha thalassemia/mental retardation syndrome X-linked gene product ATRX is required for proper replication restart and cellular resistance to replication stress. Jthenal of Biological Chemistry *288*, 6342–6350.
Lewis, P.W., Müller, M.M., Koletsky, M.S., Cordero, F., Lin, S., Banaszynski, L.A., Garcia, B.A., Muir, T.W., Becher, O.J., and Allis, C.D. (2013). Inhibition of PRC2 activity by a gain-of-function H3 mutation found in pediatric glioblastoma. Science *340*, 857–861.
Loe, T.K., Zhou Li, J.S., Zhang, Y., Azeroglu, B., Boddy, M.N., and Denchi, E.L. (2020). Telomere length heterogeneity in ALT cells is maintained by PML-dependent localization of the BTR complex to telomeres. Genes and Development *34*, 650–662.
Lovejoy, C.A., Li, W., Reisenweber, S., Thongthip, S., Bruno, J., de Lange, T., De, S., Petrini, J.H.J., Sung, P.A., Jasin, M., et al. (2012). Loss of ATRX, genome instability, and an altered DNA damage response are hallmarks of the alternative lengthening of Telomeres pathway. PLoS Genetics *8*.
Lovejoy, C.A., Takai, K., Huh, M.S., Picketts, D.J., and de Lange, T. (2020). ATRX affects the repair of telomeric DSBs by promoting cohesion and a DAXX-dependent activity. PLoS Biology *18*, e3000594.
Lu, R., O'Rtheke, J.J., Sobinoff, A.P., Allen, J.A.M., Nelson, C.B., Tomlinson, C.G., Lee, M., Reddel, R.R., Deans, A.J., and Pickett, H.A. (2019a). The FANCM-BLM-TOP3A-RMI complex suppresses alternative lengthening of telomeres (ALT). Nature Communications *10*.
Lu, R., O'Rtheke, J.J., Sobinoff, A.P., Allen, J.A.M., Nelson, C.B., Tomlinson, C.G., Lee, M., Reddel, R.R., Deans, A.J., and Pickett, H.A. (2019b). The FANCM-BLM-TOP3A-RMI complex suppresses alternative lengthening of telomeres (ALT). Nature Communications *10*.
de Magis, A., Manzo, S.G., Russo, M., Marinello, J., Morigi, R., Sordet, O., and Capranico, G. (2019). DNA damage and genome instability by G-quadruplex ligands

are mediated by R loops in human cancer cells. Proceedings of the National Academy of Sciences of the United States of America *116*, 816–825.
Marinello, J., Chillemi, G., Bueno, S., Manzo, S.G., and Capranico, G. (2013). Antisense transcripts enhanced by camptothecin at divergent CpG-island promoters associated with bursts of topoisomerase I-DNA cleavage complex and R-loop formation. Nucleic Acids Research *41*, 10110–10123.
Min, J., Wright, W.E., and Shay, J.W. (2017). Alternative Lengthening of Telomeres Mediated by Mitotic DNA Synthesis Engages Break-Induced Replication Processes.
Napier, C.E., Huschtscha, L.I., Harvey, A., Bower, K., Noble, J.R., Hendrickson, E.A., and Reddel, R.R. (2015). ATRX represses alternative lengthening of telomeres.
Nguyen, D.T., Voon, H.P.J., Xella, B., Scott, C., Clynes, D., Babbs, C., Ayyub, H., Kerry, J., Sharpe, J.A., Sloane-Stanley, J.A., et al. (2017a). The chromatin remodelling factor ATRX suppresses R-loops in transcribed telomeric repeats . EMBO Reports *18*, 914–928.
Nguyen, D.T., Voon, H.P.J., Xella, B., Scott, C., Clynes, D., Babbs, C., Ayyub, H., Kerry, J., Sharpe, J.A., Sloane-Stanley, J.A., et al. (2017b). The chromatin remodelling factor ATRX suppresses R-loops in transcribed telomeric repeats . EMBO Reports *18*, 914–928.
Olivieri, M., Cho, T., Álvarez-Quilón, A., Li, K., Schellenberg, M.J., Zimmermann, M., Hustedt, N., Rossi, S.E., Adam, S., Melo, H., et al. (2020). A Genetic Map of the Response to DNA Damage in Human Cells. Cell *182*, 481-496.e21.
O'Sullivan, R.J., Arnoult, N., Lackner, D.H., Oganesian, L., Haggblom, C., Corpet, A., Almouzni, G., and Karlseder, J. (2014a). Rapid induction of alternative lengthening of telomeres by depletion of the histone chaperone ASF1. Nature Structural and Molecular Biology *21*, 167–174.
O'Sullivan, R.J., Arnoult, N., Lackner, D.H., Oganesian, L., Haggblom, C., Corpet, A., Almouzni, G., and Karlseder, J. (2014b). Rapid induction of alternative lengthening of telomeres by depletion of the histone chaperone ASF1. Nature Structural and Molecular Biology *21*, 167–174.
Pan, X., Drosopoulos, W.C., Sethi, L., Madireddy, A., Schildkraut, C.L., and Zhang, D. (2017a). FANCM, BRCA1, and BLM cooperatively resolve the replication stress at the ALT telomeres. Proceedings of the National Academy of Sciences of the United States of America *114*, E5940–E5949.
Pan, X., Drosopoulos, W.C., Sethi, L., Madireddy, A., Schildkraut, C.L., and Zhang, D. (2017b). FANCM, BRCA1, and BLM cooperatively resolve the replication stress at the ALT telomeres. Proceedings of the National Academy of Sciences of the United States of America *114*, E5940–E5949.
Pan, X., Chen, Y., Biju, B., Ahmed, N., Kong, J., Goldenberg, M., Huang, J., Mohan, N., Klosek, S., Parsa, K., et al. (2019). FANCM suppresses DNA replication stress at ALT telomeres by disrupting TERRA R-loops. Scientific Reports *9*.
Pepe, A., and West, S.C. (2014). MUS81-EME2 promotes replication fork restart. Cell Reports *7*.
Pfister, S.X., Markkanen, E., Jiang, Y., Sarkar, S., Woodcock, M., Orlando, G., Mavrommati, I., Pai, C.C., Zalmas, L.P., Drobnitzky, N., et al. (2015). Inhibiting WEE1 Selectively Kills Histone H3K36me3-Deficient Cancers by dNTP Starvation. Cancer Cell *28*, 557–568.
Raghunandan, M., Yeo, J.E., Walter, R., Saito, K., Harvey, A.J., Ittershagen, S., Lee, E.A., Yang, J., Hoatlin, M.E., Bielinsky, A.K., et al. (2020). Functional cross talk between the Fanconi anemia and ATRX/DAXX histone chaperone pathways promotes replication fork recovery. Human Molecular Genetics *29*, 1083–1095.

Ray Chaudhuri, A., Hashimoto, Y., Herrador, R., Neelsen, K.J., Fachinetti, D., Bermejo, R., Cocito, A., Costanzo, V., and Lopes, M. (2012). Topoisomerase i poisoning results in PARP-mediated replication fork reversal. Nature Structural and Molecular Biology *19*, 417–423.
Roumelioti, F., Sotiriou, S.K., Katsini, V., Chitheea, M., Halazonetis, T.D., and Gagos, S. (2016). Alternative lengthening of human telomeres is a conservative DNA replication process with features of break-induced replication . EMBO Reports *17*, 1731–1737.
Sagie, S., Toubiana, S., Hartono, S.R., Katzir, H., Tzur-Gilat, A., Havazelet, S., Francastel, C., Velasco, G., Chédin, F., and Selig, S. (2017). Telomeres in ICF syndrome cells are vulnerable to DNA damage due to elevated DNA:RNA hybrids. Nature Communications *8*.
Schwartzentruber, J., Korshunov, A., Liu, X.Y., Jones, D.T.W., Pfaff, E., Jacob, K., Sturm, D., Fontebasso, A.M., Quang, D.A.K., Tönjes, M., et al. (2012a). Driver mutations in histone H3.3 and chromatin remodelling genes in paediatric glioblastoma. Nature *482*, 226–231.
Schwartzentruber, J., Korshunov, A., Liu, X.Y., Jones, D.T.W., Pfaff, E., Jacob, K., Sturm, D., Fontebasso, A.M., Quang, D.A.K., Tönjes, M., et al. (2012b). Driver mutations in histone H3.3 and chromatin remodelling genes in paediatric glioblastoma. Nature *482*, 226–231.
Sfeir, A., Kosiyatrakul, S.T., Hockemeyer, D., MacRae, S.L., Karlseder, J., Schildkraut, C.L., and de Lange, T. (2009). Mammalian Telomeres Resemble Fragile Sites and Require TRF1 for Efficient Replication. Cell *138*, 90–103.
Silva, B., Pentz, R., Figueira, A.M., Arora, R., Lee, Y.W., Hodson, C., Wischnewski, H., Deans, A.J., and Azzalin, C.M. (2019). FANCM limits ALT activity by restricting telomeric replication stress induced by deregulated BLM and R-loops. Nature Communications 10.
Smolka, J.A., Sanz, L.A., Hartono, S.R., and Chédin, F. (2021). Recognition of RNA by the S9.6 antibody creates pervasive artifacts when imaging RNA:DNA hybrids. Journal of Cell Biology 220(6).
Sollier, J., Stork, C.T., García-Rubio, M.L., Paulsen, R.D., Aguilera, A., and Cimprich, K.A. (2014). Transcription-Coupled Nucleotide Excision Repair Factors Promote R-Loop-Induced Genome Instability. Molecular Cell 56, 777–785.
Sordet, O., Redon, C.E., Guirouilh-Barbat, J., Smith, S., Solier, S., Douarre, C., Conti, C., Nakamura, A.J., Das, B.B., Nicolas, E., et al. (2009). Ataxia telangiectasia mutated activation by transcription- and topoisomerase I-induced DNA double-strand breaks. EMBO Reports *10*, 887–893.
Spiegel, J., Adhikari, S., and Balasubramanian, S. (2020). The Structure and Function of DNA G-Quadruplexes. Trends in Chemistry *2*, 123–136.
Tammaro, M., Barr, P., Ricci, B., and Yan, H. (2013). Replication-dependent and transcription-dependent mechanisms of DNA double-strand break induction by the topoisomerase 2-targeting drug etoposide. PLoS ONE *8*.
Taylor, M.R.G., and Yeeles, J.T.P. (2018). The Initial Response of a Eukaryotic Replisome to DNA Damage. Molecular Cell *70*, 1067-1080.e12.
Udugama, M., Sanij, E., Voon, H.P.J., Son, J., Hii, L., Henson, J.D., Lyn Chan, F., Chang, F.T.M., Liu, Y., Pearson, R.B., et al. (2018). Ribosomal DNA copy loss and repeat instability in ATRX-mutated cancers. Proceedings of the National Academy of Sciences of the United States of America *115*, 4737–4742.
Wang, Y., Yang, J., Wu, W., Shah, R., Danussi, C., Riggins, G., Kannan, K., Sulman, E., Chan, T., and Huse, J. (2018). G-quadruplex DNA drives genomic instability and

represents a targetable molecular abnormality in ATRX-deficient malignant glioma. G-Quadruplex DNA Drives Genomic Instability and Represents a Targetable Molecular Abnormality in ATRX-Deficient Malignant Glioma 347542.
Watson, L.A., Solomon, L.A., Li, J.R., Jiang, Y., Edwards, M., Shin-Ya, K., Beier, F., and Bérubé, N.G. (2013). Atrx deficiency induces telomere dysfunction, endocrine defects, and reduced life span. Jthenal of Clinical Investigation *123*, 2049–2063.
Weinberg, D.N., Allis, C.D., and Lu, C. (2017). Oncogenic mechanisms of histone H3 mutations. Cold Spring Harbor Perspectives in Medicine *7*.
Wong, L.H., McGhie, J.D., Sim, M., Anderson, M.A., Ahn, S., Hannan, R.D., George, A.J., Morgan, K.A., Mann, J.R., and Choo, K.H.A. (2010). ATRX interacts with H3.3 in maintaining telomere structural integrity in pluripotent embryonic stem cells. Genome Research *20*, 351–360.
Xue, Y., Gibbons, R., Yan, Z., Yang, D., Mcdowell, T.L., Sechi, S., Qin, J., Zhou, S., Higgs, D., and Wang, W. (2003). The ATRX syndrome protein forms a chromatin-remodeling complex with Daxx and localizes in promyelocytic leukemia nuclear bodies.
Yang, Z., Takai, K.K., Lovejoy, C.A., and de Lange, T. (2020). Break-induced replication promotes fragile telomere formation. Genes & Development.
Zellweger, R., Dalcher, D., Mutreja, K., Berti, M., Schmid, J.A., Herrador, R., Vindigni, A., and Lopes, M. (2015). Rad51-mediated replication fork reversal is a global response to genotoxic treatments in human cells. Jthenal of Cell Biology *208*, 563–579.
Zeng, S., Xiang, T., Pandita, T.K., Gonzalez-Suarez, I., Gonzalo, S., Harris, C.C., and Yang, Q. (2009). Telomere recombination requires the MUS81 endonuclease. Nature Cell Biology *11*, 616–623.
Zhang, J.M., Yadav, T., Ouyang, J., Lan, L., and Zou, L. (2019a). Alternative Lengthening of Telomeres through Two Distinct Break-Induced Replication Pathways. Cell Reports *26*, 955-968.e3.
Zhang, T., Zhang, Z., Shengzhao, G., Li, X., Liu, H., and Zhao, Y. (2019b). Strand break-induced replication fork collapse leads to C-circles, C-overhangs and telomeric recombination. PLoS Genetics *15*.
Zhang, T., Zhang, Z., Shengzhao, G., Li, X., Liu, H., and Zhao, Y. (2019c). Strand break-induced replication fork collapse leads to C-circles, C-overhangs and telomeric recombination. PLoS Genetics *15*.